1998

Phototherapeutic and clinical aspects of nitric oxide and related compounds.

Marie Antonios. Tannous
University of Windsor

PHOTOTHERAPEUTIC AND CLINICAL ASPECTS OF NITRIC OXIDE AND RELATED COMPOUNDS

By

Marie Antonios Tannous

A Dissertation
Submitted to the College of Graduate Studies and Research
through the Department of Chemistry and Biochemistry
in Partial Fulfillment of the Requirements for
the Degree of Doctor of Philosophy at the
University of Windsor

Windsor, Ontario, Canada
1998

ABSTRACT

By

Marie Antonios Tannous

Perhaps the most challenging problem of nitric oxide-photodynamic therapy is the choice of an appropriate nitric oxide (NO) carrier. In the first part of this study, two NO carriers were investigated: Metallothionein and dendrimers. Metallothionein has the ability to carry eighteen nitric oxide molecules, whereas each dendrimer upon conjugation to thiols, has the ability to carry up to ten nitric oxide molecules. In testing both carriers, the cytotoxic potential of this light-activated nitric oxide generating system was demonstrated towards human colon adenocarcinoma cells (SW 948) in culture. 98% cell death occurred in light irradiated samples after a 72 h incubation period.

Since nitric oxide-photodynamic therapy has proven to be toxic towards tumor cells in culture, the photodynamic effects of S-nitrosoglutathione and aminolevulinic acid were tested on ocular fibrosis *in vitro* to improve glaucoma filtration surgery. Upon investigation of the mode of cell death post S-nitrosoglutathione photodynamic treatment, a direct evidence of necrotic mode occurred.

In the second part of this study, nitric oxide synthase (NOS) isoform-dependent peroxynitrite production was monitored in control and diabetic platelets. Using dichlorofluorescein for the detection of peroxynitrite, and in the presence of extracellular L-arginine, diabetic platelets displayed a ~5-fold higher fluorescent level in comparison to controls. Upon using a NOS inhibitor, the dichlorofluorescein

fluorescence was nearly abolished. Furthermore, immunoblot analysis of intraplatelet proteins indicated that the induced (NOS) is detected in diabetic platelets and not in controls.

The change in the intraplatelet nitric oxide isozymes was also investigated in hyperlipidemic subjects treated with the hypercholesterolemic drug Atorvastatin in an 8-week study. The results correlated with cholesterol, low-density lipoprotein, high-density lipoprotein and triglycerides indicated that with Atrovastatin endothelial NOS levels increased, as cholesterol levels decreased. Interestingly, levels of nitrotyrosylated platelet proteins, an indication of peroxynitrite damage, decreased as endothelial NOS increased in presence of the drug. Another potential benefit of Atorvastatin was the fact that the level of intraplatelet induced NOS was lowered by this drug.

Dedicated to my parents Hannie and Antonios Tannous
and my brothers, Bakhos, Joseph, Sam, Max, Elias and Mike
for their love, support and encouragement

ACKNOWLEDGMENTS

I wish to begin by thanking my supervisor Dr. Mutus, for all his guidance and support throughout my study. I would also like to thank my committee members, Dr. Lafreniere, Dr. Szabo, Dr. Taylor, and my external examiner Dr. Johnston.

Special thanks to Dr. Zielinski and her lab for microscopy assistance; Dr. Hutnik for her assistance in the glaucoma study; Dr. Lee for the critical reading of this dissertation; Hotel Dieu/Grace hospital for blood supply. I wish to acknowledge the Natural Sciences & Engineering Research Council of Canada and The University of Windsor for the financial assistance provided.

Thanks to all Essex Hall students, staff and faculty for their guidance, assistance, and kindness. Thanks to my colleagues who contributed to this work Arianna Vignini, Joanna Klapacz, Niro Ramachandran, Pat Cervini and Sanjay Jacob. I am grateful for the many scientific discussions I have had with my colleague Stephanie White. Thanks to all my friends.

Finally I would like to especially thank my family. I could never have made it this far without the love, support, prayers and encouragement of my mom and dad, my brothers, Bakhos, Joseph, Sam, Max, Elias, Mike and the rest of my family, Laura, Sonia, Laurie, Anthony, Mia, Tony, Joseph and Maxine. I appreciate all that you have done for me.

TABLE OF CONTENTS

PART II

CHAPTER 1

INTRODUCTION

CHAPTER 2

MATERIALS

CHAPTER 3

METHODS

LIST OF TABLES

LIST OF FIGURES

LIST OF ABBREVIATIONS

ALA	aminolevulinic acid
BCIP	5-bromo-4-chloro-3-indoyl phosphate
BH_4	tetrahydrobiopterine
BSA	bovine serum albumin
cGMP	cyclic guanosine monophosphate
cNOS	constitutive nitric oxide synthase
Cys	cysteine
DCF	dichlorofluorescein
DEF	Desferal
DMEM	Dulbecco's modified Eagle's medium
DMSO	dimethylsulfoxide
DNA	deoxyribonucleic acid
DNS	dansyl
DTNB	5,5'-dithio-bis-2-nitrobenzoic acid
DTT	dithiothreitol
ECL	enhanced chemiluminescent
EDAC	1-ethyl-3-[3'-(dimethylamino)propyl]carbodiimide
EDTA	ethylenediaminetetra-acetic acid
eNOS	endothelial nitric oxide synthase
FBS	fetal bovine serum
GFS	glaucoma filtration surgery
GOD	glucose oxidase
GSH	glutathione (reduced)
GSNO	S-nitrosoglutathione
GSSG	glutathione (oxidized)
GTP	guanosine triphosphate
HCys	homocysteine
HDL	high density lipoprotein
HEPES	N-(2-hydroxyethyl)piperazine-N'-(2-ethanesulfonic acid)
HMG-CoA	β-hydroxy-β-methylglutaryl coenzyme A
IDDM	insulin-dependent diabetes mellitus
iNOS	induced nitric oxide synthase
Da	dalton
L-15	Leibovitz's 15
LDL	low density lipoprotein
MT	metallothionein
NADPH	nicotinamide adenine dinucleotide phosphate (reduced form)
NBT	nitroblue tetrazolium
NHS	N-hydroxysuccinimide
NMMA	N^G-monomethyl-L-arginine

NO	nitric oxide
NOS	nitric oxide synthase
ONOO	peroxynitrite
OxyHb	oxyhemoglobin
PAGE	polyacrylamide gel electrophoresis
PAMAM	polyamidoamine
PBS	phosphate buffered saline
PDT	photodynamic therapy
PS	phosphatidylserine
PpIX	protoporphyrin IX
PRP	platelet rich plasma
RSNO	S-nitrosothiol
SDS	sodium dodecyl sulfate
SPDP	N-succinimidyl-3-(2-pyridyldithio)propionate
T	thionein
TBS	tris buffer saline
TG	triglyceride
TFA	trifluoroacetic acid
TMB	tetramethylbenzidine
TTBS	Tween tris buffer saline
UV	ultraviolet
VLDL	very low density lipoprotein

PART I

CHAPTER 1

INTRODUCTION

1.0 Overview

Photodynamic therapy (PDT), a combination of visible light and non-toxic light-absorbing chemicals, is a promising new cancer treatment that faces many drawbacks. Previous studies in our laboratory revealed that S-nitrosothiols are photolabile. S-nitrosoglutathione which can only deliver one NO per mole, was shown to be cytotoxic. In this study, the toxicity of S-NO/PDT was further explored using a cysteine rich apoprotein (thionein) as a potential NO carrier with an ability to deliver up to 20 nitric oxide molecules per thionein. Owing to the fact that thionein was difficult to purify and very unstable to polymerization, other potential NO carriers were sought. To this end, starburst dendrimers were conjugated with thiol groups and tested as a delivery system for NO in photodynamic therapy. To further explore the effect of S-NO/PDT, we tested the potential use of this therapy to improve glaucoma filtration surgery by the inhibition of fibroblast proliferation, thus eliminating the main cause of the failure of glaucoma filtration surgery (GFS).

The mechanism of PDT-mediated cell killing is not yet well defined. Two kinds of cell death can arise from post-photodynamic therapy: apoptosis and necrosis. A major discrimination between apoptosis and necrosis is the effect on neighboring cells. Apoptotic cells are rapidly sequestered by phagocytes, whereas necrotic cells burst

open with uncontrolled spillage of their contents causing inflammation to surrounding area. Therefore, it is crucial to identify the mode of cell death post S-NO/PDT.

This introduction discusses various aspects of photodynamic therapy, the role of nitric oxide, the two potential NO carriers in PDT, the role of PDT in improving glaucoma filtration surgery, and the mode of cell death post PDT.

1.1 Photodynamic therapy (PDT)

1.1.1 The principle of photodynamic therapy and historical overview

Photodynamic therapy (PDT) (also known as photoradiation therapy, phototherapy, or photochemotherapy) is an innovative and attractive modality for cancer treatment (Ochsner *et al.*, 1997). It is based on the use of exogenously administered or endogenously formed photosensitizers which are activated by light to induce cell death via formation of singlet oxygen and other free radicals (Fritsch *et al.*, 1998).

The earliest therapeutic use of light-sensitive substances can be traced back over 6000 years to ancient Egypt, where skin depigmentation was treated with plant extract and sun light (Forrest *et al.*, 1980). Around the turn of the century, Jesionek and Tappenier were the first to use chemically enhanced phototherapy for cancer treatment (Fritsch *et al.*1998). The appearance of lasers on the market in the 1970s gave a new boost to PDT, where the use of haematoporphyrin derivatives (HPD) and laser light for selective tumour destruction was reported (Dougherty *et al.*, 1974). Since then many photosensitizers have been developed, each with a specific affinity for a specific cancer.

1.1.2 The components of photodynamic therapy

Photodynamic therapy is a combination of visible light and photosensitizer. In general, any visible light source with high output at an absorption maximum of the photosensitizer can be used in PDT (Fritsch *et al.*, 1998). Many lasers are currently available for applications of PDT.

A large number of photosensitizers have been used in PDT, but a single photosensitizer with ideal properties does not yet exist. First generation photosensitizers are effective, but cause prolonged skin photosensitivity (4-8 weeks). On the other hand, second generation photosensitizers have been shown to produce significantly low skin photosensitivity. A few are now under clinical investigation such as protoporphyrin IX (PpIX) which is easily induced by aminolevulinic acid (ALA) (Peng *et al.*, 1997). Interestingly, ALA itself is not a sensitizing agent, but it acts as a physiological precursor and induces the biosynthesis of PpIX in the mitochondria of both normal and tumour cells (Ochsner *et al.*, 1997).

1.1.3 Clinical applications of PDT

At the beginning of the PDT era, the emphasis of tumour treatment focused on diseases accessible by light such as carcinomas of the skin (McCaughan *et al.*, 1989), the upper digestive tract (Barr *et al.*, 1994), lung cancer (Furuse *et al.*, 1993), and superficial bladder cancer (Lum *et al.*, 1991). A wide variety of non-tumourous diseases such as skin lesions, benign prostate hyperplasia, and opthalmic disorders (diabetic retinopathy or macular degeneration of the retina), were proven to be good

candidates for PDT (Jori *et al.*, 1990; Levy *et al.*, 1996). Also more recently in the cardiovascular field, diagnosis of atherosclerotic plaques and prevention of restenosis following balloon angioplasty are new and promising targets of PDT (Nyamekye *et al.*, 1995).

1.1.4 Advantages and disadvantages of PDT

Since photodynamic therapy is not painful, anesthesia is not necessary. Significant advantages of PDT are the ability to treat multiple lesions in one setting, good patient acceptance and apparent lack of major side effects. There is no significant morbidity associated with PDT, especially when second generation photosensitizers are used. Every year a large number of drugs are proposed as potential new photosensitizers in PDT. Overall, PDT can be selective, as tumour cells accumulate more of the sensitizers than normal cells, thus leading to selective destruction of tumour cells (Moan *et al.*, 1992).

Photodynamic therapy has not yet been widely accepted due to a few drawbacks, including the light source. Many lasers are expensive and require special electrical installation and external water cooling systems making their use impractical in most clinical settings (Castro *et al.*, 1996). Another major downfall of PDT is the lack of a suitable photosensitizer; there is not a chemical substance, easily and consistently manufactured which does not induce skin phototoxicity. Most of currently used photosensitizers have a slow rate of clearance from the body, which leads to severe phototoxic damage upon exposure to sunlight. In addition, most of these

photosensitizers produce many other side effects such as nausea, vomiting, a metallic taste in the mouth and eye sensitivity to light.

1.2 Nitric oxide (NO)

1.2.1 Chemistry of Nitric oxide

Nitric oxide is an inorganic gas composed of seven electrons from nitrogen and eight electrons from oxygen, with one unpaired electron in the highest occupied orbital, making NO a free radical molecule (Beckman *et al.*, 1996). The solubility of NO in H_2O at 25°C and 1 atm is 1.8 mM and remains unchanged over the pH 2-13 (Butler *et al.*, 1993).

The biological half life of nitric oxide depends mostly on its initial concentration (Stamler *et al.*, 1992). Upon reaction of NO with 5-10 fold molar excess of oxygen in phosphate buffer saline (PBS) pH 7.4, the half life of NO (10-20μM) was estimated to be approximately 130 seconds (Ford *et al.*, 1993). Reaction of NO with O_2 in a gas phase is second order with respect to NO; $v=k[NO]^2[O_2]$ (Stamler *et al.*, 1992). This rate remains the same in aqueous solution with $k=5\times10^6$ dm^6 mol^{-2} s^{-1}. Thus a saturated solution of NO is ~2 mM and has a half-life of < 1s in water (Beckman *et al.*, 1996). Consequently, half-life of NO is not a constant value and is inversely proportional to the concentration of nitric oxide. The reaction rate slows down by a factor of approximately 1 million to 400 million, when nitric oxide is diluted to physiologically relevant concentrations; NO at a concentration of 5 nM has a half-life of > 70 h (Beckman *et al.*, 1996).

The reaction mechanism of NO and O_2 is as follows (Scheme 1) (Kharitonov *et al.*, 1995).

$$NO + \tfrac{1}{2} O_2 \longrightarrow NO_2$$

$$NO_2 + NO \longrightarrow N_2O_3$$

$$N_2O_3 + H_2O \longrightarrow 2HNO_2 \longrightarrow 2H^{+} + 2NO_2^{-}$$

(Scheme 1)

One of the biological effects of NO is the activation of guanylate cyclase, the enzyme responsible for the conversion of guanosine triphosphate (GTP) to cyclic guanosine monophosphate (cGMP). Since NO is a highly diffusible molecule, it can be produced in one cell and exert its actions in another (Fig. 1.1).

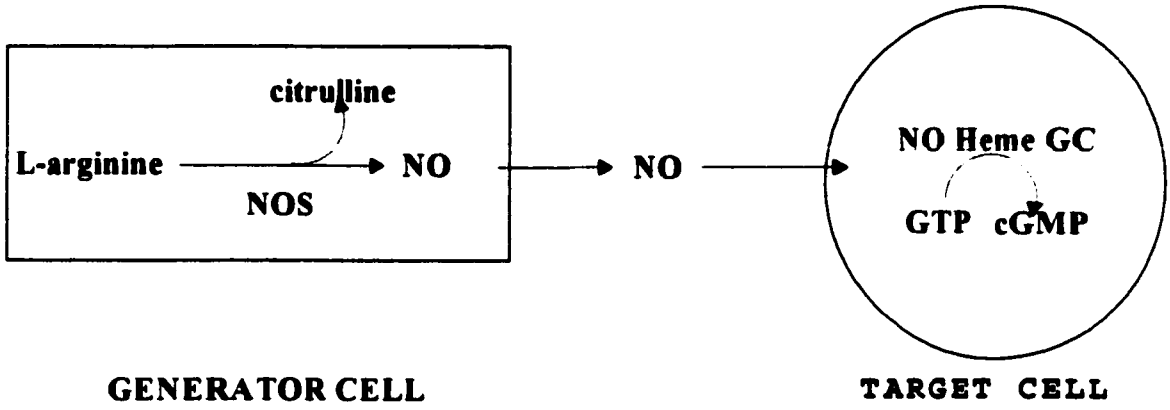

Figure 1.1- The L-arginine:nitric oxide pathway (MacAllister *et al.*, 1996). Abbreviations: NOS (nitric oxide synthase), Heme GC (heme moiety of guanylate cyclase), GTP (guanosine triphosphate), cGMP (cyclic guanosine monophosphate).

The generally accepted theory is that the interaction of NO with the iron of guanylate cyclase-bound heme may weaken or break the axial ligand and thereby pulling the iron out from the plane of porphyrin ring. This conformational change may expose the catalytic site to GTP and therefore constitute enzyme activation (Fig.1.2).

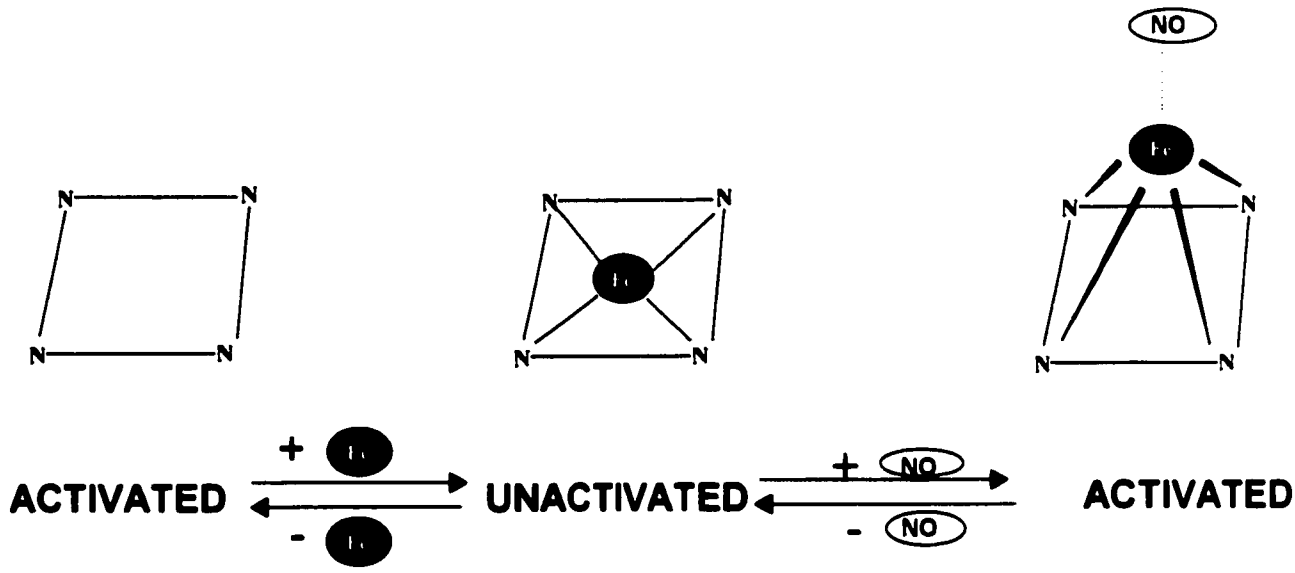

Figure 1.2- Schematic representation of the activation of guanylate cyclase by nitric oxide (Ignarro *et al.*, 1984).

1.2.2 S-Nitrosothiols

S-Nitrosothiols (RSNO) are a group of potent compounds that are readily formed through the reaction of thiols with either N_2O_3, or alkyl nitrite (Liu *et al.*, 1998; Butler *et al.*, 1997) (Scheme 2).

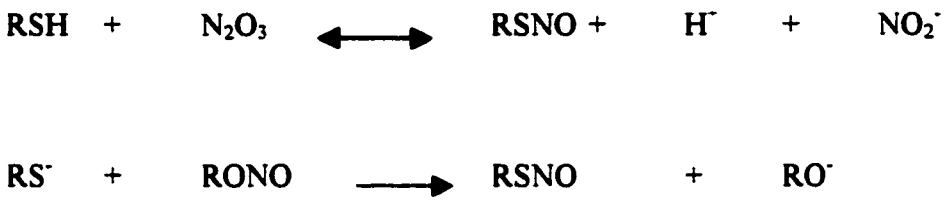

(Scheme 2)

Arnelle *et al.* (1995) had demonstrated the ability of S-nitrosothiols to act as NO^+, NO, and NO^- donors under physiological conditions. S-nitrosothiols can undergo nitrosonium NO^+ transfer to other thiols through a process of transnitrosation.

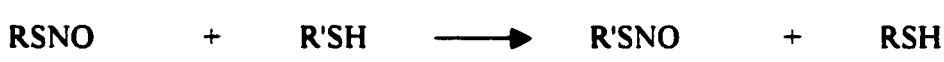

RSNOs have a significantly longer half life than NO (40 min half life) (Upchurch *et al.*, 1995), they are known to stabilize NO and potentiate its biological effects *in vivo*. Under certain conditions, these S-nitrosothiols can be unstable, thus easily decompose thermally (Williams *et al.*, 1996) or photochemically (Sexton *et al.*, 1994) to give nitric oxide and disulfide.

UV-visible light treatment results in homolytic cleavage of the sulfur-nitrogen bond, leading to the release of NO and a thiyl radical ($RS^{\bullet}$) (Singh *et al.*, 1995). The decomposition pathway as shown by Wood *et al.* (1997) (Scheme 3).

$$RSNO \xrightarrow{h\upsilon\ (355\ nm)} RS^{\bullet} + NO^{\bullet}$$

$$RS^{\bullet} + RSNO \longrightarrow RSSR + NO^{\bullet}$$

$$RS^{\bullet} + O_2 \longrightarrow RSOO^{\bullet}$$

$$RSOO^{\bullet} + RSNO \longrightarrow RSSR + NO^{\bullet} + O_2$$

(Scheme 3)

Unlike the photolytic release of NO from S-nitrosothiols (Sexton *et al.*, 1994), thermal decomposition of RSNO has been shown to be dependent on the presence of copper catalyst (Williams *et al.*, 1996).

Scheme 4 shows the thermal decomposition of RSNO in the presence of copper (Williams 1996).

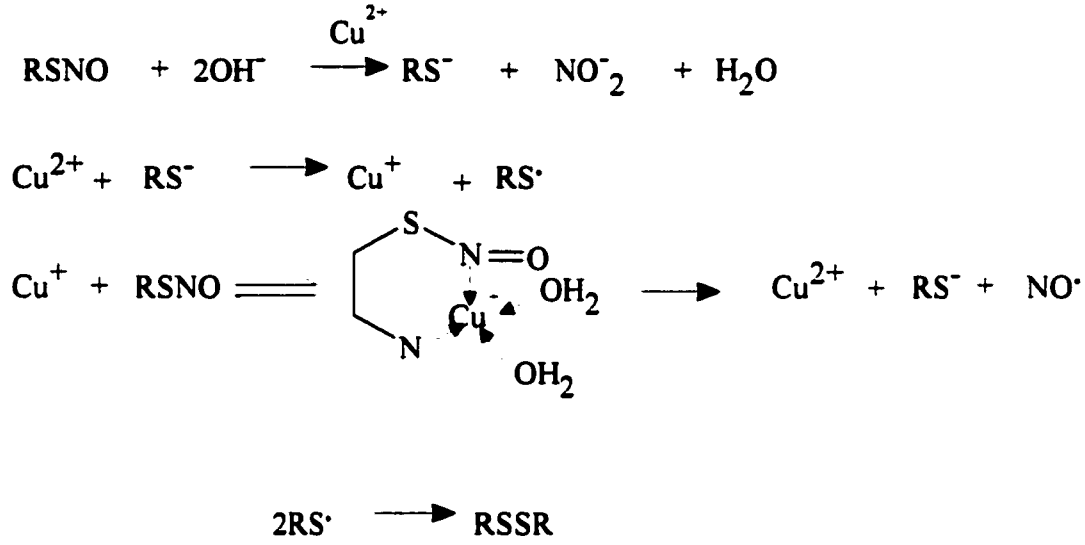

(Scheme 4)

It is believed that in the presence of an oxidizing agent such as hydrogen peroxide, Cu^{+} can be oxidized back to Cu^{2+} through an intermediate RSNOCu^{+} ring. This intermediate can therefore be a 6 or 5 member ring as it is the case for cysteine-NO (CysNO) and GSNO; whereas when an unstable 7 member ring is formed, the rate will be reduced to zero as is the case for homocysteine-NO (HcysNO) (Williams *et al.*, 1996).

1.2.3 Peroxynitrite

1.2.3.1 Peroxynitrite production

Peroxynitrite ($ONOO^-$) is a powerful oxidant with cytotoxic properties and a half life of 1 s at physiological conditions (Pryor *et al.*, 1995; Beckman *et al.*, 1990). It is formed by the rapid reaction of nitric oxide (NO) and superoxide anion ($O_2^{-\bullet}$) with a rate constant near the diffusion controlled limit ($4\text{-}7\times10^9\ M^{-1}s^{-1}$) (Huie *et al.*, 1993).

$$NO^{\bullet} + O_2^{-\bullet} \longrightarrow ONOO^-$$

Peroxynitrite formation has also been proposed via the reaction of NO with hydrogen peroxide in the presence of catalytic amounts of Fe^{3+}. Two possible routes for $ONOO^-$ production have been proposed (Farias-Eisner et al, 1996) (Scheme 5):

$$NO + Fe^{3+} \longrightarrow [Fe^{3+}\text{-}NO \longleftrightarrow Fe^{2+}\text{-}NO^{\bullet}]$$

$$Fe^{2+} + H_2O_2 \longrightarrow Fe^{3+} + HO^- + HO^{\bullet}$$

$$[Fe^{3+}\text{-}NO \longleftrightarrow Fe^{2+}\text{-}NO^{\bullet}] + H_2O_2 \longrightarrow Fe^{2+} ONOO^- + 2H^+$$

or:

$$HO^{\bullet} + H_2O_2 \longrightarrow H_2O + {}^{\bullet}OOH$$

$$NO + {}^{\bullet}OOH \longrightarrow ONOO^- + H^+$$

(Scheme 5)

In alkaline solutions, $ONOO^-$ is quite stable. However, at neutral pH peroxynitrite (pKa 6.8) is partly protonated and can form peroxynitrous acid, which rapidly decomposes to H^+ and NO_3^- at a rate of 1.3 s^{-1} at 25°C (Koppenol *et al.*, 1992). This occurs through an intermediate complex possessing characteristics of both nitrogen dioxide ($NO_2^\bullet$) and hydroxyl radical ($OH^\bullet$).

Peroxynitrite can exist as cis and trans isomers, where the cis- conformation has proven to be more stable than the trans-isomer. The isomerization to nitrate is thought to require a conformational change to the trans form (Crow *et al.*, 1994).

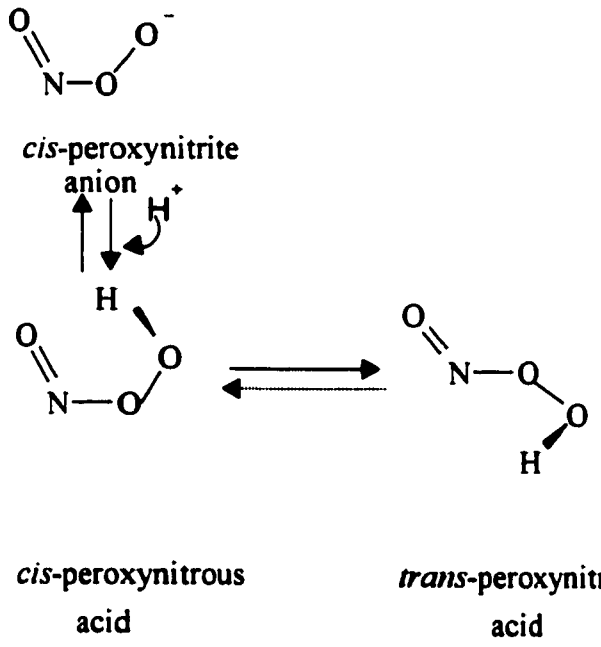

Figure 1.3- Peroxynitrite isomerization (Beckman *et al.*,1996)

In proteins, peroxynitrite decomposition most commonly leads to the nitration of tyrosine (Tyr) and phenylalanine (Phe) side chains as well as the oxidation of tryptophan (Trp) (Ischiropoulos *et al.*, 1995). It has been proposed that a transition metal catalyzes tyrosine nitration by $ONOO^-$ due to formation of an intermediate characteristic of nitronium ion (NO_2^+) (Beckman *et al.*, 1996).

$$ONOOH + H^- \longrightarrow ONOOH_2^- \longrightarrow NO_2^{\cdot} + H_2O$$

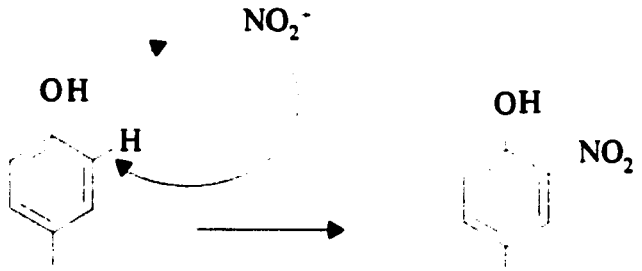

Figure 1.4- Nitration of a tyrosine residue (Beckman *et al.*, 1996)

$NO_2^{\cdot}$ is responsible for nitration (Ramezanian *et al.*, 1996), where a nitro group is added to the ortho position of the phenolic ring of free and protein-associated tyrosines to form 3-nitro-L-tyrosine.

1.2.3.2 Peroxynitrite mediated cell damage

Originally, the formation of $ONOO^-$ was thought to protect against NO mediated cell damage, since it can act as an oxygen radical scavenger. Now it is known that much of the NO-related injury is due to the generation of peroxynitrite (Szabo *et al.*, 1996). The formation of peroxynitrite has a toxic effect on cells. It can inhibit mitochondrial electron transport and respiration, with a negative effect on cellular energy production (Szabo *et al.*, 1996). Moreover it also has the ability to cause mitochondrial calcium efflux (Packer *et al.*, 1995), resulting in calcium overload and eventually cell death. Similarly, peroxynitrite is a potent initiator of DNA damage through mutations caused by oxidation of guanine to nitroguanine (Szabo *et al.*, 1997). Peroxynitrite formation has been detected in activated macrophages and other cells associated with eucaryotic defense mechanisms which can generate both NO and superoxide in large amounts (Radi *et al.*, 1991; Ischiropoulos *et al.*, 1992).

The mode of cell death caused by peroxynitrite is not yet clear. Peroxynitrite was demonstrated to cause apoptosis in primary cultured rat thymocytes (Salgo *et al.*, 1995), HL-60 human leukemia cells (Lin *et al.*, 1995), and in neuronal PC12 cells (Estevez *et al.*, 1995) by non-specifically breaking DNA strands (Zingarelli *et al.* and Szabo *et al.*, 1996). However, it was ineffective in inducing apoptosis in other cell types, such as umbilical cord endothelial cells and normal blood monocytes (Lin *et al.*, 1995).

1.3 Metallothionein

Metallothioneins (MTs) are a class of low molecular weight (6,000-7,000 Da) metal-binding proteins (Kagi *et al.*, 1987). As the name implies, MTs contain numerous thiol groups, owing to their high cysteine content (20 out of 61 amino acid are cysteine residues), which provide the basis of high affinity binding of metal ions such as Cu, Zn, Cd, and Hg (Kagi *et al.*, 1979). MTs are ubiquitous in nature, but lack aromatic and histidine residues (Munger *et al.*, 1985). MT is known to play a role in both essential metal homeostasis and resistance to heavy metal toxicity (Hamer *et al.*, 1986), and because of its high cysteine content, it tends to bind and inactivate a variety of radicals (Cherian *et al.*, 1993).

Five major MT isoforms are identified in humans (Suzuki *et al.*, 1993). Metallothionein has a half-life of ~15-25 h in eucaryotic cells (Kershaw *et al.*, 1992). Metals can be stripped from metallothionein to form apometallothionein (thionein). Thionein is known to be 1500 times more susceptible to proteolytic degradation than metallothionein (Moffatt *et al.*, 1997). Due to its high cysteine contents each thionein molecule has the potential to carry up to 20 nitric oxide molecules upon transnitrosation with excess S-nitrosothiols.

1.4 Dendrimers

1.4.1 Starburst Polyamidoamine (PAMAM) Dendrimers

Starburst polyamidoamine (PAMAM) dendrimers, are structurally defined, spherical macromolecules composed of repeating polyamidoamino subunits, (Qin *et*

al., 1998). These macromolecules, available in commercial quantities, possess known molecular weights, dimension, and number of terminal functional groups depending on the generation of the dendrimer (Tomalia *et al.*, 1990; Roberts *et al.*, 1990).

The major structural differences in PAMAM dendrimers relate to the core molecule. There are two series, N series using ammonia (NH_3) as a trivalent initiator core or E series using ethylenediamine as a tetravalent initiator core (Kukowska *et al.*, 1996). The core molecules can then react in sequence first with methylacrylate and then with ethylenediamine to form a generation zero (G0) dendrimers. Each free amino group can subsequently react with two additional molecules of methylacrylate monomer, then with two more ethylenediamine molecule to form generation one (G1).

This two step reaction sequence is repeated to provide subsequent generations of these polymers. Thus each generation has a defined molecular weight and a known number of terminal functional groups (Fig. 1.5; table 1.1). (e.g generation 3 (E series) has a molecular weight of 6,909 and 32 terminal amino groups) (Singh *et al.*, 1994).

1.4.2 Dendrimer-thiols conjugations

Since their synthesis was first reported by Tomalia (Tomalia *et al.*, 1990), dendrimers have been used in various applications. Dendrimer-antibody conjugates have been used as enhancers for immunoassay sensitivity (Singh *et al.*, 1994), as

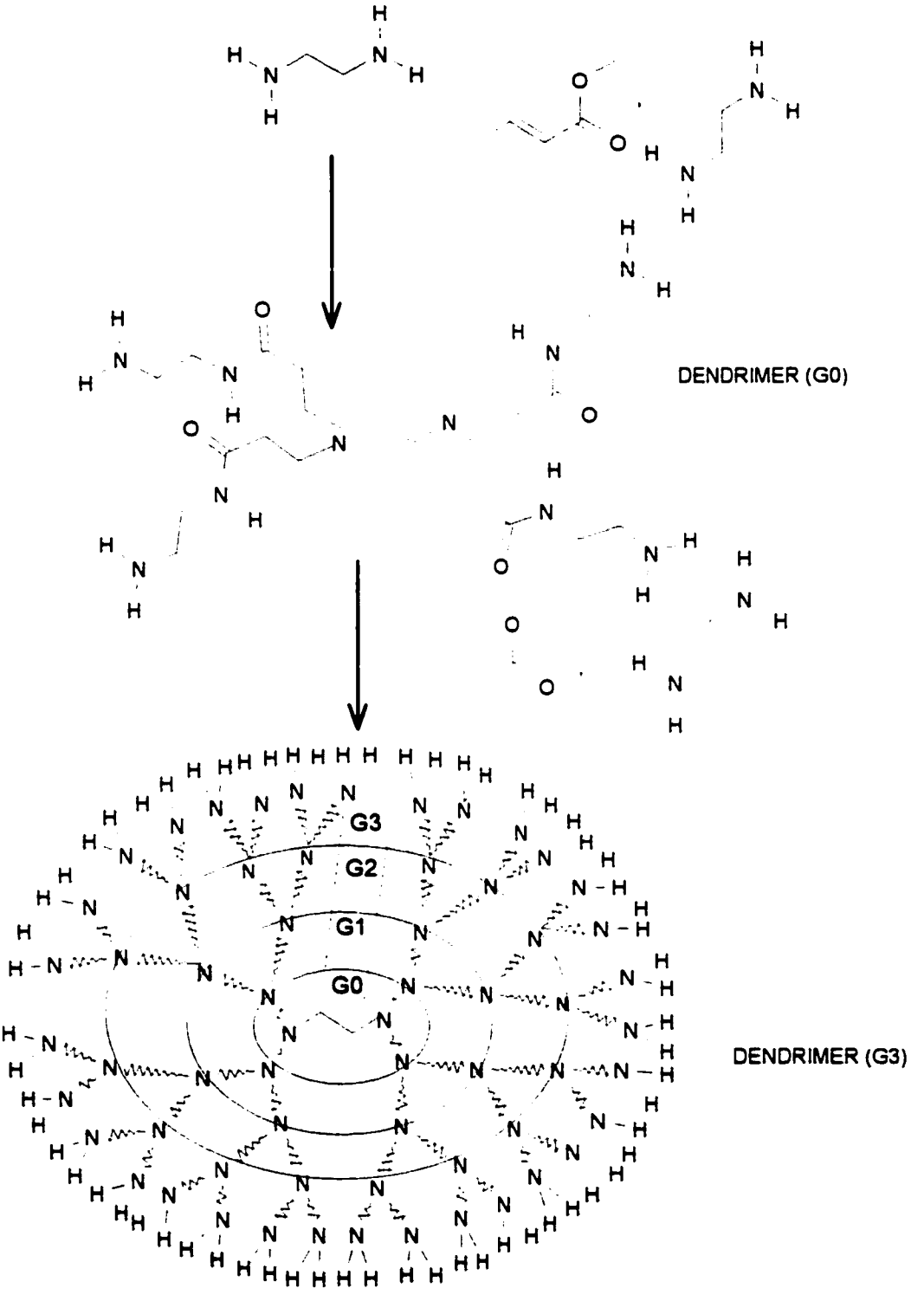

Figure 1.5- Schematic representation of Starburst Dendrimer synthesis.

Table 1.1: Characteristics of Starburst Dendrimers (generations 1-5).

GENERATION	TERMINAL GROUPS	M. W.
0	4	516.69
1	8	1429.88
2	16	3,256
3	32	6,909
4	64	14,215
5	128	28,947

potential delivery system for neutron capture therapy (Barth *et al.*, 1994), as carriers of regulatory nucleic acids for the suppression of gene expression (Bielinska *et* al., 1996) and as a linker for radiolabelled antibodies therapy (Roberts *et al.*, 1990).

Dendrimers can easily be coupled to thiol groups (e.g. glutathione, cysteine, homocysteine) via the reaction with 1-ethyl-3-[3'-(dimethylamino) propyl]carbodiimide (EDAC) in the presence of N-hydroxysuccinimide (NHS) (Fig.1.6). This method involves the initial activation of the carboxylate group of the thiol followed by coupling to terminal amino groups on the dendrimer. The other crosslinker used is N-Succinimidyl 3-(2-pyridyldithio)propionate (SPDP), it reacts directly with dendrimer (Fig. 1.7).

1.5 Application of PDT in Glaucoma filtration surgery

1.5.1 Glaucoma

Glaucoma includes a complex of disease entities that have in common an increase in intraocular pressure sufficient to cause degeneration of the optic disk and defects in the visual field. It is a prevalent disease affecting approximately 0.5-1% of the population (Leske *et al.*, 1979) and is a major cause of blindness (Fig. 1.8). Glaucoma is divided into two major categories, primary and secondary glaucoma.

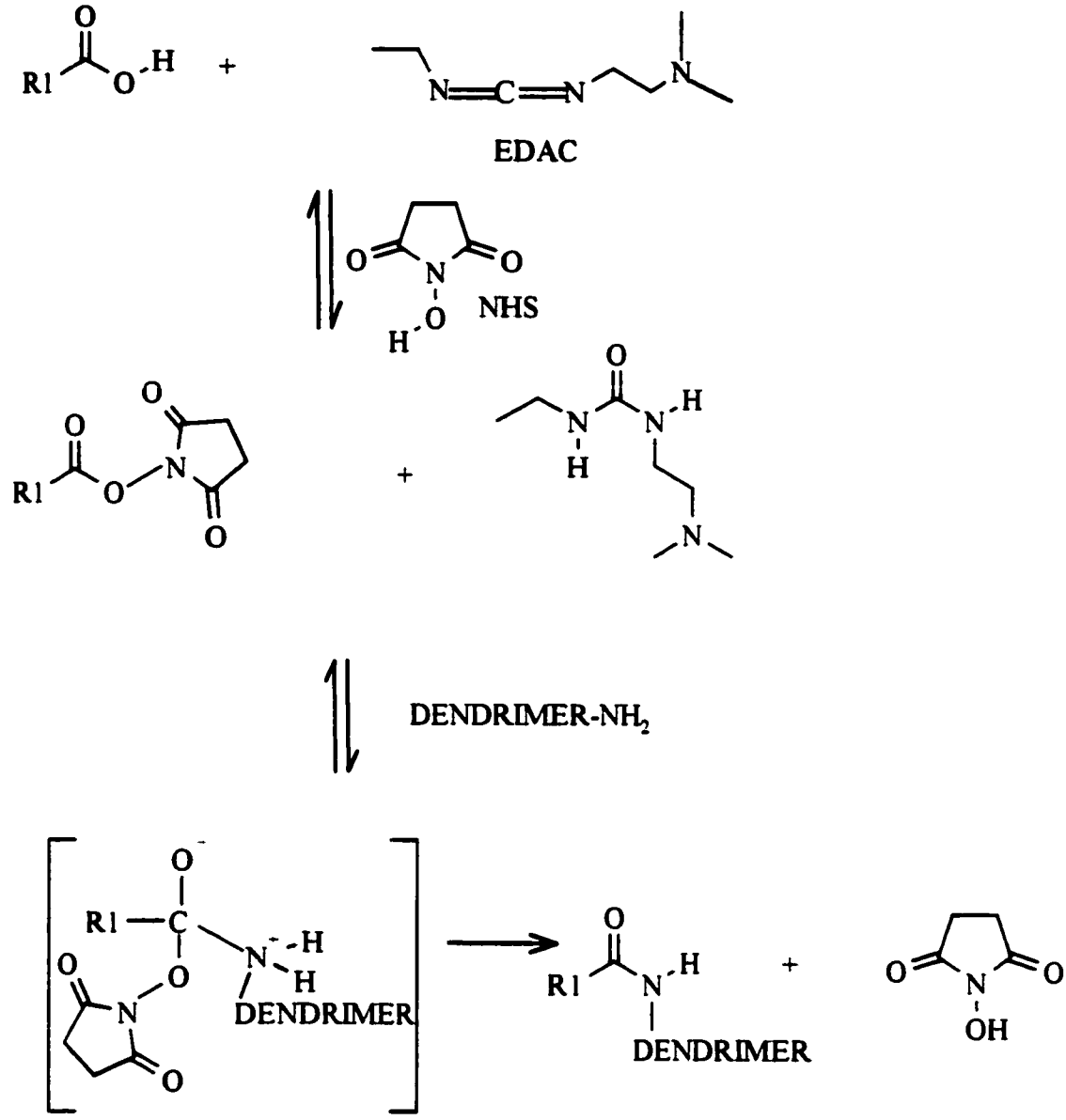

Figure 1.6- Conjugation of dendrimer to thiols via EDAC/NHS.

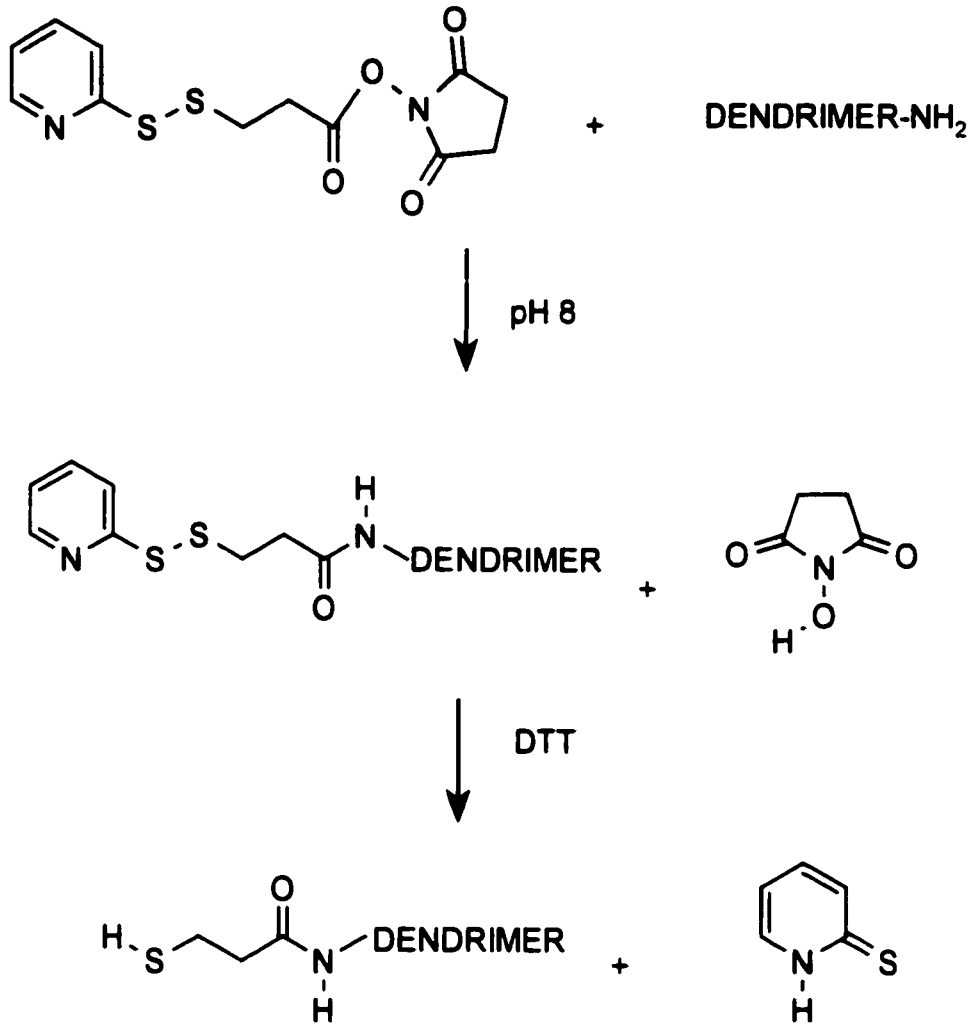

Figure 1.7- Conjugation of dendrimer to SPDP.

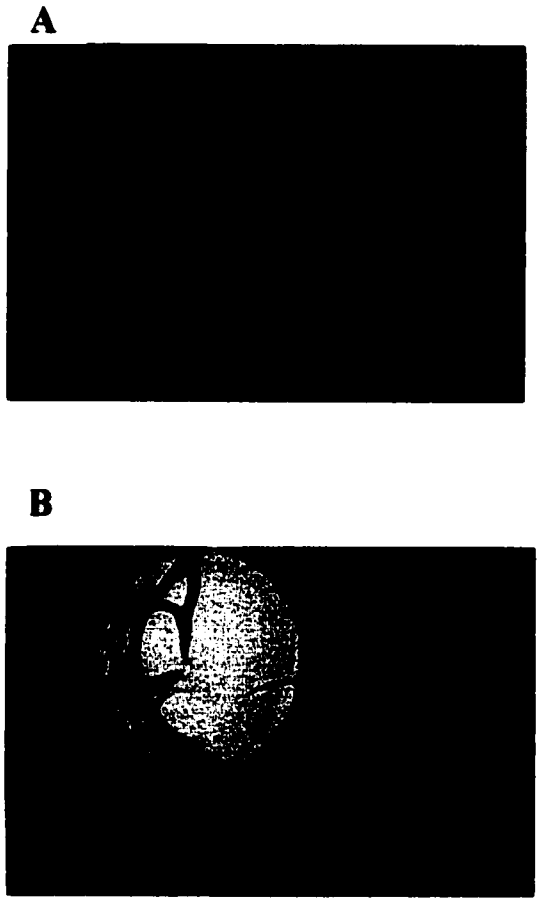

Figure 1.8- Represent a human eye where (A) is normal and (B) is glaucomatous condition.

Primary glaucoma can occur as a slow progressive process with no symptoms or signs until visual impairment occurs or as an acute process with severe pain and sudden visual loss. An increase in intraocular pressure as a result of some other intraocular disease (such as lens dislocations) is known as secondary glaucoma.

1.5.2 Glaucoma treatment

Operative treatment is sometimes indicated in the later stages of glaucoma when medical management is no longer sufficient to control the intraocular pressure. The success of glaucoma filtration surgery (GFS) to lower intraocular pressure is achieved by creation of a functional bleb. Failure is mainly attributed to the exaggerated wound-healing response leading to bleb scarring. Such scarring is more common in younger individuals and those who have had previous ocular surgery. Excessive proliferation of Tenon's Capsule fibroblasts is thought to be the principle mechanism for scar formation (Jampel *et al.*, 1988; Desjardins *et al.*, 1986; Addicks *et al.*, 1983). Recently the success of GFS has been greatly improved by the use of agents that inhibit fibroblast proliferation.

1.5.3 Current therapy post GFS

Current therapies for the prevention of fibrosis after GFS can be effective but often produce unwanted side effects (Gillies *et al.*, 1991). In an attempt to prolong bleb survival, the antimetabolites 5-fluorouracil and mitomycin C have been used to inhibit fibroblast proliferation and hence modulate the wound healing response

(Kitazawa *et al.*, 1991). Although the use of these antimetabolites has improved the success rate of filtration surgery, the risk of vision-threatening complications has also increased. Mitomycin C in particular has been associated with cystic bleb formation, unwanted wound leaks, chronic hypotony maculopathy and bleb-related endophthalmitis (Zacharia *et al.*, 1993; Greenfield *et al.*, 1996) with loss of vision and toxicity of the corneal epithelium. The rather imprecise delivery system and lack of identification of precise treatment parameters (Megevand *et al.*, 1995) have been recognized as further limitations in the use of these antimetabolites.

1.5.4 PDT effect in Ocular fibroblasts

Photodynamic therapy (PDT) is a relatively selective method of treating actively proliferating and malignant tissues by the localized application of light. Pretreatment of the tissues with photosensitizing agent results in the photochemical generation of highly reactive oxygen-related intermediates that produces cytotoxicity. Despite the common demonstration of a distinct antifibrotic effect of PDT (Noodt *et al.*, 1996; Berg *et al.*, 1996; Krammer *et al.*, 1996), few reports have examined the effects on ocular fibroblasts. Smyth *et al.* (1993) demonstrated that although the haematoporphyrin derivative (HPD) photosensitizing agent was absorbed by human subconjunctival fibroblasts and produced a certain dark toxicity, a specific phototoxic effect could not be demonstrated.

1.5.5 Aminolevulinic acid (ALA)

Aminolevulinic acid (ALA) is formed from glycine and succinyl coenzyme A (CoA). ALA itself is not a photosensitizer (Kennedy *et al.*, 1990), but is the metabolic precursor of the endogenous photosensitizer protoporphyrin IX (PpIX) in the biosynthetic pathway to heme (Fig.1.9). The synthesis of ALA is normally tightly controlled by feedback inhibition of ALA synthetase, presumably by intracellular heme levels.

ALA dehydratase induces the condensation of two molecules of ALA to yield porphobilinogen (PBG) with the elimination of two water molecules. The combined PBG deaminase and uroporphyrin III (co)synthase located in the cytosol, yield uroporphyrinogen III. A series of decarboxylations and oxidations have to take place before protoporphyrin (PpIX) is formed. The tetrapyrrole structure is now ready for the incorporation of iron by ferrochelatase to yield heme (Peng *et al.*, 1997) (Fig. 1.9).

ALA based photochemotherapy is presently being employed in the treatment of thin basal cell carcinomas in many countries. It is a simple and inexpensive form of treatment with curative rates comparable to those of established therapy modalities. Experimentally, a number of other malignant lesions accessible by light via optical fibers are being treated (Moan *et al.*, 1998).

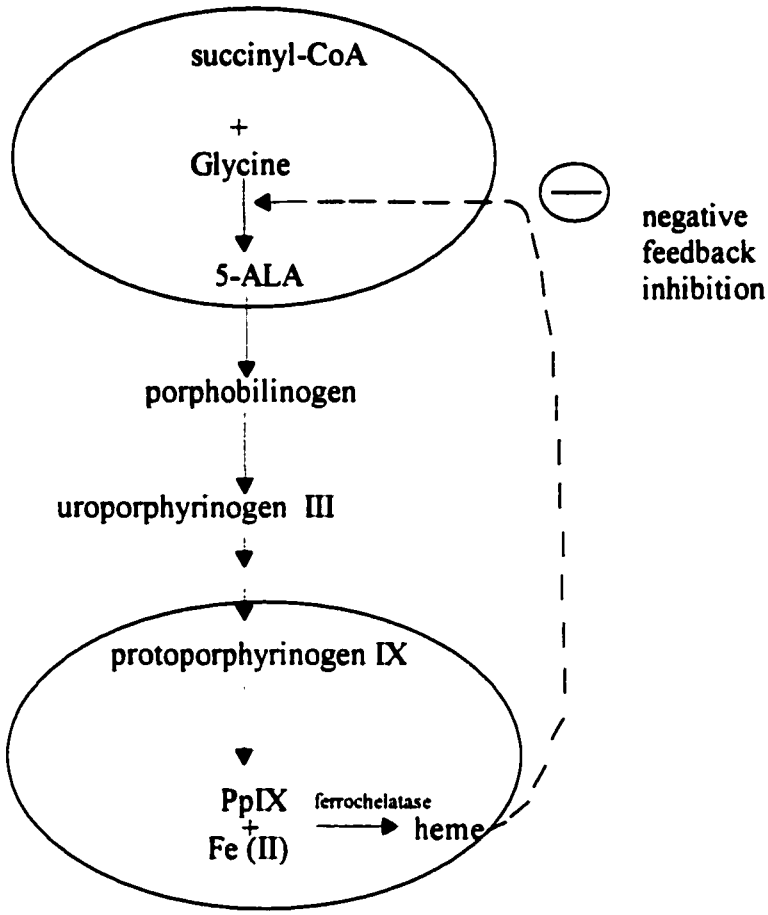

Figure 1.9- Synthesis of heme. Mitochondria are indicated as circles and the cytosol as a white area (Peng *et al.*, 1997).

Due to the hydrophilic properties of ALA, ALA-PDT may clinically be limited by the rate of ALA uptake into cells (Gaullier *et al.*, 1997) and its penetration through the tissue (Caimduff *et al.*, 1994; Wolf *et al.*, 1993). The primary site of photodamage was suggested to be the mitochondria where swelling and disruption of the cristae are observed (Iinuma *et al.*, 1994). However it has been suggested that ALA-induced PpIX may also be located in other subcellular organelles (Gaullier *et al.*, 1995).

A crucial point for the success of ALA-PDT is a low ferrochelatase activity. The use of Desferal (DEF) as an adjuvant therapeutic strategy has been shown to increase PpIX accumulation in cells and improve the phototoxic effect (Iinuma *et al.*, 1994). Desferal is an iron chelator that blocks ferrochelatase, the enzyme necessary for the conversion of PpIX to heme.

Aminolevulinic acid is unique compared with other photosensitizers because of its capacity for specific photosensitization of epithelial cells, its existence in biological pathways, and the possibility of its topical, systemic, or oral application. The main advantages of using ALA to induce PpIX photosensitization, is the rapid clearance of the sensitizer (1-2 days), which allows a repeated treatment in short time intervals. However, most investigators reported patient discomfort such as strong itching, stinging, prickling, or burning sensations during the period of light irradiation only (Caimduff *et al.*, 1994).

1.5.6 GSNO

Glutathione (L-γ-glutamyl-L-cysteinylglycine) (GSH) is a low molecular weight thiol present in millimolar levels intracellularly (0.5-10mM). It is easily reacted with $NO^{\cdot}$ to produce S-nitrosoglutathione (GSNO) (Fig.1.10). NO donors such as GSNO have been known as a stable reservoirs of NO *in vivo* (Park *et al.*, 1993) and it is the most abundant intracellular S-nitrosothiol. Owing to the fact that GSNO is easily prepared and can carry one NO molecule it is a useful model compound for providing *in vitro* evidence for the toxicity potential of S-NO/PDT.

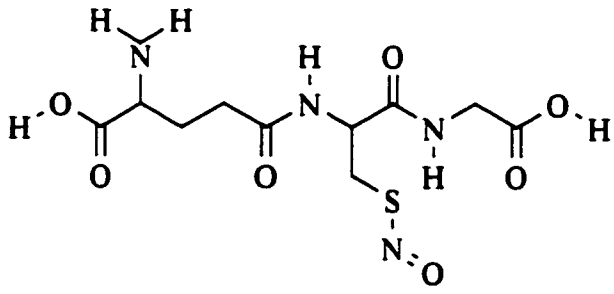

Fig.1.10- Structure of GSNO (Butler *et al.*, 1997)

1.6 Mode of cell death

Generally, both physiological cell death (apoptosis) and accidental cell death (necrosis) can occur following photodynamic therapy. Although in some systems NO effectively causes cell death by necrosis, in others generation of NO initiates apoptosis, accompanied by p53 expression (Messmer *et al.*, 1994)

1.6.1 Apoptosis

1.6.1.1 Indications of Apoptosis

Apoptosis or programmed cell death occurs during normal cell development or as the cellular response to many physiological and biochemical stimuli. Generally, it is a genetically programmed form of cellular suicide where targeted cells are removed from living tissues without causing major tissue damage or inflammation (Liang *et al.*, 1997).

Cells undergoing apoptosis are characterized and distinguished by morphological and biochemical features. They tend to shrink, display surface alterations such as the exposure of molecules normally confined to the interior of the cell such as the appearance of phosphatidylserine on the outer surface (Vanags *et al.*, 1996), membrane blebbing, chromatin condensation and nuclear DNA fragmentation (multiples of 180-200 bp). Eventually, as a result of plasma membrane shrinkage, the apoptotic cell dissociates to form apoptotic bodies (Schwartzman *et al.*, 1993).

1.6.1.2 Regulators of Apoptosis

Recently, several genes that are involved in the regulation of apoptosis were identified and grouped into three broad categories. Among these are genes that primarily suppress apoptosis, such as some members of Bcl-2 gene family, genes that act as effectors of apoptosis, for example, caspases or cysteine proteases related to interleukin-1 β converting enzyme (ICE), and intermediate genes such as p53 tumour suppressor gene (Fig 1.11). For the purpose of this study only Bcl-2 and p53 will be discussed.

Bcl-2 (26 kDa), a protein located mainly on the outer membrane of mitochondria, can protect against apoptosis caused by a variety of physiological and pathological stimuli (Hawkins, 1994). The exact mechanism is not yet clear, but it is believed that Bcl-2 blocks the release of cytochrome *c* from mitochondria (Kluck *et al.*, 1997; Reed, 1994), thus indirectly preventing caspase activation and inhibiting apoptosis. Bax a 21 kDa protein with extensive amino acid homology with Bcl-2 is pro-apoptotic relative which dimerizes with Bcl-2. The balance between Bcl-2/Bax and Bax/Bax dimers determines the fate of the cell (Korsmeyer *et al.*, 1993).

Recent studies have revealed that NO can lead to overexpression of p53 giving rise to apoptosis (Messmer *et al.*, 1994; Sandau *et al.* and Ambs *et al.*, 1997). The p53 (53 kDa) tumour suppressor protein is activated in response to DNA damage. It induces apoptosis through inhibition of Bcl-2 expression (Hale *et al.*, 1996).

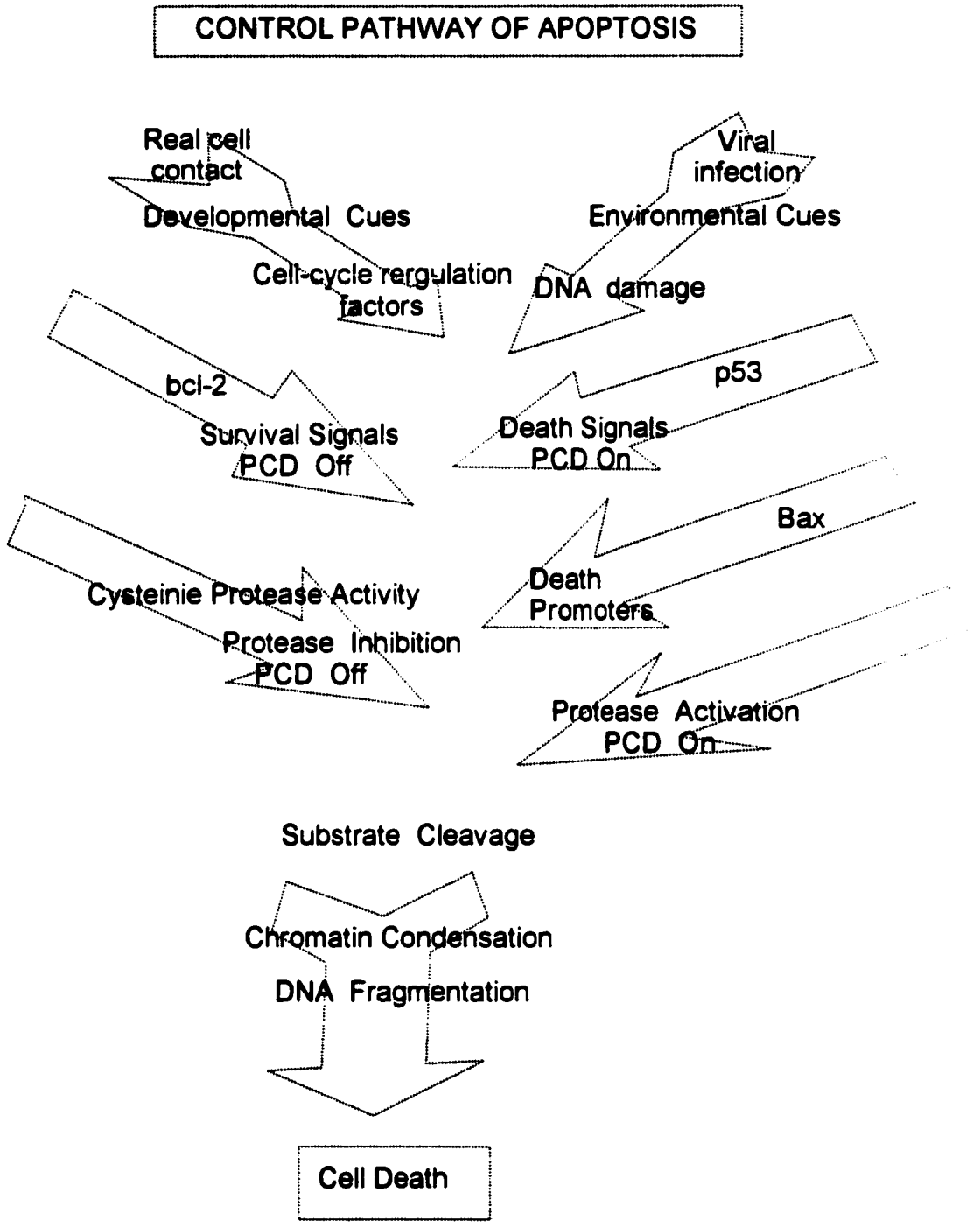

Figure 1.11- Regulation of apoptosis. Abbreviation: PCD (programmed cell death).

1.6.2 Necrosis

Generally, necrosis is the result of physical injury and is not genetically controlled. During necrosis, cells undergo early mitochondrial changes, plasma membrane loses its ability to regulate osmotic pressure causing the cell to swell and burst. Cellular contents are spilled into the surrounding tissue space where they provoke an inflammatory response (Cohen *et al.*, 1996). A cell undergoing necrosis death is characterized by mitochondrial swelling, nuclear flocculation and the loss of plasma membrane integrity leading to uncontrolled cell lysis. Morphological differentiation is shown in Fig. 1.12.

1.6.3 Mode of cell death post PDT

A major discrimination between apoptosis and necrosis is the effect of each cell on its neighbors (Leist *et al.*, 1998). Several reports demonstrated that NO and peroxynitrite either cause acute cell death (necrosis) or delayed cell death (apoptosis) in a variety of cell types (Denicola *et al.*, 1993; Mannick *et al.*, 1994; Estevez *et al.* and Messmer *et al.*, 1995). It appears that sustained exposure or low levels of NO or peroxynitrite cause apoptosis, whereas sudden exposure to high concentration of peroxynitrite or NO results in cell necrosis (Denicola *et al.*, 1993; Estevez *et al.*, 1995). Peroxynitrite has been implicated in cortical neuronal apoptosis (Bonfoco *et al.*, 1995) and as an inducer of apoptosis in various cell lines such as leukemic HL-60 cells (Lin *et al.*, 1997; Troy *et al.*, 1996) and murine leukemia P388 or L1210 cells.

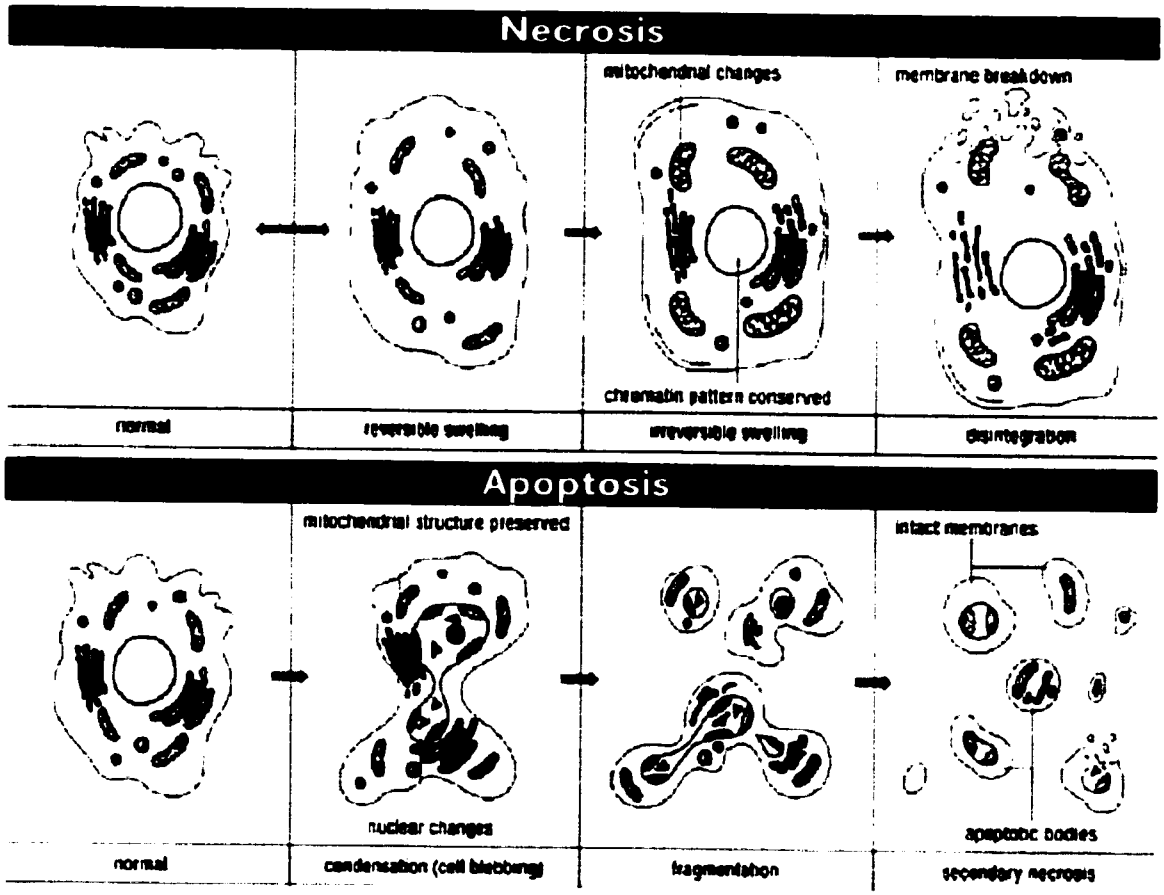

Figure 1.12- Two different types of cell death (Boehringer Mannheim 1998)

1.7 Aims of this study

PDT is a powerful new modality for cancer treatment; however due primarily to the various drawbacks including improper photosensitizers and secondly to the light source, much effort has gone into improving the mode of this therapy. In recent years, new photosensitizers have been developed, but to date there is no ideal photosensitizer. Perhaps then the most challenging problem associated with PDT is the photosensitizer. In this study, we tested a system that has all the advantages of PDT, but lacks the major disadvantages of phototoxicity. We investigated potential NO carriers: metallothionein and thiol-derivatized-Dendrimer. Metallothionein is a low molecular weight protein with high cysteine content.

The apoprotein thionein, has the potential to carry up to twenty NO molecules. Thionein-NO was toxic toward cancer cells in culture, but the problems encountered in metallothionein purification render it unfavorable to be used in a routine therapeutic method. Thus we became interested in exploring the use of commercially available compounds that could act as NO carriers with minimum chemical modification. The compound of choice was Starburst PAMAM Dendrimers (Generation3) which contain defined numbers of amino groups (32) on the surface of the polymer. The amino functionality can be easily coupled to thiols containing amino acids and peptides. Dendrimer NO-derivatives were made and their potential use in S-NO-PDT was fully explored.

Besides the significant interest in the potential role of NO as phototoxic agent for cancer treatment we wanted to further explore the use of S-NO/PDT, on non-cancerous cells. To this end we investigated the potential use of PDT as a treatment

for fibrosis post glaucoma filtration surgery. We compared the novel application of S-nitrosoglutathione photolysis to the well characterized porphyrin precursor 5-aminolevulinic acid in achieving *in vitro* antiproliferation of both standard Hamster lung and human Tenon's capsule fibroblasts.

Although S-NO-PDT is shown to be toxic to cells, neither the mechanism nor the mode of the cell death is yet clear. There are many morphological differences between an apoptotic and a necrotic cell death. These differences make apoptosis the preferred mode of cell death. Thus the aim of this final step was to examine the mode of cell death post S-NO/PDT.

CHAPTER 2

MATERIALS

The following materials are used throughout the course of this study.

2.1 Chemicals, Biochemicals and supplies

- Rabbit liver was obtained from local slaughter house.
- Diethylaminoethyl cellulose (DEAE), Sephadex G-25 and G75, gelatin, Triton X-100, Trizma hydrochloride, dithiothreitol, glutathione, 5-aminolevulinic acid, dansyl chloride, Dulbecco's phosphate buffered saline, antibiotic antimycotic, glucose oxidase, catalase were obtained from Sigma (St. Louis, MO).
- [^{3}H]-glutathione were obtained from Mandel Scientific Company Ltd. (Quelph, ON).
- Developer and fixer for hyperfilm were purchased from Kodak Canada (Toronto, ON).
- Metallothionein monoclonal mouse antibody was obtained from Dako Corporation (Carpinteria, CA).
- SDS-PAGE molecular standards, Tween-20, protein assay dye reagent were obtained from Bio-Rad Laboratories (Hercules, CA).
- L-15 and DMEM medium, fetal bovine serum, Trypsin/EDTA, trypan blue were obtained from GIBCO (Grand Island, NY).

- Human colon adenocarcinoma cells (SW-948, Batch F-12139), V-79 Chinese hamster lung fibroblast (CCL-93), Hep G2 human hepatocellular carcinoma cells were obtained from the American Type Culture Collection (Rockville, MD).
- MCF-7 human breast cancer cell line was obtained from Dr. M. Dufresne (Department of biological science, Windsor, ON).
- Human Tenon's capsule fibroblasts were obtained from Dr. Hutnick (Victoria Hospital, London, ON).
- Cells were grown in 25 cm^2 polystyrene culture flasks obtained from Corning (Corning, NY).
- Disposable 3 and 10 cc syringes and disposable 10 mL graduated, plugged polystyrene serological pipettes by Falcon were obtained from Dickinson Labware (Lincoln Park, NY).
- Sterile cell scrapers were obtained from Sarstedt (Newton, N.C).
- Nalgene disposable 25 mm syringe filters (0.2 μm pore size) and disposable glass pasteur pipettes were obtained from Baxter Diagnostics Corp. (Toronto, ON).
- Fluorescein anti-mouse IgG and Vectashield were obtained from Vector Laboratories (Burlingame, CA).
- Dendrimer, EDAC and NHS were obtained from Aldrich (Milwaukee, WI).
- Tissue culture dishes were obtained from Becton Dickenson Labware (Lincoln Park, NJ).

- Square sterile cover slips (22mm), sterile conical 15 mL and 50 mL graduated polypropylene centrifuge tubes and nitrocellulose membrane BA-S-83 were obtained from VWR Scientific Inc. (Mississauga, ON).
- DEF was obtained from Ciba Pharmaceuticals (Mississauga, ON).
- DNA fragmentation and annexin/propidium iodide kits were obtained from Boehringer Mannheim (GmbH, Germany).
- Bcl-2 and p53 antibodies were obtained from Oncogene research Products (Cambridge, MA).
- Hydrogen peroxide and sodium nitrite were obtained from BDH Inc. (Toronto, ON).

All other reagents were of reagent grade or better.

2.2 Equipment

The following is a list of equipment used in the performance of the described experiments:

Amerlite shaker/incubator from Amersham Canada Ltd. (Oakville, ON);

Beckman J-6B centrifuge (Palo Alto, CA);

Beckman LS 6500 multi-purpose scintillation counter, Beckman Instruments Inc. (Mississauga, ON);

Bench top Eppendorf shaker, Brinkmann Instruments Ltd. (Mississauga, ON);

Bio-Rad Econo System (Hercules, CA);

Bio-Rad HPLC system (Hercules, CA);

Bio Rad imaging densitometer model GS-670 (Hercules, CA);

Bio-Rad Mini gel and Trans-Blot electrophoretic apparatus (Hercules, CA);

BioRad MRC 600 and 1024 Confocal Laser Scanning Microscope (Hercules, CA);

Bio-Rad power supply model Power Pac 300 (Hercules, CA);

Brightline Hemocytometer, Reichert-Jung, Hausser Scientific, (Horsham, Pa);

Chemiluminescent NOx analyzer (Thermo Environmental instruments Model 42);

CO_2 free incubator, VWR, (Mississauga, ON);

Eppendorf Model 5415C microcentrifuge from Baxter/ Canlab, Inc. (Mississauga, ON);

Fisher Scientific micro-centrifuge model 59A (Pittsburgh, PA);

Fisher Scientific 10L water bath (Pittsburgh, PA);

Hitachi model F-3010 Spectrofluorometer, Naka Works, Hitachi Ltd. (Tokyo, Japan);

Laminar flow hood, Nuare (Plymouth, MN);

Laser flash photolysis (Continuum, Santa Clara CA);

Lyophilizer Labconco, Model 4451F, Labequip Limited (Markham, ON);

Mettler AJ100 balance, Mettler Instrument Corp. (Hightstown, New Jersey);

Microtiter plate washer, model EAW II from SLT-Lab Instruments, (Groedig/Salzburg, Austria);

Microplate reader. BIO-TEK instruments Inc. (Burlington, Vermont);

Millipore filtration apparatus, Millipore Corp. (Milford, MA);

Nikon TMS-F #210999 light Microscope (Japan);

Nuare Autoflow 5% CO_2 regulated incubator (Plymouth, MN 55447);

Orion 420A pH meter, Orion Research Inc. (Boston, MA);

300 W quartz halogen lamp from an overhead projector;

Shimadzu UV-160 spectrophotometer (Kyoto, Japan);

Waring commercial blender, model 33BL12 (New Hartford, Connecticut);

2.3 Reagents and Buffers

- SW-948 complete culture medium consisted of 90% (v/v) L-15, 10%(v/v) FBS.
- V-79 hamster fibroblast, Tenon Capsule fibroblast, MCF-7 human breast cancer and Hep G2 cells complete culture media consisted of 90% (v/v) DMEM, 10 % FBS, 100 units penicillin G, 0.01% streptomycin, 0.25 μg of amphotericin B.
- Cell freezing media consisted of 10%(v/v) DMSO in complete culture media.
- Homogenizer buffer A consisted of 20 mM Tris-Cl, 250 mM Glucose, 100 mM β-mercaptoethanol, pH 9.3.
- Rabbit inducing solution consisted of sterile saline Buffer (0.1 M Phosphate, 0.15 M NaCl) and 80 mg/mL $ZnCl_2$.
- 10 % SDS gel consisted of resolving and stacking gels.
    - Resolving gel consisted of 1.9 mL H_2O, 11.7 mL of 30% acrylamide mix, 1.3 mL of 1.5 M Tris pH 8.8, 50 μL of 10% SDS, 50 μL of 10 % ammonium persulfate, and 2 μL of TEMED.
    - Stacking gel consisted of: 680 μL of H_2O, 170 μL of 30% acrylamide mix, 130 μL of 1 M Tris pH 6.8, 10 μL of 10 % SDS, 10 μL of 10 % ammonium persulfate, and 1 μL of TEMED.
- TBS consisted of 20 mM Tris, 500 mM NaCl, pH 7.5.
- TTBS consisted of TBS and 0.5 % Tween 20.
- Gel running buffer consisted of 15 g/L Tris, 72 g/L glycine, 5 g/L SDS, pH 8.3.
- Transfer buffer consisted of 25 mM Tris base, 192 mM glycine, 20% methanol.

- Blocking buffer consisted of 50 mM Tris, pH 7.4, 0.5 M NaCl and 2 % polyvinylpyrrolidone.
- Color development buffer consisted of 0.1 M Tris, 0.5 mM $MgCl_2.6H_2O$

For DNA fragmentation assay

- Coating buffer is prepared shortly before use, by diluting 0.2 mL of anti DNA antibody with 9.8 mL of 1x coating buffer.
- Blocking buffer consisted of 20 mL of 2x incubation buffer (BSA, EDTA, Tween 20) and 20 mL of distilled Water.
- Stop Solution consisted of 560 µL of H_2SO_4 and 9.40 mL of distilled water.
- Nuclease buffer consisted of 66 mM Tris, 0.66 mM $MgCl_2$, 1 mM β-mercaptoethanol, pH 8.
- Exonuclease III solution consisted of dilution of exonuclease III with 1 x nuclease reaction buffer to a final concentration of 10 U/mL.

CHAPTER 3

METHODS

3.1 Thionein as potential NO carrier for PDT

3.1.1 Metallothionein (MT) purification

3.1.1.1 Extraction of MT

Rabbits were injected subcutaneously with $ZnCl_2$ (100 μg/kg body weight) daily for 7 days in order to induce MT. Rabbit liver (50g) was homogenized in 80 mL of cold (5°C) buffer A (20 mM Tris-Cl, 250 mM glucose, 100 mM β-mercaptoethanol, pH 9.3). The cytosolic fraction (~50 mL) which was obtained by centrifugation was chromatographed on a column of Sephadex G-75 (5 cm x 50 cm) equilibrated with buffer B (Buffer A without glucose). The low molecular weight fraction with characteristic red-orange fluorescence was collected and applied to a column of DEAE-cellulose (2.5 cm x 5 cm) which was then washed with 50 column volumes with buffer B. The crude MT was eluted with a NaCl gradient (0-0.25 M).

3.1.1.2 Western blot analysis to detect the purity of MT

3.1.1.2.1 SDS-PAGE

Sodium dodecyl sulfate polyacrylamide electrophoresis (SDS-PAGE) was performed using mini gels (8 cm x 10 cm). 10 μL of each fraction collected in section 3.1.1.1 was treated with an equal volume of sample application buffer (0.017 M Tris, 1% SDS, 20% glycerol, 4% saturated bromophenol blue and 10% β-mercaptoethanol v/v at pH 6.8). The mixture was boiled for 10 min. 10 μL of the reduced, denatured sample

was applied to 15% SDS-PAGE for electrophoresis at 100 V for 1 hour or until the dye front reached the bottom of the gel.

3.1.1.2.2 Immunoblot Analysis

Resolved protein bands were transferred electrophoretically from 10% SDS-polyacrylamide gels onto a nitrocellulose support medium at 100 V for 60 min using a transfer buffer of 25 mM Tris base/192 mM glycine/20% methanol. The blots were blocked overnight with 50 mM Tris base, pH 7.4 containing 0.5 M sodium chloride (TBS) and 2% polyvinylpyrrolidone. After washing with TBS containing 0.05% Tween-20, pH 7.5, (TTBS) the blots were incubated for one hour with anti-metallothionein (mouse monoclonal IgG) diluted 1:1000 in TTBS. The excess antiserum was removed by 4 x 5 min washings with TTBS. The blots were then treated with a 1:3000 dilution of anti-mouse IgG conjugated to alkaline phosphatase in TTBS for 1 h. After two washes in TTBS, one wash in TBS, bromochloroindolyl phosphate/nitroblue tetrazolium substrate was added to visualize the primary/secondary antibody complexes. Following color development, the blots were washed with distilled water and dried between paper towels.

3.1.2 Apo-Metallothionein preparation

The isolated protein was incubated with 50 μL of TFA for 2 h, 20°C in order to remove the metal ions from MT. The concentration of thionein was determined using its molar absorption coefficient at 214 nm (48,200 M^{-1} cm^{-1}) (Buhler *et al.*, 1983).

3.1.3 Sulfhydryl titration (Ellman, 1958)

Thionein (~20 mg in 5.0 mL Buffer B) was incubated overnight with dithiothreitol (DTT) (50 mg) at 5°C. Excess DTT was removed by chromatography on a column (1.5 cm x 20 cm) of Sephadex G-25 (superfine). The Ellman's reagent was used to determine the free thiol concentration in the thionein by using 5,5'-dithio-bis-2-nitrobenzoic acid (DTNB) in 100 mM Tris, 1 mM EDTA, pH 7.5 and using ε_{412} =13,600 M^{-1} cm^{-1} (Ellman, 1958).

3.1.4 GSNO Synthesis (Hart 1985)

GSNO was prepared by adding 0.345g of sodium nitrite to an ice-cold mixture consisting of 1.5g of GSH in 8 mL of H_2O and 2.5 mL of 2 M HCl. After the entire mixture was stirred at 4°C for 40 minutes, 10 mL of acetone was added followed by an additional 10 minutes stirring. Using a vacuum filtration system, the pink precipitated product was then collected and lyophilized after several washes with ice cold H_2O (5x 1 mL), acetone (3x 10 mL), and diethyl ether (3x 10 mL). The final product was dried in the dark and quantified using ε_{545} = 15.9 M^{-1} cm^{-1} then stored in the dark at 4°C until further use (Hart 1985).

3.1.5 T-NO synthesis

T-NO was formed by incubating the thionein solution (in 100 mM Tris-Cl, pH 8.0), with 100-fold molar excess (over free thiols) of S-nitrosoglutathione (GSNO) for 30 min at room temperature. The excess GSNO was removed by chromatography on a column (1.5 cm x 20 cm) of Sephadex G-25 (superfine) equilibrated with 100 mM Tris-

Cl, pH 8.0. T-NO was protected from light by aluminum foil. The molar extinction of thionein NO was estimated, where the absorbance of T-NO (334 nm) was divided by the product of free thiols/ T (determined by Ellman's reagent and the extinction coefficient of T (214 nm)) and [T-NO] ([T-NO]= [T] x dil factor in G-25 chromatography).

$$E_{334nm} = \frac{A_{334\,nm}}{\frac{\text{mol SH}}{\text{mol T}} \times [T-NO]\frac{(mol)}{L}}$$

The molar absorption of thionein S-NO estimated by this procedure was 1,820 M^{-1} cm^{-1} at 334 nm.

3.1.6 Preparation of oxyhemoglobin

Oxyhemoglobin was prepared according to Murphy and Noack (1994). Human hemoglobin (30 mg) was reduced by incubation with excess sodium dithionite (60 mg) followed by separation using Sephadex G-25 column equilibrated and eluted with degassed H_2O. The concentration of oxyhemoglobin was determined spectrophotometrically at 425 nm using ε=131 mM^{-1} cm^{-1} (Murphy *et al.*, 1994)

3.1.7 Measurement of photolytic NO-release from T-NO by flash photolysis

The laser flash photolysis apparatus was essentially as described in Krieg *et al.*(1993) and Aveline *et al.* (1993). The excitation source was the frequency-tripled output of a Quantel YG660A Nd/YAG laser at 355 nm (pulse duration of 10 ns, 620 μJ/pulse). A solution containing T-NO (1.2 μM) plus oxyhemoglobin (10 μM) in sodium phosphate (100 mM, pH 7.4) was exposed to five 3.3 mJ pulses. The change in

absorbance (425 nm and 405 nm), subsequent to each pulse, was monitored as a function of time.

3.1.8 Measurement of photolytic NO-release of T-NO by direct measurement on an NO_x analyzer

T-NO (1.2 μM total volume 1.0 mL) was placed in a glass screwcap test tube 15 mL) fitted with a rubber septum which was equilibrated with N_2 gas. The headspace gas was withdrawn with a gas tight syringe (25 mL) and directly injected into a chemiluminescent NO analyzer (Thermo Environmental instruments Model 42). The gas withdrawn was replaced with N_2 and NO measurement was obtained.

3.1.9 The stability of T-NO to transnitrosation by other thiols

T-NO (22.3 μM) was incubated with 1 mM of each of the thiols GSH, L-Cys , β-mercaptoethanol in the dark. The transnitrosation rate constants were then estimated by monitoring the decrease in the thionein-S-NO absorbance at 334 nm as a function of time.

3.1.10 Cytotoxicity effect of T-NO/PDT on SW 948 Colon adenocarcinoma cells in culture

3.1.10.1 Culturing cells

The human colon adenocarcinoma cells SW 948 (batch F-12139) were thawed by rapid agitation and immediately washed with cultured medium consisting of 90% Leibovitz's L15 medium (Gibco) plus 10% heat-inactivated fetal bovine serum. Cells

were pelleted by centrifugation at 300x g for 5 min, resuspended in 3 mL of cultured medium, and pipetted into a single 25 cm^2 culture flask. The cells were grown as a monolayer in a CO_2 free incubator with atmospheric air at 37°C. The culture medium was replaced with fresh medium every 2-3 days depending on the cell density.

3.1.10.2 Subculturing and freezing cells

SW 948 cells were grown in Leibovitz's L-15 medium, 90%; fetal bovine serum, 10%; antibiotic-free. Once they became confluent, the expired medium was aspirated and the cells were detached using 0.25% trypsin, 0.03% EDTA for 15 min at 37°C, resuspended in fresh media and centrifuged twice. They were then transferred to four sets of 12-well plates at a final concentration of 1,210,000 cells/mL. To store cells for later use, cell pellets were resuspended in freezing media consisting of 95% cultured media and 5% DMSO at a minimum density of $1x10^6$ cells/mL and alliquoted into 1 mL cryogenic vials. Vials were immediately stored at -20°C for 1 hour in an upward position then transferred to -80°C until further use.

3.1.10.3 The effect of glucose oxidase on cells in culture

Trypsinized SW 948 cells were transferred onto 15 separate wells (12-well plates) at a final concentration of 1,810,000 cells/mL where they were exposed to 5 different treatments: 1-GOD (50 mg/mL), 2- GOD (5 mg/mL), 3-GOD (0.5 mg/mL), 4-GOD (0.05 mg/mL), 5- control. Samples where then incubated at 37°C in a 5% CO_2 incubator and cell viability was monitored for 24 h using trypan blue dye.

3.1.10.4 The effect of various T-NO concentrations on cells in culture

Trypsinized SW-948 cells were transferred onto separate wells at a confluence of 205,000 cells/mL, then they were exposed to 4 different treatments: 1-T-NO (300 μM),

2- T-NO (30 μM), 3- T-NO (3 μM), 4-Control (cells in media). One set of each treatment was exposed to light (10 cm above *InFocus ®* overhead projector) for 1 hr while the second set was protected from light but kept at the same conditions. All samples were then incubated at 37°C in a 5 % CO_2 incubator and monitored for 24 h.

3.1.10.5 Cytotoxicity effects of combined T-NO and GOD on cells in culture

Trypsinized cells were transferred to four sets of 12-well plates at a final concentration of 1,210,000 cells/mL. Then exposed to one of the following treatments, using (+/-) catalase (1 mg/mL) in each treatment, (in triplicate, total volume 1.0 mL): treatment 1- T-NO, (60 μM); treatment 2- T-NO, (60 μM); GOD, (10 mg/mL); treatment 3- GOD, (10 mg/mL); 4- control- cells in 1.0 mL of medium. Two sets were covered with aluminum foil, the other two sets were exposed to light (10 cm above *InFocus ®* overhead projector) for 60 min, both placed in a 37°C incubator. The dark and the light-exposed samples were monitored for cell viability at 1 and 72 h after exposure to the various treatments.

3.1.10.6 Cell viability Assay

Following treatment, cells were scraped gently using a cell scraper, an aliquot of the suspended cells was diluted 2 fold with trypan blue dye and placed on a hemocytometer grid. The cells in the outer 4 corners were counted and an average cell number/square was obtained. This value was then divided by the volume of the total square (1 mm x 1 mm x 0.1 mm = 1 x 10^{-4} mL) and multiplied by the dilution factor of 2 to give the number of cells/mL.

3.1.11 Measurement of peroxynitrite formation by monitoring nitration of tyrosine

3.1.11.1 SDS-PAGE

Four 1.0 mL samples of L-15 medium containing BSA, (3 mg/mL) T-NO, (10 μM); glucose oxidase (1.65 mg/mL) were made. To two of these samples 1.25 mg/mL of catalase, was added. Two samples, one with catalase and one without, were exposed to light from an overhead projector for one hour while the other two (± catalase) were protected from light. 20 μL of each sample was treated with an equal volume of sample application buffer (0.017 M Tris, 1% SDS, 20% glycerol, 4% saturated bromophenol blue and 10% 2-mercaptoethanol v/v at pH 6.8). The mixture was boiled for 10 min. 10 μL of the reduced, denatured sample was applied to 10 % SDS-PAGE for electrophoresis at 100 V for 1 hour or until dye front reached the bottom of the gel.

3.1.11.2 Immunoblot analysis

Resolved protein bands were transferred electrophoretically from 10% SDS-polyacrylamide gels onto nitrocellulose support medium at 50 V for 30 min using a transfer buffer of 25 mM Tris base/192 mM glycine/20% methanol. The blots were blocked overnight with 50 mM Tris base, pH 7.4 containing 0.5 M sodium chloride (TBS) and 2% polyvinylpyrrolidone. After washing with TBS containing 0.05% Tween-20, pH 7.5, (TTBS) the blots were incubated for one hour with anti-nitrotyrosine (rabbit monoclonal IgG) diluted 1:400 in TTBS. The excess antiserum was removed by 4 x 5 min washings with TTBS. The blots were then treated with a 1:3000 dilution of anti-rabbit IgG conjugated to alkaline phosphatase in TTBS for 1 h. After two washes in TTBS, one wash in TBS, bromochloroindolyl phosphate/nitroblue tetrazolium substrate

was added to visualize the primary/secondary antibody complexes. After color development, the blots were washed with distilled water and dried between paper towels.

3.2 Dendrimer as potential NO carrier for PDT

3.2.1 Dendrimer-thiols conjugation

3.2.1.1 Dendrimer-thiols conjugation via EDAC/NHS method

This method is a modified version of Roberts *et al.* (1990), where 65 μmol of thiols (GSH, Cys, HCys) was incubated with 260 μmol of 1-ethyl-3-[3'-(dimethylamino)-propyl]carbodiimide (EDAC) and 260 μmol of N-hydroxysuccinimide (NHS) in 900 μL 0.1 M phosphate buffer pH 5, 7.2 and 8 for 1 hour at room temperature. During this time, 200 μL PAMAM dendrimer solution (20% w/v methanol) was rotovaped for approximately 10 minutes to eliminate methanol. Dendrimer and reaction samples were then combined and incubated at room temperature for minimum of three hours. The resulting conjugate was purified by passing over HPLC Sephadex-G25 desalting column equilibrated with distilled H_2O. The purified conjugate was then quick-frozen in liquid nitrogen and lyophilized overnight.

3.2.1.2 Dendrimer-thiol conjugation via SPDP method

To the 200 μL rotovaped PAMAM dendrimer (generation 3) resuspended in 500 μL of 0.1 M phosphate buffer (pH 8), 20 mg of N-succinimidyl 3-(2-pyridyldithio)propionate (SPDP) prepared in 400 μL ethanol was added dropwise. The reaction mixture was stirred for 1 h under nitrogen and then fractionated on a G-25 column eluted with 0.1 M phosphate buffer (pH 8). The fractions containing Dendrimer-PDP were pooled together and quick-frozen in liquid nitrogen and lyophilized overnight.

3.2.2 Reduction of thiols

Lyophilized products from sections 3.2.1.1 and 3.2.1.2 were each dissolved in 450 μL H_2O then incubated with excess dithiothreitol (DTT) (30 mg) at room temperature for 1 h. Excess DTT was removed by passing over a Sephadex G25 desalting column (1.5 cm x 20 cm) equilibrated in distilled H_2O.

Ellman's assay was used to determine free thiol groups (as previously described in section 3.1.3).

3.2.3 Dendrimer-S-NO synthesis

Dendrimer-GSNO was synthesized by incubation dendrimer-GSH (in distilled H_2O) with 100 fold molar excess (over free thiol) of S-nitrosoglutathione (GSNO) for 30 min at room temperature. The excess GSNO was removed by chromatography on a column (1.5 cm x 20 cm) of Sephadex G-25 (superfine) equilibrated and eluted with filtered distilled H_2O. Dendrimer-GSNO was protected from light by aluminum foil and stored at -20°C until further use.

3.2.4 Estimation of dendrimer toxicity towards cells in culture

3.2.4.1 Cytotoxicity effect of Dendrimers on V-79 fibroblasts

V-79 fibroblasts were grown to confluence in DMEM medium (90%) and FBS (10%) then treated with Dendrimers (85 μM) in the presence and absence of light.

3.2.4.2 Cytotoxicity effects of dendrimer-GSNO on SW-948 cells in culture

SW-948 cells were grown to confluence (as per section 3.1.10.1) then were transferred to four sets of 12-well plates at a final concentration of 1,960,000 cells/mL. Then exposed to one of the following treatments, using (+/-) catalase (2 mg/mL) in each treatment, (in triplicate, total volume 1.0 mL): treatment 1- Dendrimer-GSNO, (85 μM); treatment 2- Dendrimer-GSNO, (85 μM); GOD, (9.2 μg/mL); treatment 3- GOD, (9.2 μg/mL); 4- control- cells in 1.0 mL of medium. Two sets were covered with aluminum foil, the other two sets were exposed to light (10 cm above *InFocus* ® overhead projector) for 60 min, both placed in a 37°C incubator (5% CO_2). Cell viability of all samples was monitored at 1 h and 72 h after exposure to the various treatments (as per section 3.1.10.6).

The same experiment was repeated with varying dendrimer-GSNO concentrations (8.5 μM and 0.85 μM).

3.3 Application of PDT in glaucoma filtration surgery

3.3.1 Tenon capsule and V-79 fibroblasts Culture

Fibroblasts were cultured as previously described in section 3.1.10 and maintained in Dulbecco's modified eagle's medium (DMEM), containing 10% heat-inactivated fetal bovine serum and 100 units penicillin G, 0.01% streptomycin and 0.25 micrograms of amphotericin B in a 5% carbon dioxide incubator with atmospheric air at 37°C.

3.3.2 Uptake studies of aminolevulinic Acid (ALA)

Both V79 and TC fibroblasts were treated in an identical manner. The cells were grown to confluence. They were incubated for 24 hours at three different concentrations of aminolevulinic acid (0.05 mM, 0.1 mM, 1.0 mM) prepared in phosphate buffered saline (PBS), pH 7.4, both in the absence and presence of 1.0 mM Desferal (DEF). After the 24 h incubation, the cells were removed from the dish by trypsinization (as per section 3.1.10.2) and resuspended in 3.0 mL of PBS. The fluorescence emission spectrum was recorded on a Hitachi F-3010 spectrofluorometer at an excitation wavelength of 408 nm.

3.3.3 Uptake studies of S-nitrosoglutathione (GSNO)

Both V79 and TC fibroblasts were treated in an identical manner. The cells were grown to confluence on 22 mm sterile cover slips inside of 60 mm tissue culture dishes. Uptake was assessed by two different methods.

3.3.3.1 Uptake studies-dansylated GSNO (DNS-GSNO)

3.3.3.1.1 Preparation of DNS-GSNO

Oxidized glutathione (100 mg in 20 mL of 0.1 M Tris buffer, pH 8.0) was shaken at room temperature for 24 h with 0.01 M dansyl chloride in 1.0 mL of absolute ethanol. The mixture was passed over a G-25 Sephadex 2.5 x 10 cm gel filtration column. The first fluorescent fraction was collected and lyophilized. This material was reduced with 10 mM β-mercaptoethanol. Gel exclusion chromatography was repeated and the first fluorescent fraction was collected and lyophilized. Transnitrosylation was performed by incubating this material (in Dulbecco's phosphate buffered saline, pH 7.4), with 100-fold

molar excess (over free thiol) of GSNO for 1 h at room temperature. GSNO was prepared (as previously reported in section 3.1.4). The DNS-GSNO was protected from the light by aluminum foil.

3.3.3.1.2 Treatment of cells for confocal study

The cells were removed from the incubator, the tissue culture medium removed, and the cells rinsed twice with Hank's balanced salt solution (HBSS). The cells were then incubated at room temperature with a 1.0 mM solution of DNS-GSNO in DPBS for 2, 5 and 10 minutes. The DNS-GSNO was aspirated and the cover slips were inverted onto microscope slides using vectashield fluorescence mounting medium as an interface. The cells were imaged with a Bio Rad 1024 MRC confocal laser scanning microscope. (Nikon eclipse E-800 IMT2; 20-60x objectives, 0.5 μm Z step). Digitized images were processed through confocal assistant.

3.3.3.2 Uptake studies--^{3}H-GSNO

3.3.3.2.1 Preparation of ^{3}H-GSNO

20 μCi of ^{3}H-glutathione (^{3}H-GSH, Mandel Scientific Company, Guelph, Ontario, Canada) were added to 1 mM GSNO (10 mL) which was then divided and stored in the dark at -20°C until further use.

3.3.3.2.2 Treatment of cells and measurement of radioactive uptake

1 mL fractions of ^{3}H-GSNO were diluted 20-fold in Earles Balanced Salt Solution (EBSS) to achieve a concentration of 50 μM ^{3}H-GSNO (0.1 μCi/mL). Cells were pelleted by centrifugation following trypsinization and washing in EBSS. 1 mL of ^{3}H-GSNO was added to the cell pellet and incubated for 1, 2, and 5 min intervals. The

reaction was stopped by suction filtration through a 0.45 μm nitrocellulose filter followed by washing with EBSS. The filter paper was placed in 10 mL scintillation fluid and shaken at room temperature overnight. The radioactivity was measured after 18 hours on a Beckman LS 6500 multi-purpose scintillation counter. Non-specific binding was determined by adding 1.0 mL of 50 μM ^{3}H-GSNO to the filter paper followed by identical treatment as the cell-containing specimens then was subtracted from the radioactivity measured in the presence of cells.

3.3.4 Photodynamic treatment

3.3.4.1 Effect of ALA in the presence of DEF

Chinese hamster lung V-79 fibroblasts were treated with ALA (1 mM) in the presence and absence of 1.0 mM Desferal. The cells were either incubated for an additional 4 h or 24 h at 37°C, 5% CO_2 subsequent to light treatment, or were directly treated with light without any further incubation (0 h incubation). The cells were radiated with a fibre optic spectrometer (Ocean Optics Inc. S2000) which delivered 200 msec pulses of visible light through a 3 mm aperture held at a distance of 10 cm after passing through a cupric sulphate filter (1 mM). A Spectra Physics power meter recorded energy of 0.068 watts/pulse. The radiation time was 10 minutes. Following radiation the incubation solutions were removed and replaced with fresh tissue culture medium and incubated for a further 24 h followed by cell viability assessment.

3.3.4.2 Cytotoxic effect of ALA/DEF and GSNO PDT

Human tenon's capsule and Hamster lung V-79 fibrobroblasts were treated with three different concentrations of either ALA or GSNO (0.05 mM, 0.1 mM, 1.0 mM). The ALA experiments were performed both in the presence of 1.0 mM Desferal. The cells were either incubated for an additional 4 h or 24 h at 37°C, 5% CO_2 subsequent to light treatment, or were directly treated with light without any further incubation. Cell viability was determined 24 h subsequent to light exposure. The radiation time was 10 minutes. Following radiation the incubation solutions were removed and replaced with fresh tissue culture medium then further 24 h incubation before cell viability assessment.

3.3.4.3 Cell viability study

Following 24 h from treatment with GSNO or ALA +/- DEF, cells were then scraped gently using a cell scraper. An aliquot of the suspended cells was diluted 2 fold with trypan blue dye and placed on a hemocytometer grid and percent cell viability was estimated as per section 3.1.10.6.

3.4 Mode of cell death post S-NO/PDT

3.4.1 Analysis of cell death type by annexin and propodium iodide

Surface exposure of phosphatidylserine (PS) by apoptotic cells was measured by using annexin fluorescein and propidium iodide for the differentiation from necrotic cells. MCF breast tumor cells were cultured as per section 3.3.1 until confluence. Cells were then lifted from cultured flask by trypsinization, treated for varying periods (0, 4, 24 h) of time in the presence of 1 mM GSNO plus or minus light (10 cm above *InFocus* ® overhead projector) for 10 min. Stain solution was prepared by taking diluting 20 µL of

annexin fluorescein labeling reagent (stock) in 1 mL of HEPES buffer, followed by the addition of 20 μL of propidium iodide stock solution.

MCF Cells treated with GSNO (as previously described) were gently washed with PBS and centrifuged at 200 x g for 5 minutes. Cells were then resuspended in 100 μL of staining-solution and incubated for 20-25 minutes at room temperature in the dark. Each sample was evaluated by fluorescence microscopy (using 488 nm excitation and 515 nm emmission).

3.4.2 DNA fragmentation assay

Recently developed Photometric enzyme linked imunosorbent assay to quantitatively differentiate between apoptotic and necrotic cell death.

3.4.2.1 Coating Microtiter plates

Clear, polystyrene microtiter wells were coated, by physical adsorption, with 100 μL of anti-DNA solution. The wells were covered with an adhesive cover foil, and incubated overnight at 4°C.

3.4.2.2 Blocking Procedure

Microtiter plates (MTP) were blocked after aspirating away the coating solution, 200 μL of blocking solution was added into each well. MTP was covered with an adhesive cover foil and incubated at room temperature for 30 min. then washed three times with 250 μL of washing solution for 3 min each. After removing washing buffer the wells are ready for use.

3.4.2.3 labelling cells

MCF human breast cancer cells were lifted from culture flask by trypsinization (as described in section 3.1.10.2) and resuspended in culture medium to adjust cell number to 2-4 x 10^5 cells/mL. BrdU labeling solution was added to a final concentration of 10 μM. The cell mixture was then incubated overnight at 37°C. After the appropriate incubation, cells were centrifuged for 10 min at 250 x g, then were resuspended in BrdU-free culture medium.

3.4.2.4 ELISA procedure

100 μL of labelled cells were transferred into each well of the pre-coated MTP, covered tightly with an adhesive cover foil and incubated for 90 min at room temperature. The wells were then washed three times with 250 μL washing solution for 3 min each. DNA was fixed and denatured by adding 100 μL exonuclease III solution to each well, covering MTP with an adhesive cover foil and incubating for 30 min at 37°C. After three washing steps (as previously described), 100 μL of anti-BrdU-POD conjugate solution was added to each well and incubated for 90 min at room temperature, followed by another three washing steps.

Prior to reading, washing buffer was aspirated away from the wells, and 100 μL of tetramethylbenzydine (TMB) substrate solution was added to each well. The plate was incubated in the dark on a MTP shaker until color development was sufficient. 25 μL of stop solution (H_2SO_4) was then added to each well and incubated for 1 min on the shaker. A photometric measurement at 450 nm was then taken within 5 minutes after adding stop solution.

3.4.3 Detection of Bcl-2 and p53

3.4.3.1 (8%) SDS- PAGE

Hep G2 Cell line was cultured as per section 3.3.1, then were treated with 1 mM GSNO. One set was treated with light for 10 min, while the second set was protected from light. Cells were then lysed and the collected supernatants were treated with an equal volume of sample application buffer (125 mM Tris-HCl pH 6.8, 2% SDS, 5% glycerol, 0.003% bromophenol blue, and 1% β-mercaptoethanol). The mixture was then boiled for 5 min. To each well of an 8% SDS-polyacrylamide gel, 10 μL of each sample was applied and electropheresed for 1 h at 130 V along with a set of molecular weight markers (Sigma-broad range).

3.4.3.2 Immunoblot analysis

The resolved protein bands were then transferred onto a nitrocellulose support medium at 100 V for 70 min using a transfer buffer of 25 mM Tris base/192 mM glycine/20% methanol. The blots were blocked overnight at 4°C with blocking buffer (5% non-fat milk in 10 mM Tris pH 7.5, 100 mM NaCl, 0.1% Tween 20). The blocking buffer was decanted and blots were incubated for 1 h at room temperature with primary antibody (anti-mouse Bcl-2 (5 μg/mL) or anti-mouse p53 (1 μg/mL). Blots were then washed using washing buffer (10 mM Tris pH 7.5, 100 mM NaCl, 0.1% Tween 20) for 30 min with agitation. Then incubated with the enzyme conjugate anti-mouse IgG: horseradish peroxidase, diluted 1:2500 in blocking buffer for 1 h at room temperature followed by 6 washes 5 min each with agitation.

3.4.3.3 Hyperfilm development

The blots were then incubated with ECL reagents for 5 min in the dark and exposed using Kodak cassette for 30 min onto a hyperfilm. The film was then incubated in Kodak developer reagent for 3 min or until bands were observed. Then it was moved into the neutralization solution (3% acetic acid) for another 3 min until it was fixed with Kodak fixer reagent, followed by extensive washing with water then air dried.

CHAPTER 4

RESULTS

4.1 Thionein as a potential NO carrier for PDT

During the metallothionein isolation process, protein content was quantified at each purification step (table 1.2). The overall yield was 0.5%. Most of the protein loss occurred after the acid precipitation step that was used for the removal of metal ions to produce the apoprotein (Thionein). Thionein is known to be 1500 times more succeptible to degradation than metallothionein (Moffatt *et al.*, 1997).

To confirm further the purity of metallothionein, the protein was subjected to western blot analysis, where the samples were electrophoresed, transferred onto nitrocellulose and probed with anti-metallothionein (host mouse) primary monoclonal antibody followed by anti mouse-IgG conjugated to alkaline phosphatase. The blot revealed a single band at the expected molecular weight (~6,000 Da) of metallothionein (Fig 1.13).

Conjugation of thionein and nitric oxide occurs via transnitrosation with 100 fold molar excess of GSNO. The UV/vis absorption spectra of T and T-NO are revealed in Fig.1.14 where T is spectrally transparent in the wavelength region 330 nm-500 nm.

The formation of the NO-derivative of T (Fig.1.14 filled circles) is confirmed from the characteristic S-nitroso absorbance at 334 nm. The molar absorption coefficient (at 334 nm) for thionein S-NO was estimated to be 1,820 M^{-1} cm^{-1}. This value is ~2-fold larger than S-NO absorption coefficients observed for small molecular weight thiols and ~2-fold smaller than that reported for the NO derivative of bovine serum albumin.

Table 1.2: Purification of metallothionein from rabbit liver

Steps	[Protein]
24.38 g of rabbit's liver	----------
After homogenization	3210 mg
After G-75	427 mg
After DEAE	34 mg
After acid precipitation	18 mg

Purification of metallothionein from the crude cytosolic fraction (20,000 x g) was subjected to a sequential chromatography: Sephadex G-75 and DEAE-cellulose. The eluate was stripped from its metal by acid precipitation procedure. The data represent a single typical purification procedure.

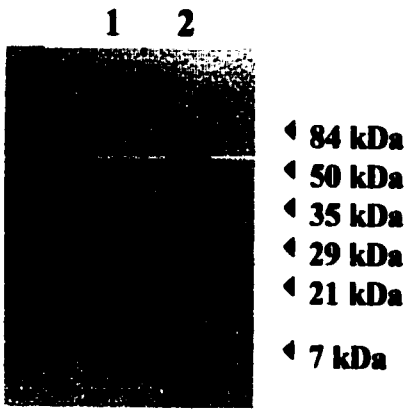

Figure 1.13- Immunoblot analysis of metallothionein. The purified protein was probed with anti-metallothionein (1:1000 dilution). Metallothionein was visualized using an alkaline phosphatase conjugated secondary antibody detection system (1:3000 dilution). Lane 1, purified metallothionein. Lane 2, pre-stained (coomasie blue) molecular weight standards (from top: Bovine serum albumin 84 kDa, ovalbumin 50 kDa, carbonic anhydrase 35 kDa, soybean trypsin inhibitor 29 kDa, lysozyme 21 kDa, aprotinin 7 kDa).

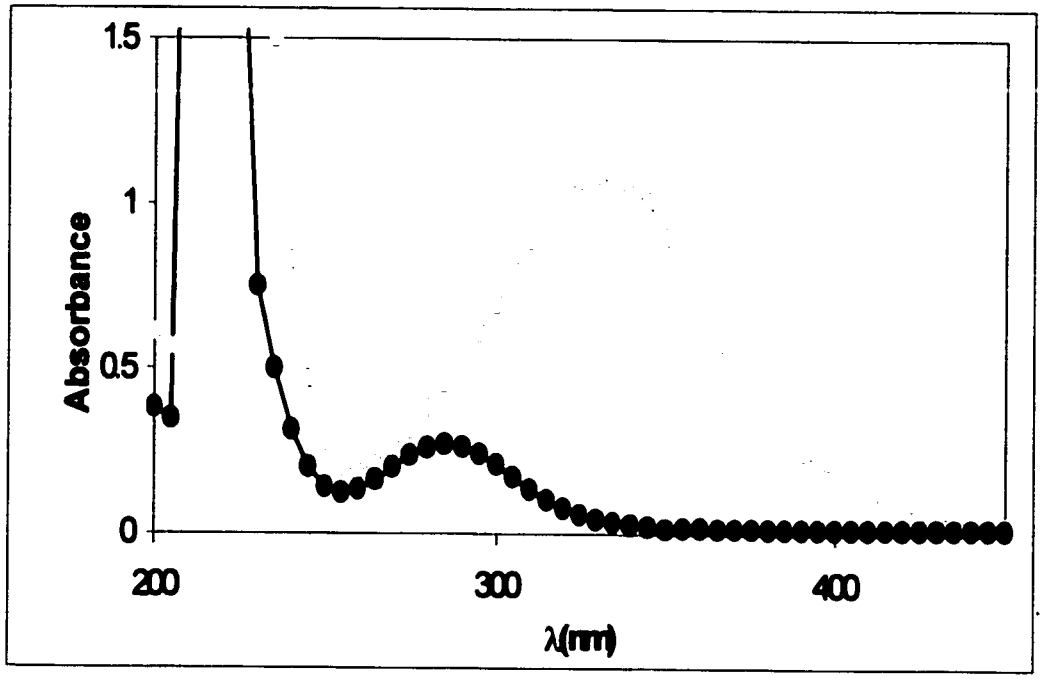

Figure 1.14- UV-vis spectra of Thionein and Thionein-NO. Absorption spectra of thionein (32μM) (filled circles) and thionein-NO (32μM) (open circles).Samples were prepared in Tris-Cl buffer pH 8.

The photolability of the S-NO bond of T-NO is demonstrated in Fig.1.15. 1.0 mL aliquots of T-NO (15 μM, 18.9 NO/mol) in phosphate buffer (0.1 M, pH 7.4) were added to 2 matched semi-micro cuvettes. One cuvette was wrapped in aluminum foil in order to protect it from light. Both cuvettes were then placed 10 cm above an overhead projector. UV/vis spectra were recorded at various time intervals following light exposure. The spectrum of the sample protected from light was unchanged after 1 h, (t=0) and (t =1 h). The absorption peak of the photo irradiated sample decreased by ~ 56% after 15 min of exposure and was nearly totally abolished after 1h of exposure.

It is well documented that NO (and not $NO^{\cdot}$ or NO^{-}) reacts with oxyhemoglobin (Fe^{2+}, λ_{max} 425 nm) converting it to methemoglobin (Fe^{3+}, λ_{max} 408 nm). In this study T-NO (1.2 μM, 18.9 NO/mol)) was photolyzed by 355 nm light in the presence of oxyhemoglobin (10 μM) in a flash photolysis instrument. The absorbance changes subsequent to the nsec flash were monitored at 425 nm and 408 nm (Fig.1.16). The liberation of NO was confirmed as the absorbance increased at 408 nm and a concomitant decrease was observed at 425 nm at the same rate.

To confirm photolytic NO-release, a sample of T-NO (1.2 μM, 18.9 NO/mol) was placed in a glass screwcap test tube (15 mL) fitted with a rubber septum. The head space gas was withdrawn with a gas tight syringe 25 mL and directly injected into a chemiluminescent nitric oxide analyzer. There was no nitric oxide detected when the sample was protected from light. However, upon exposure of the sample to light from an overhead projector for 1 h, the head space gas contained ~ 4 μM NO.

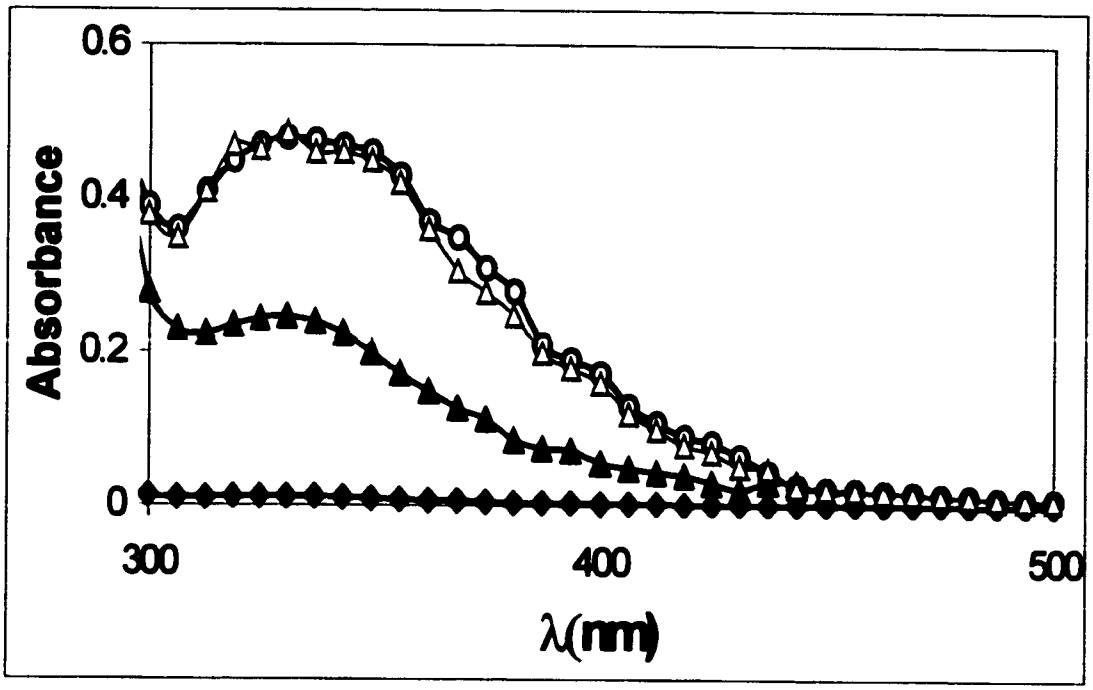

Figure 1.15- Measurement of photolytic NO release by UV-vis spectrophotometer. UV-vis spectra of thionein-NO (15 μM) protected from light (at t=0, open triangle; t=1h, open circles); thionein-NO (15 μM) exposed to light for various time intervals: t=15 min (filled triangles), t=1 h (open diamonds) in 0.1 M sodium phosphate, pH 7.4.

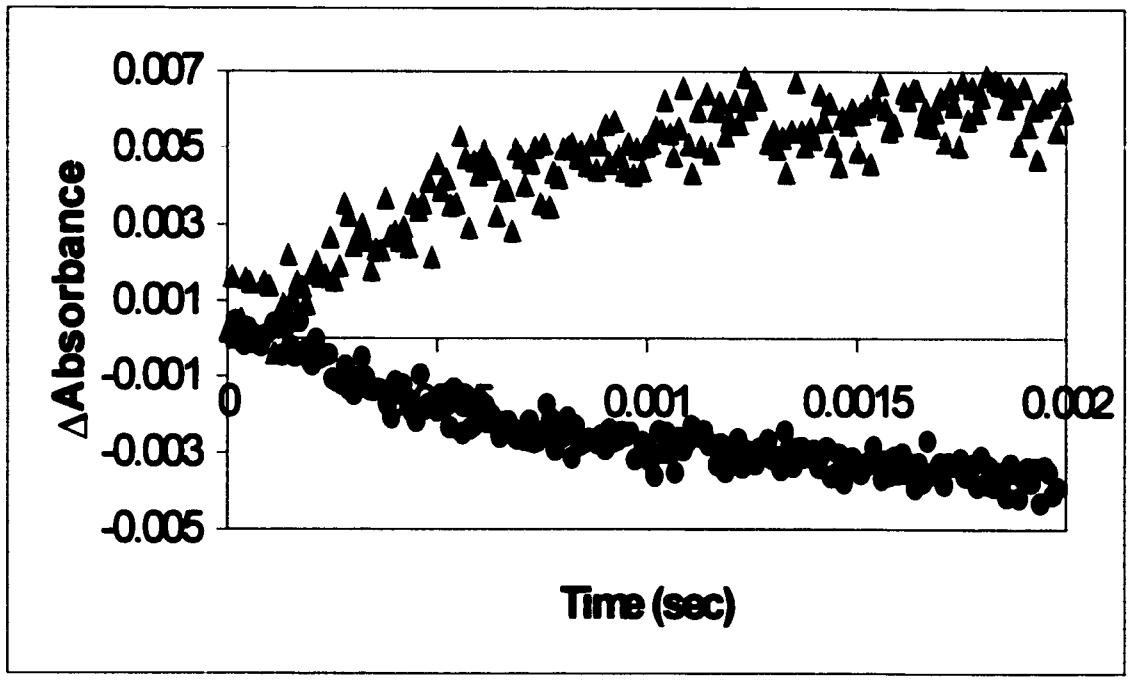

Figure 1.16- Measurement of photolytic NO release from T-NO by flash photolysis. Using a flash photolysis apparatus, transient absorption changes were measured at 408 nm (filled triangles) and 425 nm (filled circles) following direct excitation at 355 nm of T-NO (1.2 μM) in the presence of oxyhemoglobin (10 μM) in sodium phosphate (0.1 M, pH 7.4).

Transnitrosation effects by other thiols were demonstrated by adding GSH, L-Cys or β-mercaptoethanol (β-ME) (1 mM) to T-NO (22.3 μM, 18.9 NO/mol). The transnitrosation rate constants were estimated by monitoring the decrease in the thionein-S-NO absorbance at 334 nm as a function of time. The second order rate constants were estimated from the pseudo-first order treatment of the transnitrosation data (table 1.3). The largest k_2 (0.163 ± 0.0156 M^{-1} sec^{-1}) was obtained with GSH, whereas L-Cys yielded the smallest (0.000686 ± 0.000034 M^{-1} sec^{-1}). The non-physiological thiol, β-ME resulted in an intermediate rate constant (0.0340 ± 0.00481 M^{-1} sec^{-1}). These rate constants suggest very slow reaction rates for physiologically relevant concentrations of the reactants.

Previous studies have shown that H_2O_2 can be toxic to the cells, thus in our study we used GOD enzyme which catalyzes the conversion of glucose to gluconic acid plus H_2O_2 (Ignarro *et al.*, 1993). This enzyme has the ability to produce H_2O_2 from D-galactose as well, albeit at 0.5 % of the rate observed for glucose. This is significant as the media for the human colon adenocarcinoma cells (SW 948) used contains D-galactose and not D-glucose. In the process of assessing the cytotoxicity of GOD on SW-948 cells in culture, cells (1,810,000 cells/mL) were exposed to 5 different treatments: 1-GOD (50 mg/mL), 2-GOD (5 mg/mL), 3-GOD (0.5 mg/mL), 4-GOD (0.05 mg/mL), 5- control. Cells treated with 0.5 mg/mL GOD were found to exhibit 74% cell death at 24 hr after treatment. On the other hand cells treated with 50 mg/mL GOD seem to exhibit the least cell death (50%) (Fig 1.17, table 1.4).

Table 1.3: Transnitrosation effects by other thiols

Thiols	k_2
GSH	$0.163 \pm 0.0156\ M^{-1}\ sec^{-1}$
β-mercaptoethanol	$0.0340 \pm 0.00481\ M^{-1}\ sec^{-1}$
L-Cys	$0.000686 \pm 0.000034\ M^{-1}\ sec^{-1}$

SW-948 cells (205,000 cells/mL) were treated with varying T-NO concentrations (3-300 μM), in the presence of light (open bars) or in the dark (filled bars) for 1 hr. Viable cell counts was performed at 24 h and 48 h following treatment. Cells treated with 300 μM of T-NO and light exhibited the most cell death (84%) after 48 h incubation. Whereas, samples treated with the same concentration of T-NO but protected from light revealed 67% cell death (Fig. 1.18, table 1.5).

To assess the cytotoxic potential of NO/GOD. SW-948 cells in culture (1,210,000 cells/mL) treated with plus or minus catalase (1 mg/mL) then exposed to 4 different treatments: 1- T-NO (60 μM); 2- T-NO (60 μM) + GOD (10 mg/mL); 3- GOD (10 mg/mL); and 4- control (cells in 1 mL of media). One complete set was exposed to light for (60 min) by placing the 12 well plates on an overhead projector. The other set was kept in the dark (Fig.1.19). The effectiveness of T-NO and GOD in combination is evident after 1 h in the irradiated set, where the cell viability decreases by ~ 76 % without catalase and by 2% with catalase. This value increases to 98% (without catalase) and 65% (with catalase) in 72 h. In contrast, in samples receiving GOD and T-NO ± catalase and no light the cell viability is decreased by only 56% (without catalase) and 22% (with catalase) in 72 h (table 1.6).

Cell culture medium (Leibovitz's L-15) is composed of 2 mM to 140 mM inorganic salts and no metal chelators. As a result, trace Fe-ion contamination is expected. We therefore wanted to check for peroxynitrite production under the conditions employed in the cell culture experiments.

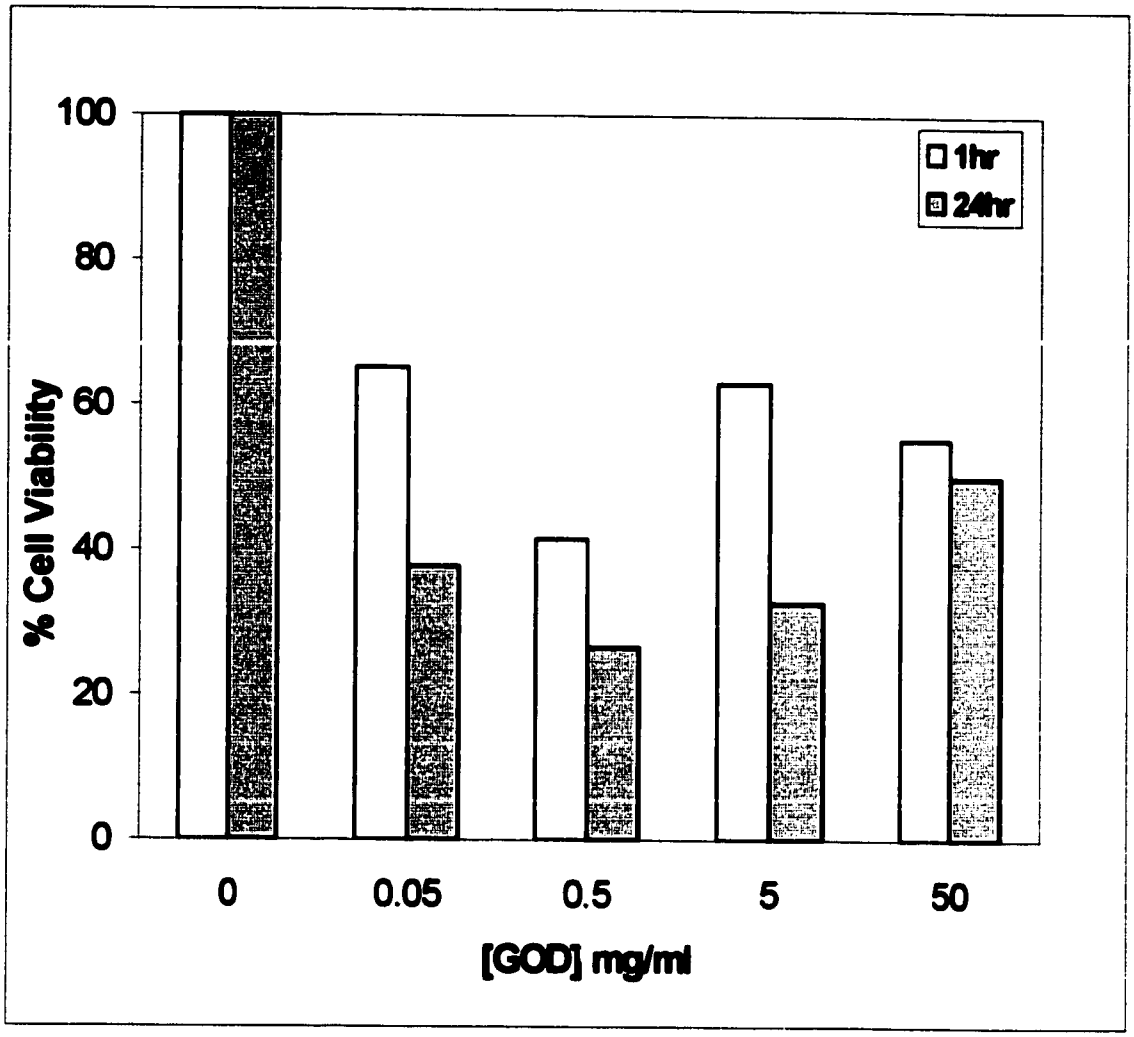

Figure 1.17- The cytotoxic effect of glucose oxidase towards human colon adenocarcinoma cells in culture. SW 948 cell viability after 1 h (open bars) and 24 hr (filled bars) after exposure to varying GOD concentrations (0-50 mg/ml). Viability is expressed as a percent of control cell density at each time point.

Table 1.4: Cell viability (%) of SW-948 treated with GOD

Cell viability (%)

[GOD] mg/mL	1 hr	24 hr
0	100%	100%
0.05	65%	37%
0.5	41%	26%
5.0	62%	32%
50	55%	50%

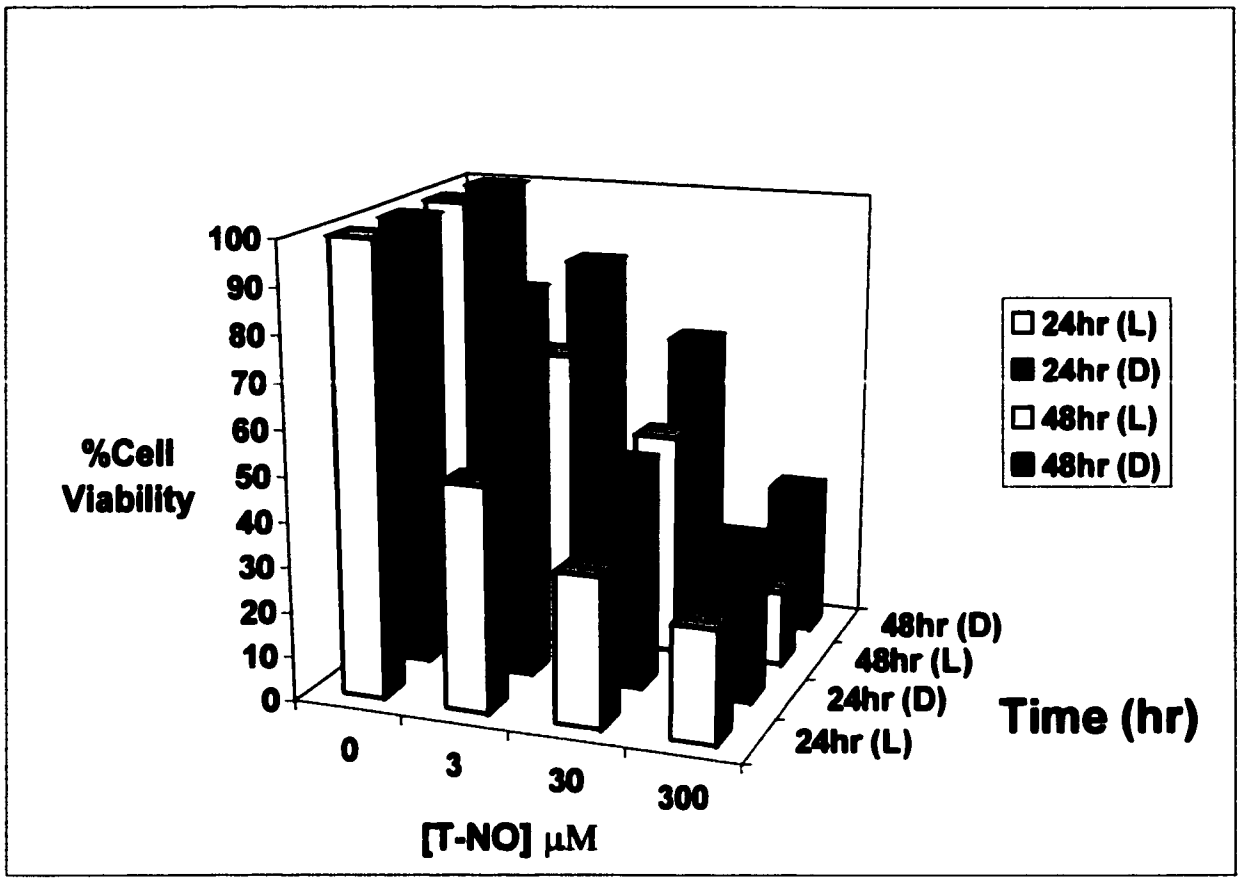

Figure 1.18- Cytotoxicity effect of T-NO towards human adenocarcinoma cells in culture. Aliquots from 205,000 cells/ml were treated with different concentration of T-NO (0-300 μM) in the dark (filled bars) or in the presence of light (open bars) for 1 h. Viable cell assay was performed after 24 h and 48 h incubation.

Table 1.5: Cell viability (%) of SW-948 cells treated with T-NO/PDT.

Cell viability (%)

[T-NO]μM	24 hr (Light)	24 hr (Dark)	48 hr (Light)	48 hr (Dark)
0	100%	100%	100%	100%
3	50%	85%	66%	83%
30	33%	50%	50%	66%
300	25%	35%	16%	33%

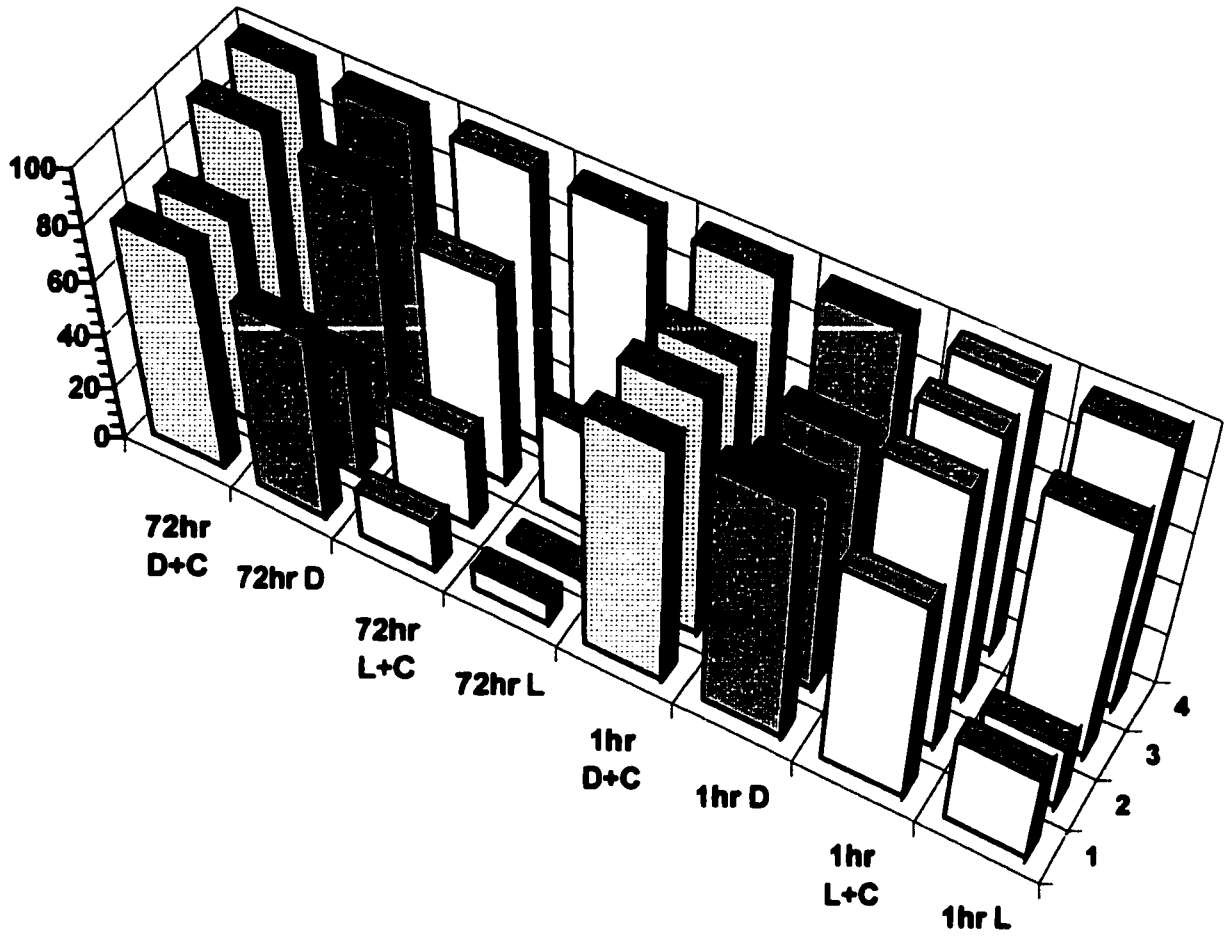

Figure 1.19- Thionein-NO photo-induced cytotoxicity in the presence of GOD. The cytotoxic effect of T-NO and glucose oxidase towards human colon adenocarcinoma cells (SW 948) in culture was monitored for 72 h after exposure to the following treatments. (1) T-NO (60 μM); (2) T-NO (60 μM) plus GOD (10 mg/ml); (3) GOD (10 mg/ml), (4) control (cells in growth medium). All treatments were maintained either in the dark no catalase (D), treated with catalase (D+C) or subsequent to 60 min of exposure to light no catalase (L), treated with catalase (L+C). Viability is expressed as a percent of control cell density (i.e. treatment 4) at each time point. Values obtained are the average of triplicate experiments.

Table 1.6: Cell viability (%) of SW-948 treated with T-NO/GOD/PDT.

Cell viability (%)

TREATMENT	1 HR (LIGHT)	1 HR (DARK)	72 HR (LIGHT)	72 HR (DARK)
T-NO	33%	90%	9%	70%
T-NO +Catalase	76%	89%	19%	81%
T-NO + GOD	24%	76%	2%	44%
T-NO + GOD + Catalase	98%	90%	35%	78%
GOD	88%	75%	36%	91%
GOD + Catalase	100%	86%	77%	94%
Control	100%	100%	100%	100%
Control + Catalase	100%	100%	100%	100%

Nitrotyrosine has been widely used as a marker of peroxynitrite formation. In these experiments, BSA samples in L-15 medium plus T-NO and GOD with or without catalase were irradiated for 1 h or kept in the dark. The samples were electrophoresed, transferred onto nitrocellulose and probed with anti-nitrotyrosine (rabbit) primary antibodies followed by anti rabbit-IgG conjugated to alkaline phosphatase. A single nitrated band at the correct molecular mass for BSA was detected when sample was treated with light for one hour in the absence of catalase (Lane 3). On the other hand, samples treated with light and catalase (Lane 2), or dark (Lane 1), showed no sign of evidence for nitrotyrosylated protein (fig.1.20).

4.2 Dendrimer as potential NO carrier for PDT

One of the aims of this work is to be able to attach the maximum number of thiol groups on to the dendrimer to deliver the maximum amount of NO during PDT. Several attempts were made to optimize the conjugation of dendrimer to three different thiols containing compounds at variant pH values using EDAC/NHS method (table 1.7).

Another approach was to use SPDP to couple thiols to dendrimer at pH 8.0. When conjugating an amine-containing compound such as dendrimer with SPDP, the conjugation would occur via NHS-ester group. Upon reduction with DTT, this conjugation yielded 10 thiols/dendrimer molecule.

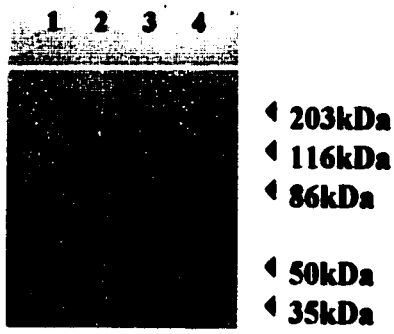

Figure 1.20- Evidence of nitrotyrosine formation on BSA irradiated in the presence of T-NO and GOD. BSA incubated with T-NO plus GOD in L-15 medium, pH 7.4 (± light for 1 h), then the mixer was separated on a 10 % SDS-PAGE gel, transferred to nitrocellulose and probed with a monoclonal anti-nitrotyrosine antibody (1:400) (host, rabbit) followed by anti-rabbit-IgG-alkaline phosphatase conjugate (1:3000). Lane 1, sample received no light. Lane 2, treated with light for 1 h in the presence of catalase. Lane 3, treated with light for 1 h. Lane 4, pre-stained (coomassie blue) molecular weight standards (from top: myosin, 203 kDa; β-galactosidase, 116kDa; BSA, 84kDa; ovalbumin, 50 kDa; carbonic anhydrase, 35 kDa).

Table 1.7: Number of thiols per dendrimer at varying pH values.

Number of Thiols per Dendrimer

Thiol	pH 5	pH 7.2	pH 8
GSH	3	2	3
CYSTEINE	3	2	3
HOMOCYSTEINE	1	2	3

The conjugation of Dendrimer-SH and nitric oxide occurs via transnitrosation with 100 fold molar excess of GSNO. The UV/vis absorption spectra of Dendrimer-GSNO are presented in Fig.1.21. The formation of the NO-derivative of dendrimer is confirmed from the characteristic S-nitroso absorbance at 334 nm.

The cytotoxicity of Dendrimer alone was tested first on Chinese hamster cells in culture (V-79) (Fig 1.22). The % cell viability (Table 1.8) clearly showed that dendrimer (85 μM) alone possess no toxicity towards these cells in culture. Thus the cytotoxicity potential of the photochemical release of NO from dendrimer-GSNO coupled via EDAC/NHS procedure was tested next on human colon adenocarcinoma (SW-948) cells (Figs.1.23 A, B, C; Tables 1.9, 1.10, 1.11). SW-948 cells in culture were exposed to 4 different treatments: 1- Dendrimer-GSNO (85 μM, 8.5 μM, and 0.85 μM, 3 NO/mol); 2- Dendrimer-GSNO (85 μM, 8.5 μM, and 0.85 μM, 3 NO/mol) + GOD (9.2 μg/mL); 3- GOD (9.2 μg/mL); and 4- control (cells in 1 mL of media). One complete set was exposed to light for (60 min) by placing the 12 well plates on an overhead projector. The other set was kept in the dark. At the highest concentration (85 μM) the effectiveness of dendrimer-NO in the presence of GOD is evident after 1 h in the irradiated set, where the cell death was 72% without catalase and 60% with catalase. This value increases to 98% (without catalase) and 62% (with catalase) in 72 h.

The cytotoxicity effect of Dendrimer-GSNO (85 μM, 3 NO/mol) in light treated samples after 72 h incubation period was comparable to T-NO (60 μM, 18.9 NO/mol) towards tumor cells in culture (Table 1.12).

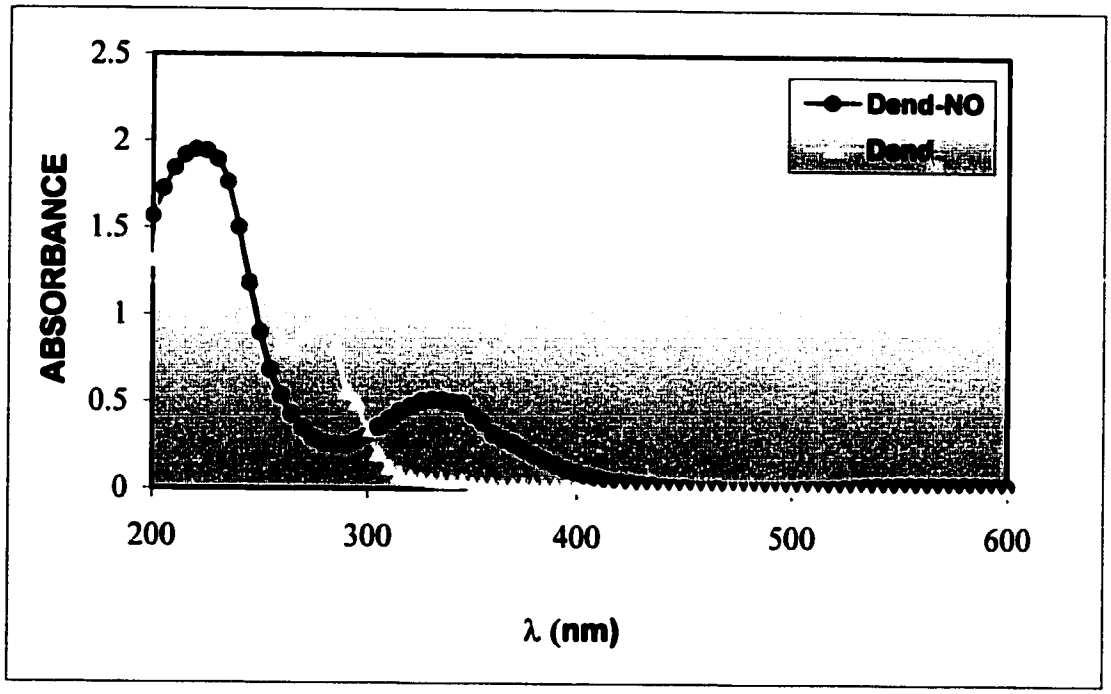

Figure 1.21- UV-vis spectra of dendrimer and dendrimer-NO. Dendrimer once it is conjugated to thiol containing compounds, it is then coupled to NO by transnitrosation with 100 fold molar excess of GSNO. Upon removal of excess GSNO, evidence of Dendrimer-NO formation was spectrally apparent by the spectrum in the wavelength range of 330-350 nm.

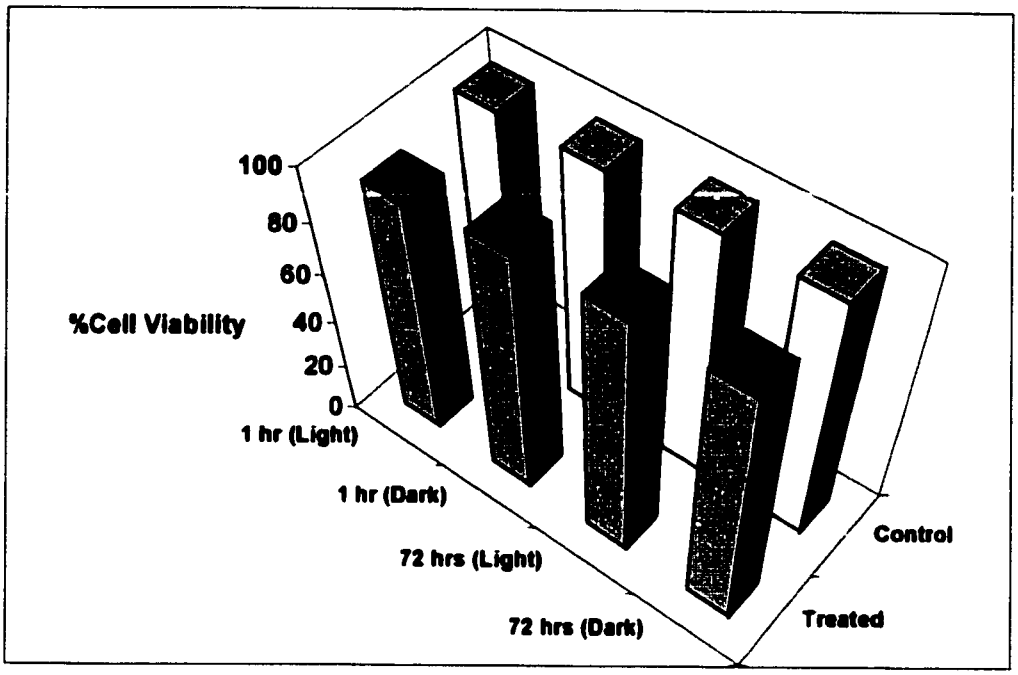

Figure 1.22- Dendrimer cytotoxicity towards cells in culture. The cytotoxic effect of dendrimer to hamster fibroblasts cells in culture was monitored for 72 h after exposure to the following treatments. (1) Dendrimer (85 μM); 2- control (cells in 1 ml of media). One set received subsequent 60 min of exposure to light (open bars) prior incubation, the other set was kept in the dark at all time (filled bars). Viability is expressed as a percent value of control cell density (i.e. treatment 4) at each time point.

Table 1.8: Cell viability (%) of V-79 treated with dendrimer (85 μM).

Cell viability (%)

TREATMENT	1 HR (LIGHT)	1 HR (DARK)	72 HR (LIGHT)	72 HR (DARK)
Dendrimer (85 μM)	94%	99%	100%	100%
Control	100%	100%	100%	100%

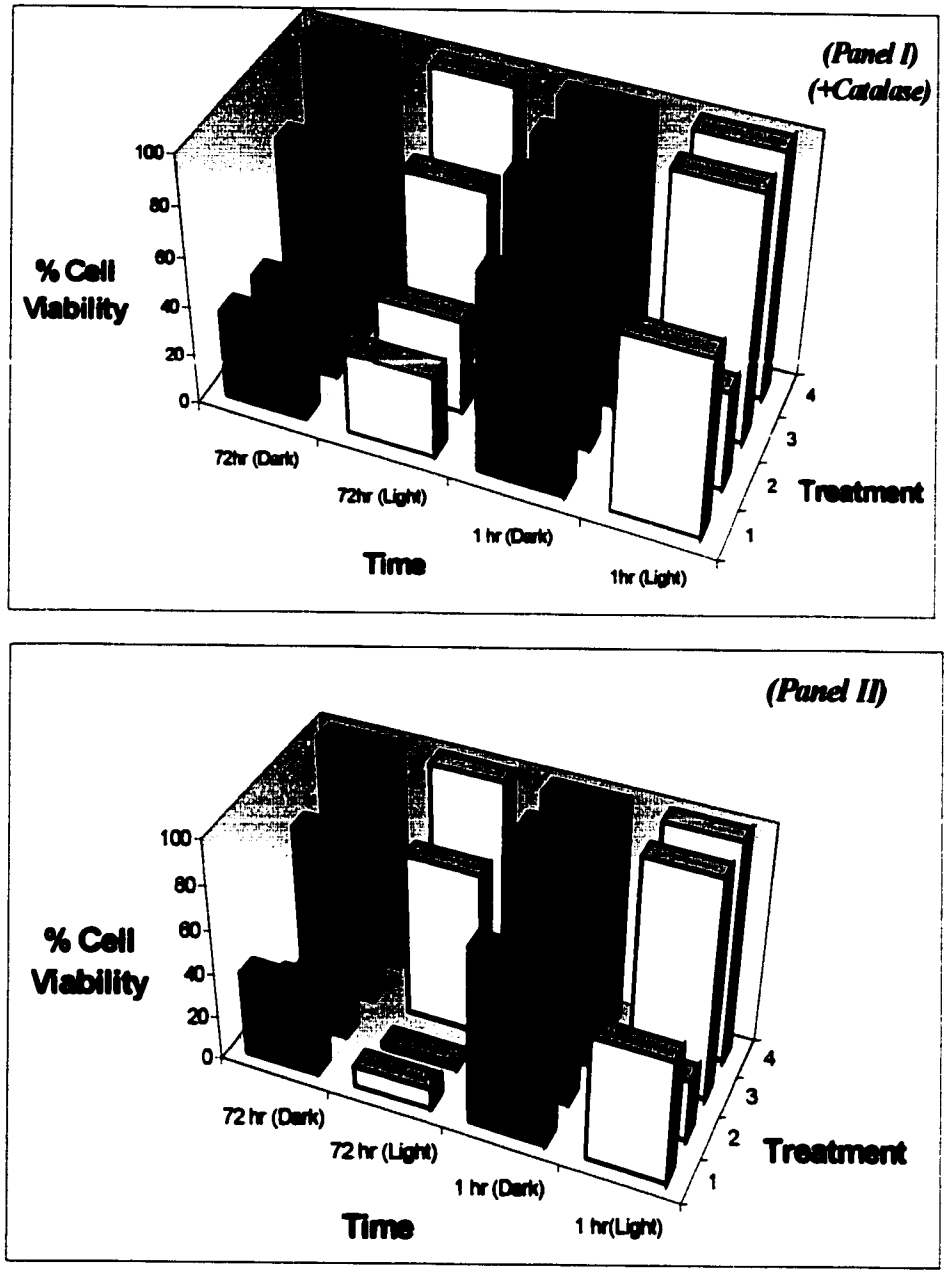

Figure 1.23A- Dendrimer-GSNO (85 μM) photo-induced cytotoxicity. The cytotoxic effect of Dendrimer-GSNO and glucose oxidase to human colon adenocarcinoma cells (SW 948) in culture was monitored for 72 h after exposure to the following treatments. (1) Dendrimer-NO (85 μM); 2- Dendrimer-GSNO (85 μM) + GOD (9.2 μg/ml); 3- GOD (9.2 μg/ml); and 4- control (cells in 1 ml of media). One set received subsequent 60 min of exposure to light (open bars) prior incubation, the other set was kept in the dark at all time (filled bars). All treatments were maintained either in the presence of catalase (Panel I), or in the absence of catalase (Panel II). Viability is expressed as a percent value of control cell density (i.e. treatment 4) at each time point.

Table 1.9: Cell viability (%) of SW-948 treated with dendrimer-GSNO (85 μM), GOD, PDT.

Cell viability (%)

TREATMENT	1 HR (LIGHT)	1 HR (DARK)	72 HR (LIGHT)	72 HR (DARK)
D-NO	56%	80%	10%	38%
D-NO + Catalase	72%	80%	33%	36%
D-NO + GOD	28%	52%	2%	19%
D-NO + GOD + Catalase	40%	100%	38%	33%
GOD	100%	100%	74%	74%
GOD + Catalase	100%	74%	74%	74%
Control	100%	100%	100%	100%
Control + Catalase	100%	100%	100%	100%

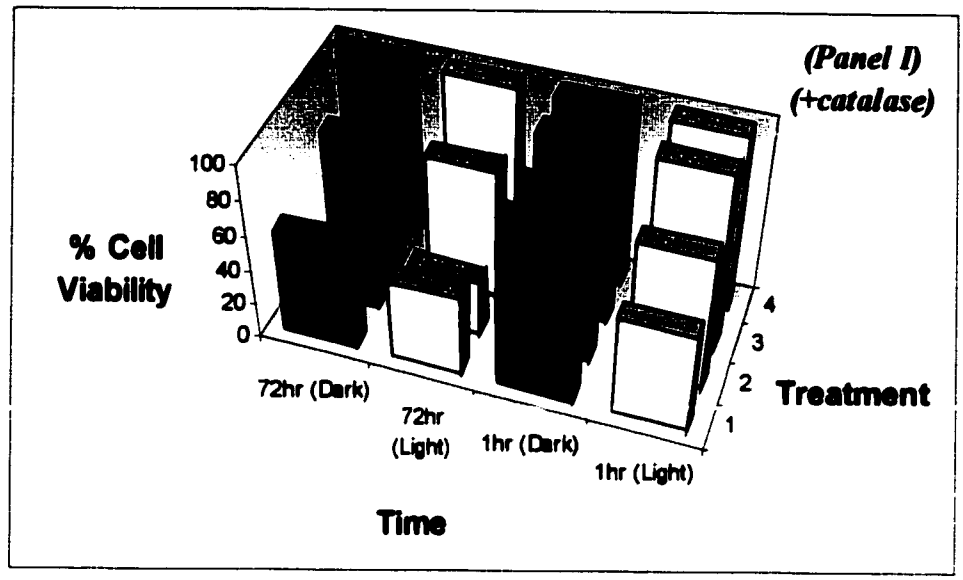

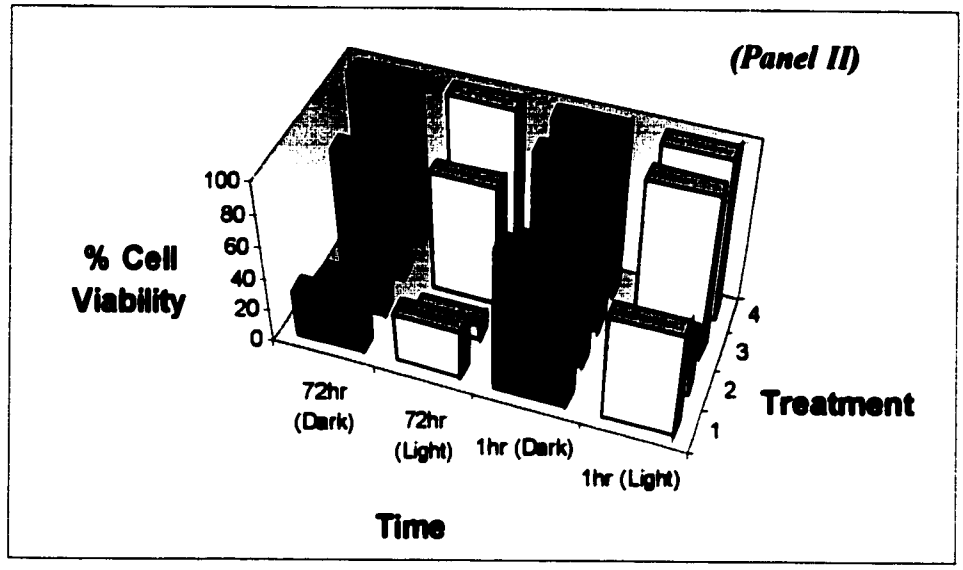

Figure 1.23B- Dendrimer-GSNO (8.5 μM) photo-induced cytotoxicity. The cytotoxic effect of Dendrimer-GSNO and glucose oxidase towards human colon adenocarcinoma cells (SW 948) in culture was monitored for 72 h after exposure to the following treatments. (1) Dendrimer-GSNO (8.5 μM); 2- Dendrimer-GSNO (8.5 μM) + GOD (9.2 μg/ml); 3- GOD (9.2 μg/ml); and 4- control (cells in 1 ml of media). One set received subsequent 60 min of exposure to light (open bars) prior incubation, the other set was kept in the dark at all time (filled bars). All treatments were maintained either in the presence of catalase (Panel I), or in the absence of catalase (Panel II). Viability is expressed as a percent value of control cell density (i.e. treatment 4) at each time point.

Table 1.10: Cell viability (%) of SW-948 treated with dendrimer-GSNO (8.5 μM), GOD, PDT.

Cell viability (%)

TREATMENT	1 HR (LIGHT)	1 HR (DARK)	72 HR (LIGHT)	72 HR (DARK)
D-NO	64%	88%	31%	29%
D-NO +Catalase	56%	96%	45%	60%
D-NO + GOD	36%	68%	10%	14%
D-NO + GOD + Catalase	76%	92%	31%	33%
GOD	100%	100%	74%	74%
GOD + Catalase	100%	100%	74%	74%
Control	100%	100%	100%	100%
Control + Catalase	100%	100%	100%	100%

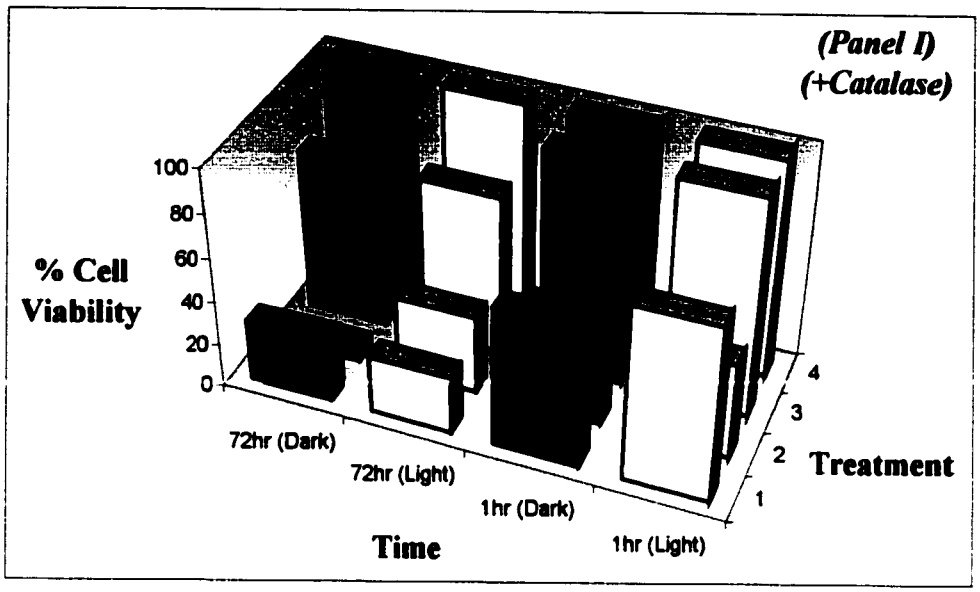

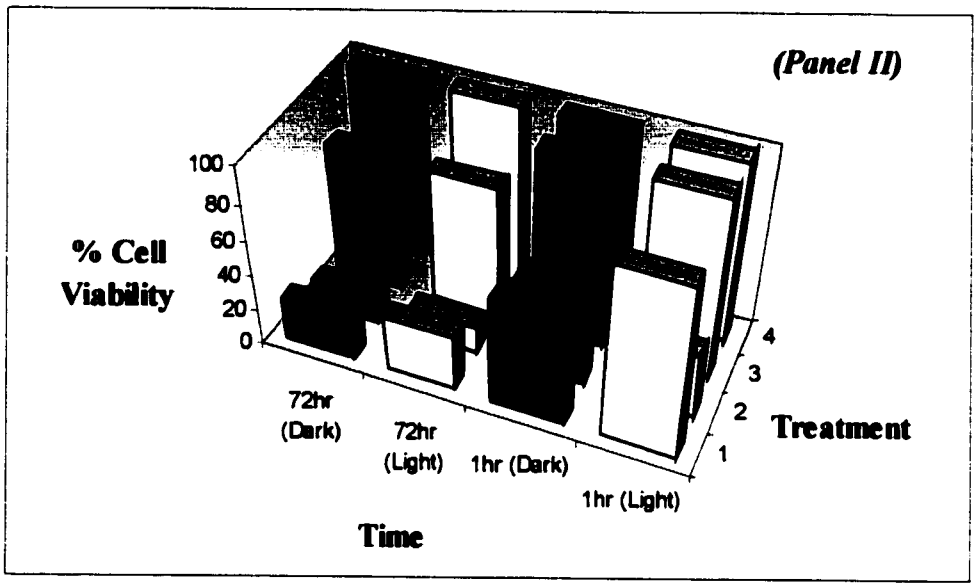

Figure 1.23C- Dendrimer-GSNO (0.85 μM) photo-induced cytotoxicity. The cytotoxic effect of Dendrimer-GSNO and glucose oxidase towards human colon adenocarcinoma cells (SW 948) in culture was monitored for 72 h after exposure to the following treatments. (1) Dendrimer-GSNO (0.85 μM); 2- Dendrimer-GSNO (0.85 μM) + GOD (9.2 μg/ml); 3- GOD (9.2 μg/ml); and 4- control (cells in 1 ml of media). One set received subsequent 60 min of exposure to light (open bars) prior to incubation, the other set was kept in the dark at all time (filled bars). All treatments were maintained either in the presence of catalase (Panel I), or in the absence of catalase (Panel II). Viability is expressed as a percent value of control cell density (i.e. treatment 4) at each time point.

Table 1.11: Cell viability (%) of SW-948 treated with dendrimer-GSNO (0.85 μM), GOD, PDT.

Cell viability (%)

TREATMENT	1 HR (LIGHT)	1 HR (DARK)	72 HR (LIGHT)	72 HR (DARK)
D-NO	96%	60%	31%	24%
D-NO +Catalase	64%	64%	26%	29%
D-NO + GOD	36%	48%	14%	14%
D-NO + GOD + Catalase	44%	48%	36%	6%
GOD	100%	100%	74%	74%
GOD + Catalase	100%	100%	74%	74%
Control	100%	100%	100%	100%
Control + Catalase	100%	100%	100%	100%

Table 1.12: The comparison of cell viability (%) of SW-948 treated with dendrimer-GSNO/GOD and T-NO/GOD.

Cell viability (%)

TREATMENT	1 HR (LIGHT)	1 HR (DARK)	72 HR (LIGHT)	72 HR (DARK)
Dendrimer-NO/GOD	28%	52%	2%	19%
T-NO/GOD	24%	76%	2%	44%

4.3 Application of PDT in glaucoma filtration surgery

A characteristic fluorescence emission spectrum of intracellular protoporphyrin IX (PpIX) was measured after treating both V79 fibroblasts with ALA (1 mM) for 24 h (Fig.1.24). Excitation of a cell suspension at 408 nm produced an emission maximum between 631-635 nm. The presence of an iron chelator Desferal (DEF) enhanced the emission intensity by over 3-fold.

Both V79 and TC fibroblasts demonstrated maximum uptake of ^{3}H-GSNO after 2 minutes of incubation (Figure 1.25). By 5 minutes, the recovered amount of radioactivity had declined. Furthermore, fluorescence microscopy of the dansyl-GSNO treated cells confirmed that, by 2 minutes, the cytoplasm of each fibroblast was qualitatively as fluorescent as those treated for longer periods (Figure 1.26).

In these studies, Tenon's capsule and V-79 fibroblasts cell lines were grown to confluence and incubated in the dark with ALA or GSNO for various time intervals (0 h, 4h, 24 h). The pretreated cells were then split into two sets. One set was treated with light for 10 min. The other set was kept in the dark. The extracellular media were removed from the cells and replaced with fresh media. Both sets of plates were incubated at 37°C in a 5% CO_2 incubator while monitoring cell viability up to 24 h after treatment. In addition to the treated samples, cells in media alone were used as a control where they were exposed to light of identical flux and duration, to account for the non-specific phototoxicity of 350 nm light.

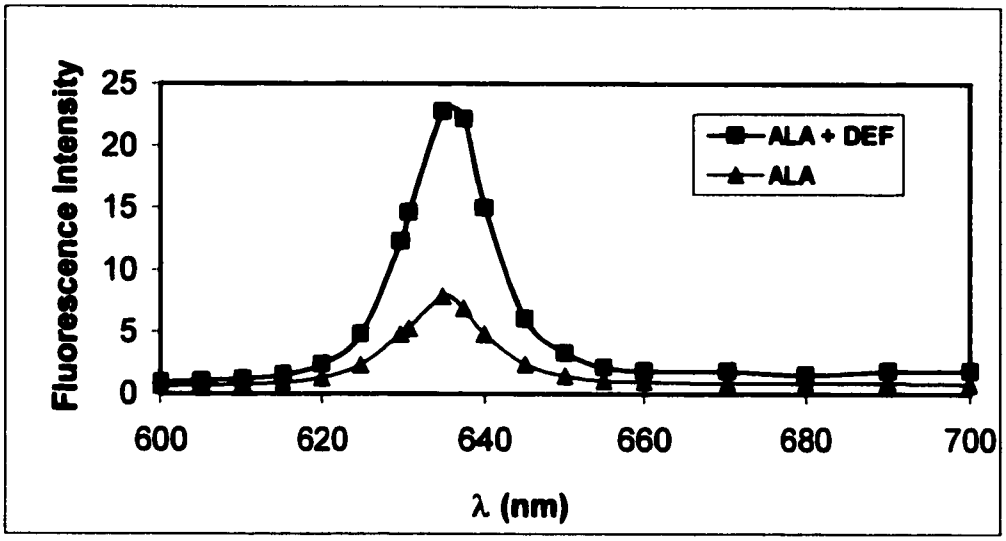

Figure 1.24- Evidence of PpIX production due to ALA ± DEF induction in cultured fibroblasts. Steady-state fluorescence emission spectrum of $1.0x10^6$ cells/mL of V79 fibroblasts after 24 hours of incubation with 1 mM of ALA ± 1 mM DEF prepared in phosphate buffered saline (PBS) pH 7.4. λ_{ex} 408 nm.

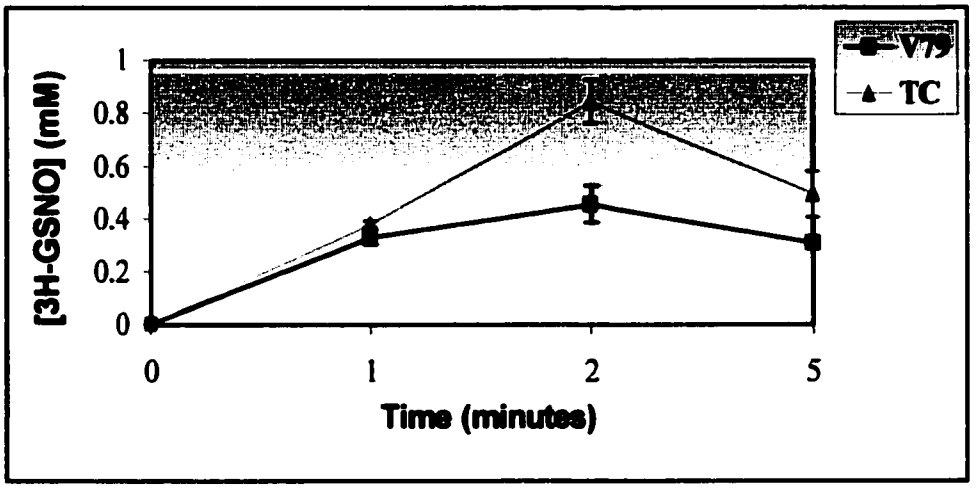

Figure 1.25- Radioactive measurement of GSNO uptake by cells in culture. Concentration of ^{3}H-GSNO was measured after treating $1.4x10^{6}$ cells/mL of both V79 and tenon's capsule fibroblasts with ^{3}H-GSNO (50 μM, 0.1 μCi/mL) at various times (1, 2, 5 min) intervals. Data shown here is the average of three separate trials and the error bars represent their standard deviation.

The presence of DEF produces a greater amount of cell death when cells are incubated with DEF at the shortest time interval (table 1.13), However, at longer periods the presence of DEF did not seem to significantly affect the viability (Fig 1.27). Treatment of the V79 fibroblasts with three concentrations of either ALA/DEF or GSNO (0.05 mM, 0.1 mM, 1.0 mM), at either 10 min, 4 h, or 24 h of incubation, showed that GSNO produced a greater amount of cell death at the shortest incubation interval (Figure 1.28). This effect was noted even at the smallest concentration (0.05 mM) where 79% cell death occurred after treatment with GSNO under these conditions compared to 4% with ALA/DEF. At the shortest incubation interval, ALA/DEF produced a greater degree of cytotoxicity (75%) at the highest (1.0 mM) concentration. This was still not as effective as 1.0 mM GSNO (90%). At the longest incubation interval (24 h), the effect of ALA/DEF on cell viability was comparable to that of GSNO at all three concentrations (table 1.14).

Treatment of TC fibroblasts with the same three concentrations of either ALA/DEF or GSNO, at the same incubation periods as previously described, produced similar trends to those seen with the V79 fibroblasts. At all incubation times, the TC fibroblasts seemed more sensitive to ALA/DEF than the V79 fibroblasts in that less cells remained viable post-photodynamic treatment (Fig. 1.29). Tenon's capsule fibroblasts at short incubation time (10 min and 4 hrs), GSNO (1 mM) resulted in greater cell death (93% and 90% respectively) than ALA/DEF (42% and 34% respectively). After 24 h of incubation, the cytotoxic effect of GSNO increased to 98% on the other hand ALA/DEF showed a 78% cell death. (Table 1.15).

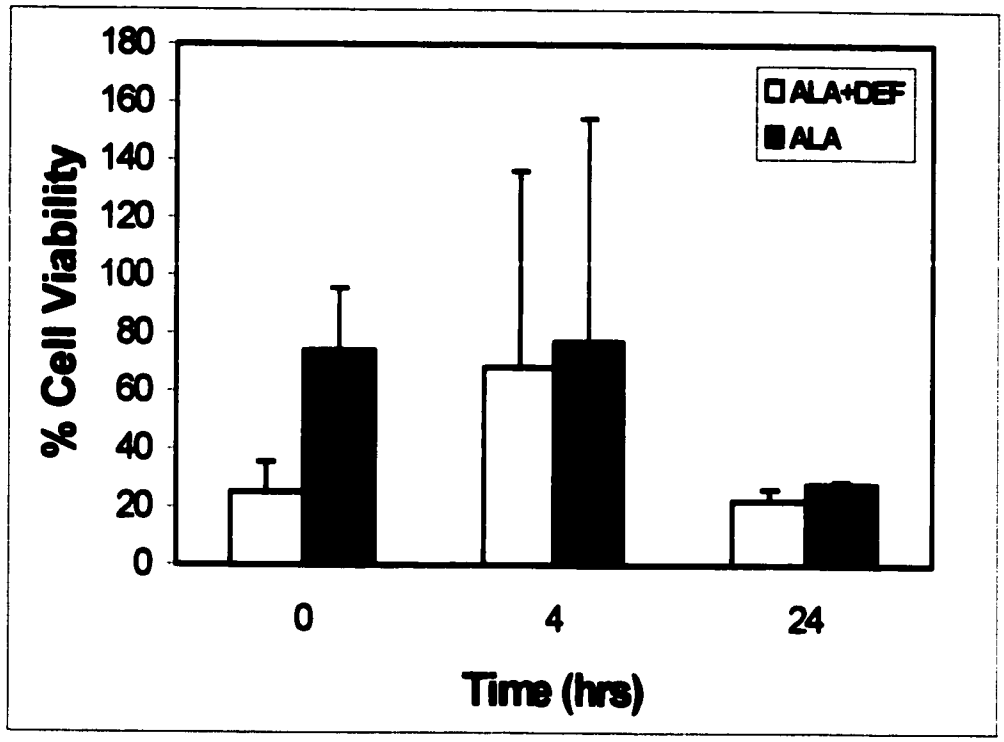

Figure 1.27- The cytotoxic effect of DEF towards cells in culture. Cell viability of V79 fibroblasts after treatment with either 1 mM ALA alone (red bars), or 1 mM ALA + 1 mM DEF (white bars) for various times. 0, 4, 24 h of incubation after addition of treatment to the cells, followed by irradiation for the standard 10 min period.

Table 1.13: Cell viability (%) of V-79 fibroblasts treated with ALA ± DEF.

Cell viability (%)

TREATMENT	10 minutes	4hrs	24hrs
ALA+DEF	25%	68%	22%
ALA	74%	77%	28%

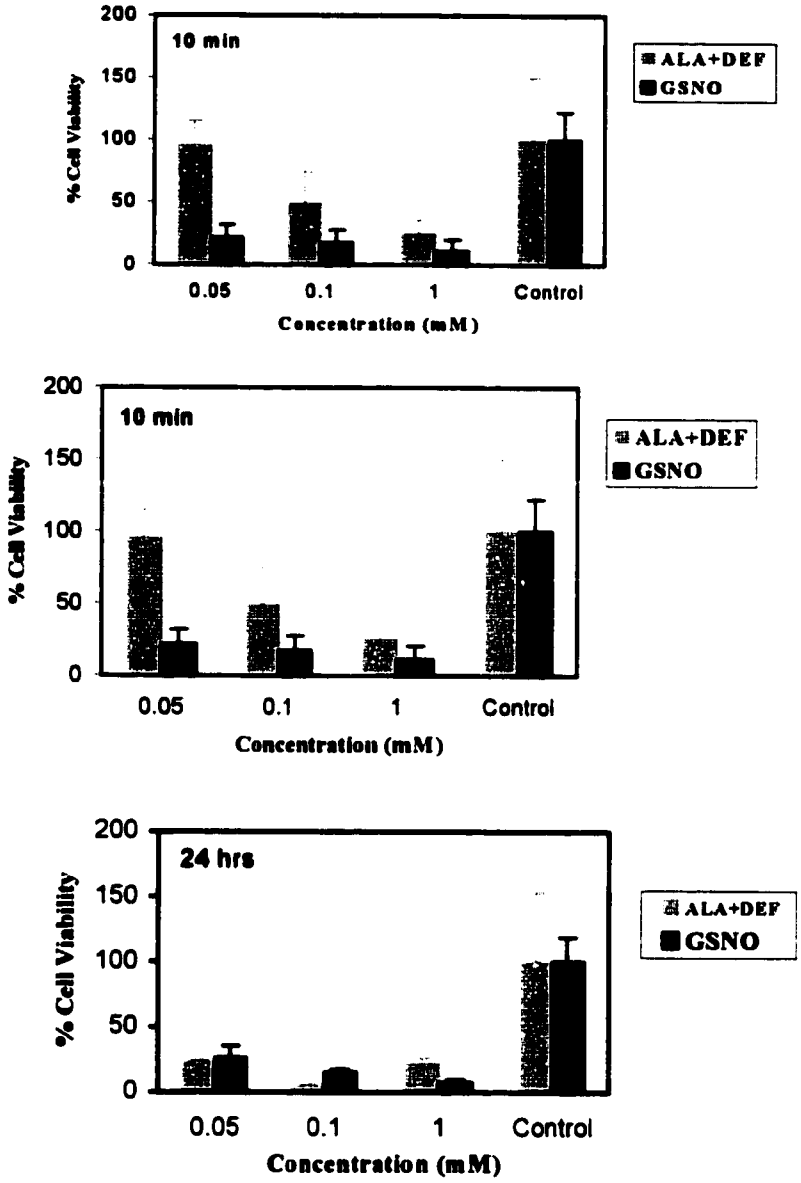

Figure 1.28 Comparison between ALA and GSNO photo-induced toxicity on V-79 fibroblasts. The cytotoxic effect of ALA + DEF and GSNO (+light), on V79 fibroblasts is expressed as percent cell viability. Cells were treated with three different concentrations of either ALA ± DEF or GSNO (0.05 mM, 0.1 mM, 1.0 mM), for various times interval (0, 4, 24 hrs), with subsequent light treatment for 10 min. Cell viability is the average of triplicate experiments.

Table 1.14: Cell viability (%) of V-79 fibroblasts treated with ALA + DEF and GSNO.

Cell viability (%)

(10 min incubation)

CONCENTRATION (mM)	ALA+DEF	GSNO
0	100%	100%
0.05	96%	21%
0.1	49%	17%
1	25%	10%

(4 h incubation)

CONCENTRATION (mM)	ALA+DEF	GSNO
0	100%	100%
0.05	77%	17%
0.1	45%	16%
1	68%	11%

(24 h incubation)

CONCENTRATION (mM)	ALA+DEF	GSNO
0	100%	100%
0.05	23%	26%
0.1	4%	15%
1	22%	7%

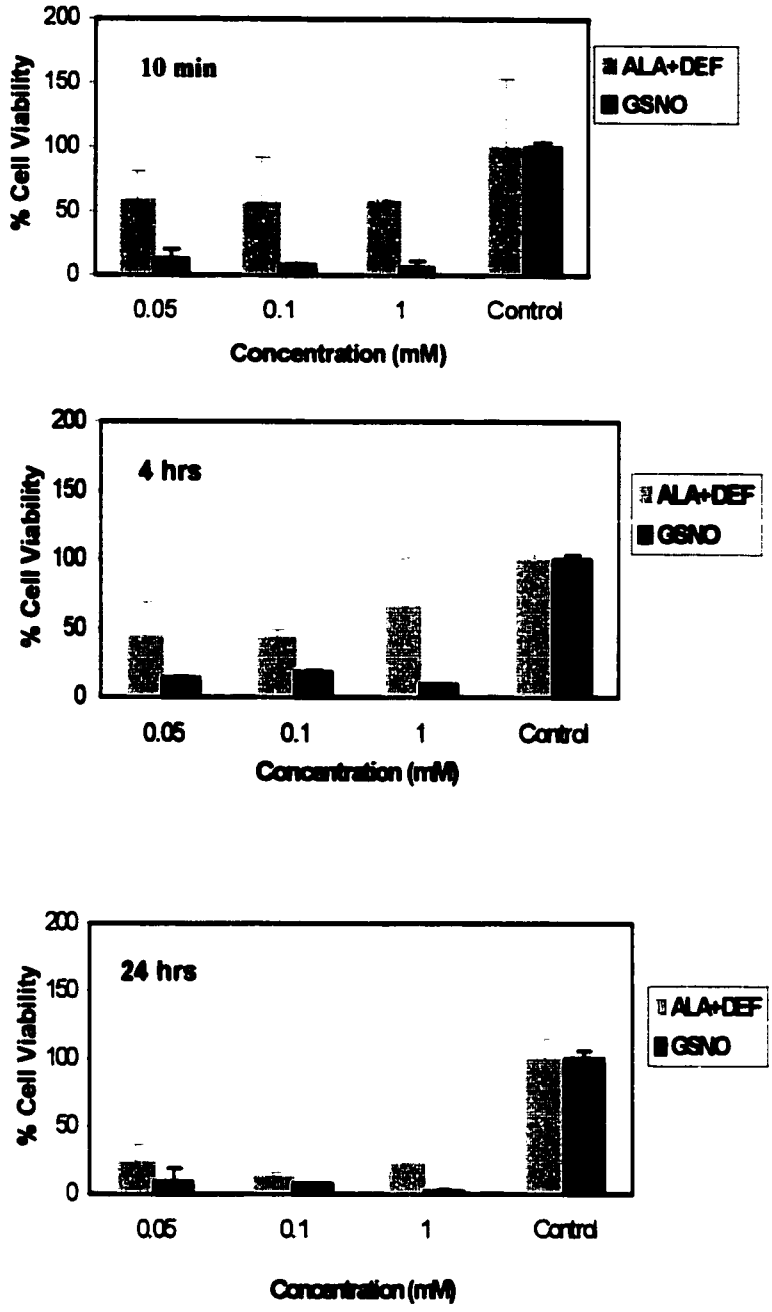

Figure 1.29- Comparison between ALA and GSNO photo-induced toxicity on TC fibroblasts. The cytotoxic effect of ALA+DEF and GSNO (+light), on Tenon's capsule fibroblasts is expressed as percent cell viability. Cells were treated with three different concentrations of either ALA ± DEF or GSNO (0.05 mM, 0.1 mM, 1.0 mM), for various times interval (0, 4, 24 h), with subsequent light treatment for 10 min. Cell viability values are the average of triplicate experiments.

Table 1.15: Cell viability (%) of Tenon's capsule fibroblasts treated with ALA + DEF and GSNO.

Cell viability (%)

(10 min incubation)

CONCENTRATION (mM)	ALA+DEF	GSNO
0	100%	100%
0.05	58%	12%
0.1	56%	8%
1	58%	7%

(4 h incubation)

CONCENTRATION (mM)	ALA+DEF	GSNO
0	100%	100%
0.05	44%	14%
0.1	43%	18%
1	66%	10%

(24 h incubation)

CONCENTRATION (mM)	ALA+DEF	GSNO
0	100%	100%
0.05	24%	9%
0.1	12%	7%
1	22%	2%

4.4 Mode of cell death post S-NO/PDT

In the early stages of apoptosis, changes occur at the cell surface, where phosphatidylserine (PS) gets translocated from the inner side of the plasma membrane to the outer layer. Annexin being a Ca^{2+}-dependent phospholipid-binding protein with affinity for PS, can be used as an excellent detection agent for PS. But since necrotic cells also expose PS as a result of loss of membrane integrity, both apoptotic and necrotic cells were detected. The simultaneous application of propidium iodide, a DNA stain allows the discrimination of necrotic cells and apoptotic cells by dye exclusion test. Annexin and propidium iodide were used to probe the cells after GSNO-PDT exposure (Fig 1.30). Both apoptotic and necrotic cells showed a positive signal with annexin, whereas only necrotic cell showed a positive signal with propidium iodide stain (table 1.16).

To quantitatively differentiate between the two cell death pathways, cells in culture were incubated with the non-radioactive thymidine analogue BrdU, which is incorporated into the genomic DNA. Then BrdU-labeled DNA fragments are released from the cells into the cell cytoplasm during apoptosis or into the cell culture during cell mediated cytotoxicity. These DNA fragments are detected immunologically by the ELISA technique (Fig. 1.31). Upon increased time of exposure to the apoptosis-inducing agent GSNO-PDT, DNA fragments appeared first in the supernatant. No BrdU-labeled DNA fragments were detected in the cell lysate during the first 4 hours after cell death induction, indicating that DNA fragmentation occurs after plasma membrane lysis. Therefore cell death is due to necrosis rather than apoptosis.

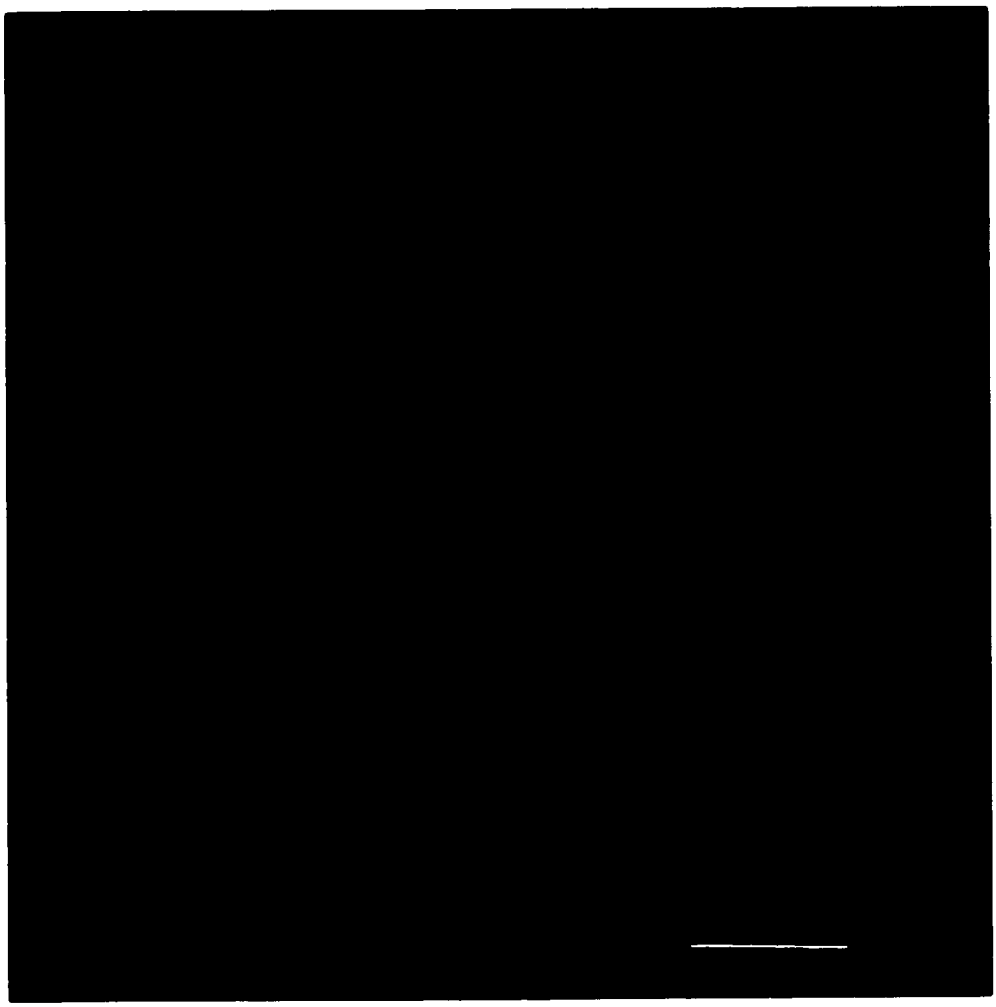

Figure 1.30- Analysis of the mode of cell death by annexin and propidium iodide. Cells treated with GSNO (1 mM) and light for 10 min, were stained with annexin/propidium iodide stain solution for 15 min at room temperature. Then each sample was evaluated by confocal scanning microscope. This picture reveals the visualization of NO-induced phosphatidylserine translocation by fluorescently labeled annexin in apoptotic MCF breast cancerous cells in culture (green color) and the visualization of NO-induced nuclear stain by fluorescently labeled propidium iodide in necrotic MCF breast cancerous cells in culture (red color). The scale bar represents 50 μm.

Table 1.16: Analysis of the mode of cell death by annexin and propidium iodide

CELL TREATMENT	CELLS	CELLS + GSNO (LIGHT)	
		APOPTOSIS	NECROSIS
Annexin	–	+	+++
Propidium Iodide	–	–	+++

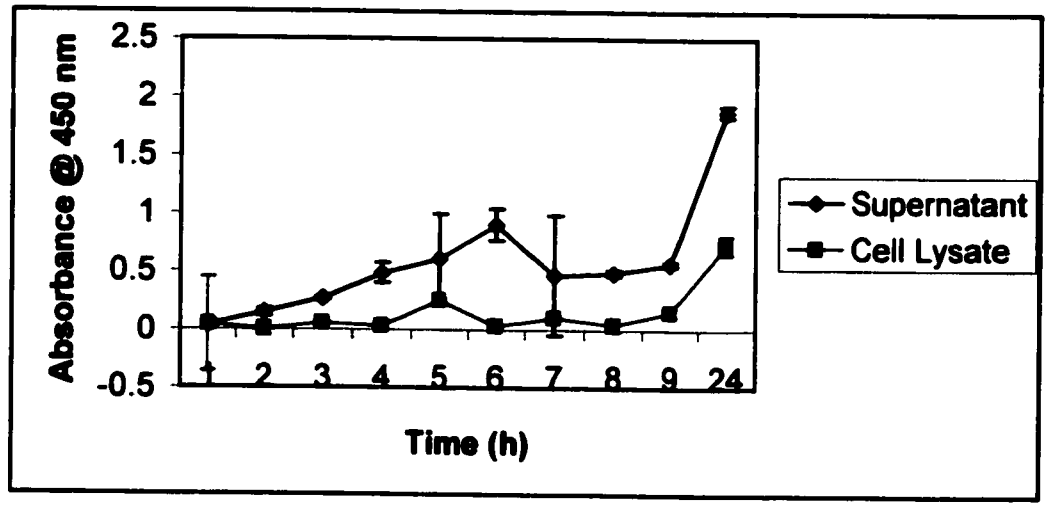

Figure 1.31- Kinetics of GSNO-induced cell death in MCF cells. 10^4 BrdU-labeled cells/well were incubated with 1 mM GSNO for 1 to 24 hrs 37°C followed with light exposure for 10 min. After the time indicated, 100 µl/well supernatant and 100 µl/well cell lysate were removed and tested by ELISA. Color development was assessed by horseradish peroxidase substrate tetramethylbenzidine (TMB) at 450 nm.

Recent studies have shown NO-mediated p53 over-expression, which is well known as a regulator of the cellular response to apoptosis. In contrast to the apoptotic effect in p53, Bcl-2 blocks the process of apoptosis. Here, we investigated the expression of p53 and Bcl-2 in modulation of apoptosis. Immunoblot analysis for Bcl-2 and p53 revealed that p53 level was increased in light-exposed, GSNO treated, Hep G2 cells in culture (Fig.1.32A), while Bcl-2 level was low or non-existent (Fig.1.32B). On the other hand cells treated with GSNO and protected from light showed a higher level of Bcl-2.

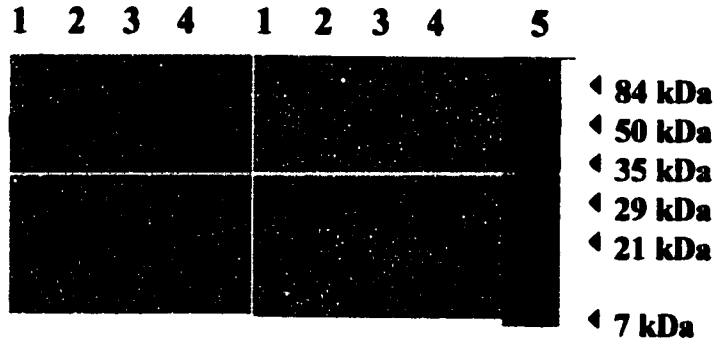

Figure 1.32 A, B- Immunoblot analysis for the detection of p53 and Bcl-2 in Hep G2 cells in culture. Cells were treated with GSNO in DMEM medium, pH 7.4 (±light for 10min), then Cells were lysed and proteins were separated on a 10 % SDS-PAGE gel, transferred to nitrocellulose and probed with a monoclonal antibody (anti-p53, panel A) or (anti-Bcl-2, panel B) followed by anti-IgG-HRP conjugate. Lane 1, Cells received light. Lane 2, cells received no light. Lane 3, treated with GSNO and light. Lane 4, treated with GSNO and no light. Lane 5, pre-stained (coomasie blue) molecular weight standards (from top: Bovine serum albumin 84 kDa, ovalbumin 50 kDa, carbonic anhydrase 35 kDa, soybean trypsin inhibitor 29 kDa, lysozyme 21 kDa, aprotinin 7 kDa).

CHAPTER 5

DISCUSSION

5.1 Thionein as a potential NO carrier for PDT

Photodynamic therapy (PDT) has been recognized as an effective and controlled method of cancer therapy since the late 1980's, but yet has suffered the same skepticism that all new therapeutic modalities face upon introduction into the clinical forum (Bown *et al.*, 1990). A large number of photosensitizing agents have been reported (Fritsch, 1998) yet none of these current agents seem to have ideal therapeutic properties. S-nitrosothiols (S-NO) are photolabile compounds, which upon exposure to light at 330 nm can generate nitric oxide (NO). Previous studies in our laboratory revealed the cytotoxic effect of GSNO in the presence of light toward cells in culture. However GSNO can only produce one mol of NO per mol. Therefore we looked for a NO carrier that is rich in thiols such as thionein. Thionein was able to carry 18 mol of NO per mol, thus delivered larger concentrations of NO to target cells during PDT.

The photolability of T-NO was explored when T-NO sample treated with light was monitored for various time intervals using a UV-Vis spectrophotometer. The absorption spectrum was totally abolished after 1 h light exposure. Thus the maximum time needed for S-NO to photolytically release all NO was estimated to be 1 hour.

In view of reports that S-NO exhibits higher cytotoxicity in the presence of H_2O_2 and in order to produce H_2O_2, an enzyme based method for the production of H_2O_2 was chosen. The enzyme of choice was glucose oxidase which catalyses the conversion of glucose to gluconic acid and H_2O_2 in the presence of oxygen. The presence of H_2O_2 simultaneously with T-NO after 72 h incubation showed a maximum cell death of 98% in

light treated samples. Conversely, upon addition of catalase, which removes H_2O_2, only 65% cell death occurs, thereby indicating that H_2O_2 indeed enhances T-NO toxicity towards targeted cells.

The site of action of T-NO/GOD/PDT on tumor cells is not yet clear. NO has been proposed to be an important cytotoxic mediator (Szabo *et al.*, 1996). However, recent data challenged the fact that NO is independently toxic. Accumulating evidence suggested that much of the NO-related injury may be due to the generation of peroxynitrite (Hausladen *et al.*, 1994). While NO is known to react with aconitase to inhibit mitochondrial respiration (Hausladen *et al.*, 1994), thus causing reversible inactivation of mitochondrial enzymes, peroxynitrite was shown to cause permanent suppression of mitochondrial function (Brunelli *et al.*, 1995). NO-induced aromatic ring nitration by a major pathway that involves the production of peroxynitrite, this was evident in our study where a single nitrated band at the correct molecular mass of BSA was detected in a BSA sample treated with T-NO/GOD in the presence of light. On the other hand samples protected from light showed no sign of nitration. These results indicated that some peroxynitrite is generated when NO is photolytically released in the presence of H_2O_2. Thus the cytotoxicity observed may be caused directly by NO/H_2O_2 or indirectly by the production of peroxynitrite.

Colon adenocarcinoma (SW 948) cells exposed to a combination of T-NO and GOD exhibited a significant difference in the cell death values between the light (98%) and dark (56%) conditions at 72 h following treatment (Fig.1.19). But there was an apparent cytotoxic effect in the dark treatment in comparison to controls. This is not surprising, as a recent study has shown that S-NO can produce peroxynitrite upon

reacting with superoxide in the dark (Jourd'heuil *et al.*, 1998). From previous reports, superoxide is known to be formed in all aerobic cells, including SW 948 cells, thus any aerobic cells exposed to S-NO/H_2O_2 would have had the ability to produce peroxynitrite in the dark.

$$O_2^{-\cdot} + RSNO \longrightarrow RSNO(O_2^-)$$

$$RSNO(O_2^-) + RSNO + H_2O \longrightarrow RSSR^{-\cdot} + NO_2^- + ONOO^-$$

To summarize, purification of metallothionein resulted in a very low yield after acid precipitation step. This is expected, as metallothionein once stripped from its metal ions, has the tendency to decompose 1500 times faster (Moffatt *et al.*, 1997). Clearly then, thionein is not an entirely suitable NO carrier for therapeutic settings. However, T-NO is a useful model for providing *in vitro* evidence for potential S-NO/PDT for cancer treatment. Thus we looked for a more suitable NO carrier such as dendrimer.

5.2 Dendrimer as a potential NO carrier

The effect of NO on cells is known to be dose dependent, although high concentrations of NO can be cytostatic and cytotoxic (Szabo *et al.*, 1996), low concentrations of NO may even protect some cell types from damage (Genero *et al.*, 1995). Our goal is to be able to deliver the largest amount of NO through PDT therapy. The unique properties, precise structure, and thorough characterization of starburst

dendrimers prompted us to investigate applications of these molecules as a potential NO carrier.

The conjugation of dendrimer to thiols faces several problems. Since the EDAC/NHS system used to couple thiols to G3 dendrimers at varying pH level (pH 5, 7.2, 8) yielded a maximum of 3 thiols per dendrimer only, we optimized this technique by using dendrimer/SPDP conjugation which enhanced the yield to 10 thiols per dendrimer. Even though dendrimers are not prone to polymerization like metallothionein, experimentally dendrimers could not be modified to carry more than 10 thiols per dendrimer molecule.

The toxicity of Dendrimer-NO toward SW-948 cells was enhanced in the presence of H_2O_2. Light treated samples showed a 98% cell death after 72 h incubation, on the other hand, samples protected from light showed 81% cell death. Clearly then, Dendrimer-NO is an efficient NO carrier due to its simple synthesis and high toxicity towards targeted cells. Consequently, SW 948 cells in the dark were more sensitive to Dendrimer-NO/GOD treatment (81% cell death at 72 h) than T-NO/GOD treatment (56% cell death at 72 h) at comparable concentrations. Thus in the light treated samples, the cytotoxicity of both T-NO/GOD and Dendrimer-NO/GOD were comparable at 72 h. This was expected as due to the short lifetime of NO upon light exposure, NO is rapidly released to target cells from both carriers. Under dark conditions the observed toxicity of both T-NO/GOD and Dendrimer-NO/GOD is believed to be due to possible S-NO/superoxide reaction to yield peroxynitrite.

5.3 Application of PDT in glaucoma filtration surgery

One approach for PDT is the use of the photosensitizing agent protoporphyrin IX (PpIX) which is biosynthesized when cells are treated with 5-aminolevulinic acid (ALA) (Noodt *et al.* and Krammer *et al.*, 1996; Kennedy *et al.*, 1992). It has been used to treat a variety of malignancies and skin disorders (Fritsch *et al.*, 1998). The problem with ALA is that the initial step in the ALA-induced synthesis of porphyrins is the penetration of ALA through the plasma membrane. Since ALA is a hydrophilic molecule, its hydrophilicity may be a clinical limitation for its use in PDT.

In this study, ALA photobiology has been shown to produce photosensitizing concentrations of PpIX in both the V79 Chinese Hamster lung fibroblasts and human Tenon's capsule fibroblasts. In accordance with previous reports, the presence of the iron chelator Desferal enhanced the accumulation of PpIX (Berg *et al.*, 1996), but only seemed to augment the PDT effect at short incubation times. DEF, being a highly specific membrane-permeable iron chelator, blocks ferrochelatase necessary to convert PpIX into heme. The co-administration of 1 mM Desferal and ALA significantly increased PpIX accumulation in all carcinoma cells (Iinuma *et al.*, 1994).

S-NO was shown to be toxic to cells in culture, thus we investigated the possibility of using this technique to improve glaucoma filtration surgery by inhibiting fibroblast proliferation following the surgical procedure. We have shown in this *in vitro* study that GSNO can rapidly be incorporated into both V79 and TC fibroblasts. A specific cytotoxic effect in V-79 and TC (90 and 93% respectively) was observed after incubation with GSNO (1mM) after 10 min incubation time, however ALA/DEF (1mM) performed best after 24 hours of incubation (78% and 78 % respectively)

ALA and GSNO were compared, in both standard and human Tenon's capsule fibroblasts. GSNO effectively inhibited proliferation at concentrations, incubation times and irradiation times compatible with its potential use in glaucoma filtration surgery. This effect was superior to that of 5-aminolevulinic acid at short incubation periods (minutes), but comparable when the treatment time was increased to 24 hours.

Clearly GSNO is superior to current therapy for GFS. A possible future mode of treatment is a slow release capsule incorporated in the eye during GFS to release constant dose of GSNO, thus continually inhibiting fibroblasts proliferation post surgery.

5.4 Mode of cell death post S-NO/PDT

S-NO/PDT was shown to cause cell death *in vitro*. Moreover, the mode of this cell death is not yet clear. A major difference between apoptosis and necrosis is the implications that cell death have for its neighbors (Savill *et al.*, 1993). An apoptotic cell is rapidly engulfed by phagocytes or by neighboring cells before they can lyse. On the other hand, a necrotic cell undergoes uncontrolled spillage of intracellular contents thus causing inflammation to surrounding cells.

One of the morphological characteristics associated with cell death is a loss of membrane integrity with the concomitant inability to exclude vital dyes such as trypan blue. This technique allowed us to determine the percent cell viability thus didn't give an indication of the mode of the cell death, since both necrosis and apoptosis undergoing secondary necrosis permit dye uptake. Therefore this technique was used in conjunction with more informative morphological methods such as annexin/propidium iodide stains.

After treating cells with annexin and propidium iodide stains, breast cancer (MCF) cells did not show the typical morphology of apoptotic cells and did not retain their plasma membrane integrity. Digestion of the plasma membrane was very characteristic of necrotic cell death, which allows the incorporation of propidium iodide into the cells.

To further differentiate between necrotic and apoptotic pathways, the DNA fragmentation assay was performed. The percentage of non-viable cells in each exposure group was greater than the percentage of cells undergoing apoptotic DNA fragmentation by ELISA assay over a long period of incubation time. This could suggest that cell death from NO released by photolysis is primarily necrotic and that apoptotic fragmentation plays a lesser role. Our data is comparable with a recent report stating that an inhibition of caspases and conversion of the mode of cell death to necrosis appeared upon cell exposure to nitric oxide (Dimmeler *et al.*, 1997).

Another criterion used to distinguish apoptotic from necrotic cell death has been the sensitivity of apoptosis to Bcl-2 and p53 (Jacobson *et al.*, 1994). The exact mechanism by which Bcl-2 exerts its anti cell death action is unknown. It has been shown that Bcl-2 appears to influence the level of reactive oxygen species and functions in an antioxidant pathway to prevent apoptotic (Steinman *et al.*, 1995) as well as necrotic cell death (Lindenboim *et al.*, 1995). Our investigation revealed necrotic cell death in conjunction with downregulation of Bcl-2 post S-NO/PDT in cultured MCF cells thus this was not unexpected as several studies now show that overexpression of Bcl-2 can inhibit necrotic cell death (Kane *et al.*, 1995; Zhong *et al.*, 1993). On the other hand, the true role of p53 is to hold a damaged cell in the G1 while the damage is repaired. Cells

that try to oppose the G1 block may end up by activating the suicide pathway (Lane *et al.*, 1992). Our data document transient p53 protein detection before and after S-NO/PDT towards Hep G2 cells in culture. Whether p53 had a major role in differentiating between necrotic and apoptotic cell death following S-NO/PDT is not yet clear.

The overall picture achieved is that upon photolysis of RS-NO, nitric oxide is released which then interacts with endogenous superoxide producing peroxynitrite leading to necrotic cell death. Thus S-NO/PDT was proven to be an effective method for killing cells *in vitro* and could potentially in the future be applied as a treatment of various diseases.

CHAPTER 6

CONCLUSION

Collectively, presently available information provides a basis for a tentative model for the role of NO in PDT. We have demonstrated that metallothionein, once stripped from its metal ions, can serve as a potent NO carrier. Thionein can carry up to 18 mol of NO/mol via S-nitrosylation of its 20 constituent Cys thiols and thus serve as a multiple source of NO (c.f. GSNO, which produces only one NO per molecule). T-NO is stable to transnitrosylation by the ubiquitous intra and extracellular thiols. The S-nitrosothiol bond of T-NO is photolabile and yields NO upon photolysis. This property can be utilized for photochemical release of NO from T-NO. We were able to demonstrate that the combination of T-NO with GOD in the presence of visible light can decrease cell viability of human colon adenocarcinoma cells by 98 % within 72 h.

Dendrimer-thiol conjugates, on the other hand can carry NO via S-nitrosylation of its constituent thiol. Experimentally, we were able to couple up to 10 thiols/dendrimer. We also were able to demonstrate that the dendrimer by itself is proven to be a non toxic agent to the cells but the combination of Dendrimer-NO and GOD in the presence of visible light showed 98% cell death in human colon adenocarcinoma cells within 72h incubation period.

In an effort to improve success of GFS, S-nitrosoglutathione was proven to inhibit effectively the proliferation of both standard and human Tenon's capsule fibroblasts at

concentrations, incubation times, and irradiation times compatible with its use in filtration surgery. Upon investigation of the mode of cell death post S-NO/PDT, MCF human breast cancer cells treated with nitric oxide-photodynamic therapy showed a direct evidence of necrotic cell death based on the annexin/propidium iodide fluorescent study which was confirmed by the quantitative DNA fragmentation assay.

PART II

CHAPTER 1

INTRODUCTION

1.0 Overview

Cardiovascular disease is the principal cause of mortality in patients with diabetes mellitus (Stamler *et al.*, 1993). Myocardial infarction and stroke representing 80% of all mortalities in non-insulin-dependent diabetes mellitus subjects (NIDDM) (Martina *et al.*, 1998). There is conclusive evidence that platelet-NO metabolism is altered in various diseases such as atherosclerosis (Buttery *et al.*, 1996), hypercholesterolemia and diabetes mellitus (Calver *et al.*, 1993). Recent studies revealed that constitutive nitric oxide synthase (cNOS) level is decreased in platelets of insulin dependent diabetes mellitus (IDDM) and non-insulin dependent diabetes mellitus (NIDDM) subjects. With this in mind, the level of induced nitric oxide synthase was investigated in diabetic and control platelets.

The benefits of cholesterol lowering for prevention of coronary artery disease have been well established. Currently, 3-hydroxy-3-methylglutaryl coenzyme A (HMG-CoA) reductase inhibitors (statins) are first-line therapy for the reduction of cholesterol level. However, Atorvastatin, which was recently introduced, has a greater efficacy in lowering LDL cholesterol than other statins. Recently these statins have been shown to have other beneficial effects other than lipid lowering (Lea *et al.*1997). Here we explored the effect of Atrovastatin on intraplatelet NO metabolism.

1.1 NOS and Diabetes Mellitus

1.1.1 Diabetes Mellitus

Diabetes mellitus, one of the most common endocrine diseases, is a syndrome of disturbed intermediary metabolism caused by inadequate insulin secretion or impaired insulin action, or both. It is grouped into two types Insulin Dependent Diabetes Mellitus (IDDM) also known as type I diabetes. It is mainly caused by lack of insulin, and usually develops at early stages of life. Non-Insulin Dependent Diabetes Mellitus (NIDDM) or Type II diabetes is caused by improper insulin secretion or lack of an insulin receptor on the cell surface and occurs at later stages of life.

1.1.2 Platelet-NO synthesis in pathological conditions

Platelets are anucleated blood elements that are produced in the bone marrow as megakaryocyte, and then get fragmented and released into circulation as platelets. Their size ranges from 0.5-1.0μm in thickness and from 1.5-2.5μm in length. They possess a lifetime of ~ 10 days (Gentry *et al.*, 1992) and human reference range of 150-450 $\times$ 10^9/ml. Under physiological conditions, when a blood vessel is ruptured, platelets become activated to form a platelet plug that prevents blood loss. The activation of platelets is tightly controlled by a number of regulating factors including nitric oxide. Nitric oxide regulates platelet activation in autocrine (NO generated inside platelets) and paracrine (NO generated outside platelets) manner. The basal production of NO for platelets could generate as much as 20 nmol NO per liter of blood (Zhou *et al.*, 1995). Platelets from patients suffering from hypertension or

diabetes are more susceptible to activation than controls (Radomski *et al.*, 1991). NO plays a major role as a regulator of vascular homeostasis and is reduced during the course of essential hypertension (Calver *et al.*, 1992), and coronary atherosclerosis (Drexler *et al.*, 1991). Moreover, it was shown that constitutive nitric oxide synthase (cNOS) is also reduced in subjects with diabetes (IDDM and NIDDM) (Rabini *et al.* and Martina *et al.*, 1998). On the other hand induction of nitric oxide synthase (iNOS) causes NO overproduction which is seen in subjects suffering from hypotension and cardiovascular collapse.

1.1.3 Biosynthesis of Nitric oxide

Nitric oxide is an important mediator of both physiological and pathological processes (Moshage *et al.*, 1997). In the cardiovascular system, NO serves as an endothelial-dependent vasodilator, an antithrombotic agent, an antiproliferative molecule and a regulator of cardiac contractility (Upchurch *et al.*, 1996).

The general scheme of NO biosynthesis (Fig.2.1) starts when a guanidino nitrogen of L-arginine undergoes oxidation via molecular oxygen to yield NO and citrulline (Dewanjee *et al.*, 1996). The co-substrate nicotine adenine dinucleotide phosphate (NADPH) provides the necessary electrons for the formation of the intermediate N-hydroxy-L-arginine and for its further oxidation (Nathan, 1992). Cofactor BH_4 has been known to play a major role in directing the electron flow in the enzyme to L-arginine (Wever *et al.*, 1997). Depletion of BH_4 resulted in uncoupling of oxygen reduction and arginine oxidation, thus generating superoxide

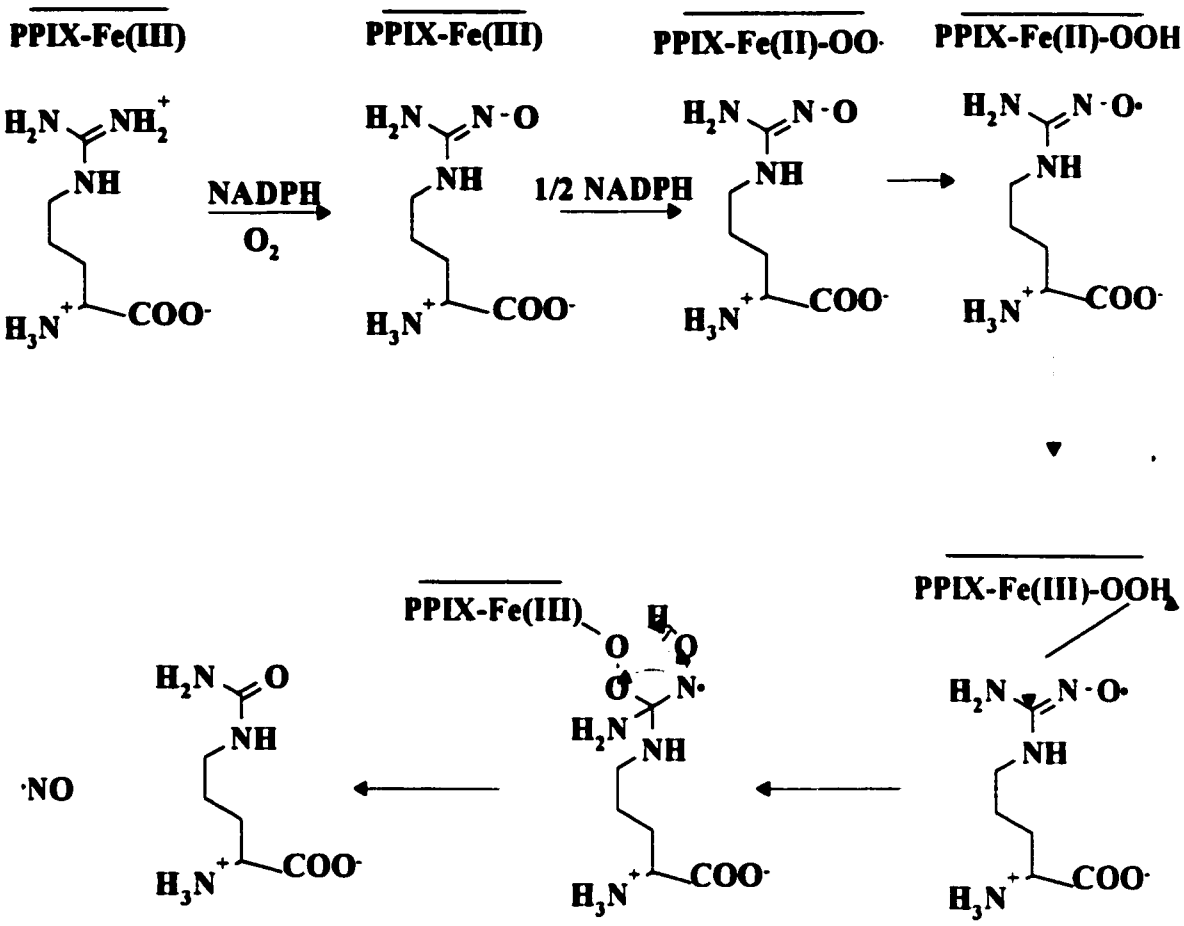

Figure 2.1-Reaction mechanism of nitric oxide synthase. Protoporphyrin IX (PpIX) conjugated to iron to form the catalytic heme group in NOS (Sexton 1994).

and hydrogen peroxide. Once NO is formed, it can then bind to several targets such as the heme groups in NOS themselves, guanylyl cyclase, sulfur-containing amino acids, hemoglobin, and other molecules (superoxide and oxygen) (Dewanjee *et al.*, 1996).

At least three isoforms of NOS have been detected. The endothelial (eNOS) and neuronal (nNOS) are continuously present and thus termed as constitutive NOS enzymes and are regulated by Ca^{2+}/calmodulin. The inducible NOS (iNOS) originally detected in macrophages and in the endothelium, is expressed in response to cytokines and cellular debris of microbial origin.

The three known NOS isoforms are all dimeric, each consists of two domains: oxygenase and reductase. Active dimeric NOS contains iron protoporphyrin IX (heme), tetrahydrobiopterin (BH_4), FAD, FMN as bound prosthetic groups, and also contains binding sites for L-arginine, calmodulin, and NADPH (Stuer *et al.*, 1997).

For Both nNOS and eNOS, the main mechanism of regulation is provided by the Ca^{2+}/calmodulin system. Bound calmodulin is necessary for the transfer of electrons from the flavin nucleotides to the heme moiety of NOS. As the intracellular free Ca^{2+} concentration increases, calmodulin binds to NOS and stimulates NO formation (Schmidt *et al.*, 1991). On the other hand, iNOS contains tightly bound calmodulin (Cho *et al.*, 1992) and is not subject to regulation by Ca^{2+} but it does requires induction by cytokines. The synthesis of nitric oxide can be easily inhibited by several L-arginine analogues, including N^G-monomethyl-L-arginine (L-NMMA), N^G-nitro-L-arginine methyl ester (L-NAME), and N^G-nitro-L-arginine (L-NA) (Knowles *et al.*, 1994; Kerwin *et al.*, 1995).

The L-arginine-NO pathway has been shown to be involved in the pathophysiology of hyperoxia-induced seizures via various regulating mechanisms (Bitterman *et al.*, 1998). NO-mediated cellular injury may be accomplished by a variety of mechanisms, including disruption of mitochondrial respiration, enzyme inhibition, lipid peroxidation and genetic mutation. Nitric oxide itself is not highly toxic but its toxic effects are largely mediated via intermediates such as N_2O_3 and peroxynitrite, arising from the reaction of NO with either molecular oxygen or reactive oxygen species (Gordge *et al.*, 1998).

It is believed that iNOS under conditions of limiting L-Arg can produce superoxide ($O_2^{-\bullet}$) as well as NO (Klatt *et al.*, 1993). Superoxide is a free radical that is shown to be released by NADPH oxidase activity during the respiratory burst of macrophages in response to several stimuli (Baggiolini *et al.*, 1990) and during autoxidation of hemoglobin, myoglobin and cytochrome c (Muijsers *et al.*, 1997). There is evidence that neuronal NOS, transfected in human kidney 293 cells, can produce both NO and superoxide when L-arginine concentration is relatively low (Xia *et al.*, 1996). Another recent study showed that the level of superoxide is highly increased in diabetes mellitus, atherosclerosis, and high renin hypertension (Munzel *et al.*, 1997). These two radicals $NO^{\bullet}$ and $O_2^{-\bullet}$ react at diffusion controlled rates to yield peroxynitrite ($ONOO^-$).

1.1.4 Pathophysiology of peroxynitrite

Recent studies have shown that iNOS-dependent peroxynitrite production has been implicated in the pathophysiology of atherosclerosis (Harrison *et al.*, 1997;

Buttery *et al.*, 1996), hypercholesterolemia (Calver *et al.*, 1993), hypertension (Huang *et al.*, 1995), and diabetes mellitus (Calver *et al.*, 1993). Peroxynitrite is a highly reactive species, which is capable of rapid oxidization of a wide variety of biomolecules including plasma, proteins, lipids, carbohydrates and nucleic acids, as well as nitration and hydroxylation of aromatic compounds, such as tyrosine (Beckman *et al.*, 1996; Pryor *et al.*, 1995). It modifies free or protein-associated tyrosine residues to give nitrotyrosines, leaving a marker detectable *in vivo*.

Overproduction and uncontrolled formation of peroxynitrite is an important factor in the tissue damaging mechanisms during pathological situations such as chronic inflammation. For example, induction of iNOS and suppression of superoxide dismutase, favoring peroxynitrite formation, were shown in experimental colitis (Seo *et al.*, 1995). On the other hand, NOS inhibition by analogs of L-arginine prevented this peroxynitrite formation as expected (Sherman *et al.*, 1992).

1.2 The effects of Atorvastatin on NOS

1.2.1 Hypercholesterolemia and heart disease

It has been known that high cholesterol levels are associated with an increased risk of atherosclerosis, thus reduction of cholesterol-carrying lipoproteins in circulation can reduce the risk of heart disease in general. Normal cholesterol level is considered to be less than 5.2 mmol/L, when it exceeds this level the first approach taken is diet therapy which includes controlling the intake of total cholesterol and saturated fat, weight control along with physical activity. If that is unsuccessful the second approach would be drug therapy. The decision of the type of drug and the

specific dosage varies between individuals with respect to age, history, and severity of hypercholesterolemia. There are a number of hypolipidemic drugs that are currently available such as β-hydroxy-β-methylglutaryl coenzyme A (HMG-CoA) reductase inhibitors (Lovastatin, Pravastatin, Simvastatin, and Atorvastatin). HMG-CoA reductase inhibitors are considered the newest class of lipid lowering drugs in use.

1.2.2 Atorvastatin

Atorvastatin is a synthetic competitive inhibitor of HMG-CoA reductase, the enzyme necessary for the conversion of HMG-CoA to mevalonate, which is a rate limiting step in cholesterol biosynthesis in the liver (Lea *et al.*, 1997). The resulting affect of Atorvastatin is a reduction in intracellular cholesterol leading to an increase in the number of low density lipoprotein (LDL)-receptors and increase in LDL-cholesterol clearance from plasma (Bocan *et al.*, 1992; Gaw *et al.*, 1993). This reduces LDL-cholesterol (LDL-c), the number of LDL particles, very low density lipoprotein-cholesterol (VLDL-C), as well as serum triglycerides (TG) (Haria *et al.*, 1997).

Atorvastatin is a new HMG-CoA reductase inhibitor. It has a high hepatic selectivity over other statin drugs and a high efficiency in reducing LDL-cholesterol. This drug appears to have the potential to claim a place alongside other HMG-CoA reductase inhibitors as a first-option drug for patients with hypercholesterolemia and because of its triglyceride-lowering properties, it may be an appropriate therapeutic option for patients with combined hyperlipidemia or hypertriglyceridemia (Lea *et al.*, 1997).

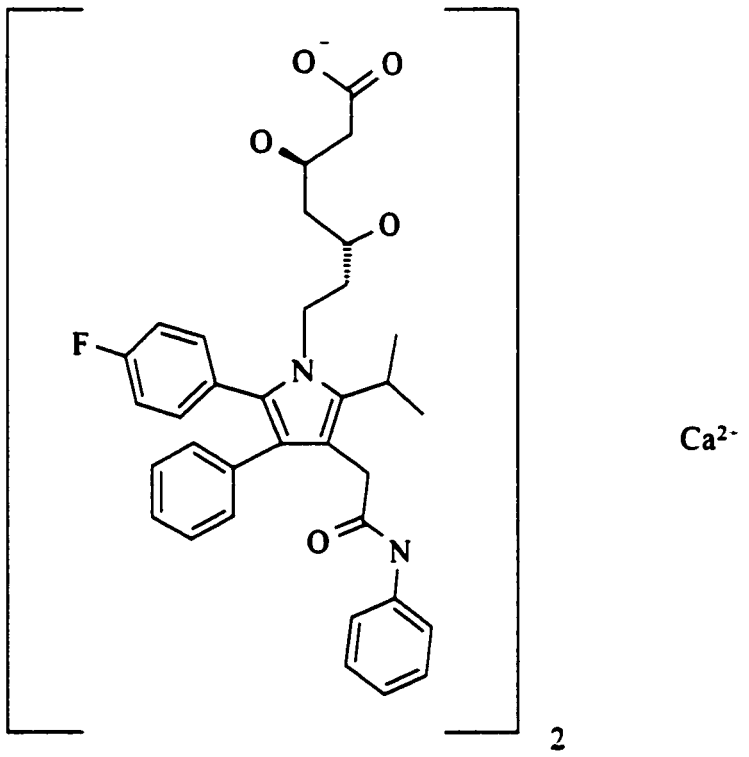

Figure 2.2-Atorvastatin Structure (Lea *et al.*, 1997)

1.3 Aims of this study

Impaired platelet function plays a major role in atherosclerosis. The aim of this study was to assess the function of NO synthesis in platelets of patients with diabetes mellitus. Since little has been known about platelet-NOS function, we investigated the role of iNOS, and the possibility of peroxynitrite production in diabetic platelets.

The second part of this study involved the assessment of the new HMG-CoA reductase inhibitor used as hypolipidemic drug, Atorvastatin. The clinical aspect of Atorvastain and its correlation with intraplatelet nitric oxide synthase isozymes were thoroughly investigated in hypercholesterolemic subjects.

CHAPTER 2

MATERIALS

The following materials are used throughout the course of this study.

2.1 Chemicals, Biochemicals and Supplies

- Human whole blood was provided by the chemistry department at the Hotel Dieu hospital (Windsor, ON).
- Platelet concentrates were obtained from the Blood bank department at the Hotel Dieu Hospital (Windsor, ON) and the University of Ancona (Ancona, Italy).
- 2,7-dichlorofluorescin diacetate (DCFDA) and N^G-monomethyl-L-arginine (L-NMMA) were obtained from Molecular Probes (Eugene, OR).
- L-Arginine from Sigma (St. Louis, MO).
- Primary antibody (anti-iNOS), secondary antibody (anti-mouse IgG-peroxidase) and mac-NOS (positive control) from Transduction Laboratories (Lexington, Kentucky).
- Anti-nitrotyrosine, (host mouse) was obtained from Upstate Biotechnology (Lake Placid, NY).
- ECL western blotting detection reagents and hyperfilm were obtained from Amersham International (Buckinghamshire, England).
- D-MEM medium, fetal bovine serum, Trypsin/EDTA were obtained from GIBCO (Grand Island, NY).

- Developer and fixer for hyperfilm were purchased from Kodak Canada (Toronto, ON).
- Hydrogen peroxide was purchased from BDH Inc. (Toronto, ON).
- SDS-PAGE molecular standards, Tween-20, protein assay dye reagent were obtained from Bio-Rad Laboratories (Hercules, CA).
- Nitrocellulose membrane BA-S-83 were obtained from VWR Scientific Inc. (Mississauga, ON).

2.2 Equipment

Beckman J-6B centrifuge (Palo Alto, CA).

Bio-Rad Mini gel and Trans-Blot electrophoretic apparatus (Hercules. CA).

Bio-Rad MRC 600 and 1024 Confocal Laser Scanning Microscope (Hercules, CA).

Bio-Rad power supply model Power Pac 300 (Hercules, CA).

Bio Rad model GS-670 imaging densitometer (Hercules, CA).

Eppendorf Model 5415C microcentrifuge from Baxter/Canlab, Inc. (Mississauga, ON).

Fisher Scientific micro-centrifuge model 59A (Pittsburgh, PA).

Hitachi model F-3010 Spectrofluorometer, Naka Works, Hitachi Ltd. (Tokyo, Japan).

Mettler AJ100 balance, Mettler Instrument Corp. (Hightstown, New Jersey).

Millipore filtration apparatus, Millipore Corp. (Milford, MA).

Orion 420A pH meter, Orion Research Inc. (Boston, MA).

Shimadzu UV-160 spectrophotometer (Kyoto, Japan).

U-V laser LSM 410 confocal microscope (Ziess, Canada)

2.3 Reagents and Buffers

- 10 % ACD buffer consisted of 0.8% citric acid, 2.2% sodium citrate and 2.4 % dextrose.
- Ca^{2+}-free Tyrode's buffer consisted of 137 mM NaCl, 2.7 mM KCl, 1.0 mM $MgCl_2$, 0.35 mM $NaHCO_3$, 119 mM glucose, pH 5.5.
- Sample buffer consisted of 125 mM Tris-HCl pH 6.8, 2% SDS, 5% glycerol, 0.003% bromophenol blue, and 1% β-mercaptoethanol).
- 8% SDS-polyacrylamide composed of resolving and stacking gels.
    - Resolving gel consisted of 2.3 mL H_2O, 1.3 mL of 30% acrylamide, 1.3 mL of 1.5 M Tris pH 8.8, 50 μL of 10 % SDS, 50 μL of 10 % ammonium persulfate, 3 μL of TEMED.
    - Stacking gel consisted of 68 μL of H_2O, 170 μL of 30 % acrylamide mix, 130 μL of 1.5 M Tris pH 8.8, 50 μL of 10 % ammonium persulfate, and 4 μL of TEMED.
    - Gel running buffer consisted of Tris 15 g/L, glycine 72 g/L, SDS 5 g/L, H_2O 0.6 L, pH 8.3.
- Transfer buffer consisted of 25 mM Tris base, 192 mM glycine, 20% methanol.
- Blocking buffer consisted of 5% non-fat milk in 10 mM Tris pH 7.5, 100 mM NaCl, 0.1% Tween 20.
- Washing buffer consisted of 10 mM Tris pH 7.5, 100 mM NaCl, 0.1% Tween 20.

CHAPTER 3

METHODS

3.1 NOS and diabetes mellitus

3.1.1 Blood Collection and preparative procedures

Blood (5 mL) from healthy and type I and type II diabetic volunteers was collected in 5 mM EDTA sterile tubes. Platelet-rich plasma (PRP) was obtained by centrifuging blood at 1,000 RPM for 10 min. PRP were then centrifuged at 3,000 RPM for 10 min using 10% ACD buffer containing 0.8% citric acid, 2.2% sodium citrate, and 2.4% dextrose. Platelet pellets were then washed three times with Ca^{2+}-free Tyrode's buffer containing 137 mM sodium chloride, 5.5 mM glucose, $NaHCO_3$ 11.9 mM, NaH_2PO_4 0.35 mM, $MgCl_2$ 1.0 mM, pH 6.5, and stored in the appropriate buffer.

3.1.2 Preparation of DCFDA

DCFDA free base was prepared daily, by mixing 0.05 mL of 10 mM DCFDA with 2 mL of 0.01 N NaOH at room temperature for 30 minutes. The mixture was neutralized with 18.0 mL of 25 mM phosphate-buffered saline (PBS), pH 7.4. This solution was maintained on ice in the dark until use.

3.1.3 Confocal microscopy study

Washed platelets from control and diabetic subjects were incubated for 15 min with 5 μM of DCF free base at 37°C. 0.1 mM of L-arginine was then added for a further 15 min of incubation. Platelets were washed twice with 25 mM phosphate buffer (pH

7.4), and were viewed with a U-V laser on a U-V laser on a Zeiss LSM 410 confocal microscope, under a 60X objective, 0.5 μm Z step. Digitized images were processed through confocal assistant.

3.1.4 Peroxynitrite synthesis

Peroxynitrite was synthesized using a quenched-flow reactor, where 0.6 M of $NaNO_2$ and 0.6 M HCl/0.7 M H_2O_2 were pumped into a tee-junction and mixed in a 3 mm diameter by 2.5 cm glass tube. The acid-catalyzed reaction of nitrous acid with H_2O_2 to form peroxynitrous acid was quenched by pumping 1.5 M NaOH at the same rate into a second tee-junction at the end of the glass tubing. Final product was quantified photometrically (ε_{302} 1670 $M^{-1}cm^{-1}$) then stored at –20°C for as long as a week.

3.1.5 Fluorimetric assay of DCF

Dichlorofluorescein diacetate (DCFH-DA) is a non-fluorescent compound which rapidly diffuses through cell membrane. Within the cell, it is hydrolysed to 2,7-dichlorofluorescein by cytosolic esterases and is oxidized to the fluorescent intracellular DCF by peroxynitrite in platelets (Kooy *et al.*, 1997). The DCFDA/L-arginine treated Platelets (as per section 3.1.3) were divided into two sets, where 0.1 mM of L-NMMA was added to one set only. After incubation for 15 min at 37°C, both sets were washed twice with pH 7.4 phosphate buffer, 25 mM. The platelet pellets were broken by resuspension in 1 mL of water, while shaking for 15 min at room temperature. The mixture was then centrifuged for 2 min at 1,000 rpm. The supernatant was diluted appropriately and the fluorescence was measured in a Hitachi Model F-2000

Spectrofluorometer at an excitation wavelength of 475 nm and emission wavelength of 520 nm. Blank samples contained all reagents except platelets.

3.1.6 Cytosolic protein estimation

Protein concentrations in platelets were estimated using the Bio-Rad microassay that uses bovine serum albumin as the standard. This assay is a modification of the Bradford assay (Bradford, 1976).

3.1.7 Western blotting for iNOS detection

3.1.7.1 (8%) SDS-PAGE

Washed platelets were hypotonically lysed (as described in section 3.1.5). The collected supernatants were treated with an equal volume of sample application buffer (125 mM Tris-HCl pH 6.8, 2% SDS, 5% glycerol, 0.003% bromophenol blue, and 1% β-mercaptoethanol). The mixture was then boiled for 5 min. To each well of an 8% SDS-polyacrylamide gel, 10 μL of each sample was applied and electrophoresed for 1 h at 130 V along with a set of molecular weight markers (Sigma-broad range). BSA (1 μg/ μL), and mouse macrophage iNOS (macNOS) were used as negative control and positive control, respectively.

3.1.7.2 Immunoblot analysis

The resolved protein bands were then transferred onto a nitrocellulose support medium at 100 V for 60 min using a transfer buffer of 25 mM Tris base/192 mM glycine/20% methanol. The blots were blocked overnight at 4°C with blocking buffer

(5% non-fat milk in 10 mM Tris pH 7.5, 100 mM NaCl, 0.1% Tween 20). The blocking buffer was decanted and blots were incubated for 1 h at room temperature with primary antibody (anti-macNOS monoclonal, host mouse) diluted 1:2500 in blocking buffer. Blots were then washed using washing buffer (10 mM Tris pH 7.5, 100 mM NaCl, 0.1% Tween 20) for 30 min with agitation. Then incubated with the enzyme conjugate anti-mouse IgG: horseradish peroxidase, diluted 1:2500 in blocking buffer for 1 h at room temperature followed by 6 washes 5 min each with agitation.

3.1.7.3 Hyperfilm development

The blot was incubated with ECL reagents for 5 min in the dark. Then exposed it using Kodak Cassette for 30 min onto a hyperfilm. The film was then incubated in Kodak developer reagent for 3 min or until bands are shown, then it can be moved into the neutralization solution (3 % acetic acid) for another 3 min until it is fixed with Kodak fixer reagent, followed by extensive washing with water then air dried.

3.2 The effects of Atorvastatin on NOS in platelets

3.2.1 Blood Collection and preparative procedures

After a dietary baseline period of 3 weeks, hypercholesterolemia. subjects were randomized to either treatment with Atorvastatin (10 mg/day) or placebo. After four weeks on this regimen, blood samples were withdrawn and analyzed for triglycerides, total as well as LDL and HDL cholesterol, intraplatelet eNOS, iNOS and nitrotyrosylated proteins. At this point, the subjects receiving Atorvastatin were given placebo and *vice versa*. Blood samples were once again sampled for the same analytes at the end of four weeks. For NOS and nitrotyrosine evaluations, blood was collected in 5 mM EDTA

sterile tubes. Platelet-rich plasma (PRP) was obtained by centrifuging blood at 1,000 RPM for 10 min. PRP were then centrifuged at 3,000 RPM for 10 min using 10% ACD buffer containing 0.8% citric acid, 2,2% sodium citrate, and 2.4% dextrose. Platelets pellets were then washed three times with Ca^{2+}-free Tyrode's buffer containing 137 mM sodium chloride, 5.5 mM glucose, $NaHCO_3$ 11.9 mM, NaH_2PO_4 0.35 mM, $MgCl_2$ 1 mM, pH 6.5, and stored in the appropriate buffer. For lipid evaluation, blood is drawn and tested at the Medical Laboratory of Windsor.

3.2.2 Cytosolic protein estimation

Protein concentrations in platelets were estimated as per section 3.1.6.

3.2.3 Western blot analysis for NOS and nitrotyrosine detection

Washed platelets were hypotonically lysed (as described in section 3.1.3). The collected supernatants were treated with an equal volume of sample application buffer (125 mM Tris-HCl pH 6.8, 2% SDS, 5% glycerol, 0.003% bromophenol blue, and 1% β-mercaptoethanol). The mixture was then boiled for 5 min. To each well of an 8% SDS-polyacrylamide gel, 10 μL of each sample was applied and electropheresed for 1 h at 130 V along with a set of molecular weight markers (Sigma-broad range). BSA (1 μg/ μL) as a negative control, and mouse macrophage iNOS (macNOS), or endothelial NOS, or nitrotyrosine as a positive control. The immunoblot analysis is followed as described in section 3.1.7.

CHAPTER 4

RESULTS

4.1 NOS and diabetes mellitus

Initially, we were interested in confirming the specificity of DCFDA assay for peroxynitrite ($ONOO^-$). To test this 2,7-dichlorofluorescin diacetate (DCFDA) (5 μM) was incubated with either 100 μM H_2O_2 or 100 μM $ONOO^-$ for 15 min in PBS at 37°C. Hydrogen peroxide was not an efficient oxidizer of dichlorofluorescin as essentially no fluorescence (~23 Relative Intensity Units) was produced (Fig.2.3). Peroxynitrite on the other hand yielded 41-fold larger fluorescence (954 Relative Intensity Units). This agrees with the recent reports of Kooy *et al.* (1997) and Possel *et al.* (1997) that peroxynitrite can oxidize the non-fluorescent molecule 2,7-dichlorofluorescin to the fluorescent 2,7-dichlorofluorescein and that NO, hydroxyl radical ($OH^\bullet$) and metal ions do not oxidize 2,7-dichlorofluorescin.

To demonstrate the dependance of intracellular dichlorofluorescin oxidation on peroxynitrite produced by intracellular L-Arg/NO pathway, washed platelets isolated from type I diabetic subjects were first preincubated for 15 min with DCFDA then incubated with increasing amounts of L-Arginine. The intraplatelet fluorescence (due to dichlorofluorescein) was directly proportional to the extracellular L-Arg concentration up to 100 μM (Fig.2.4). Above this concentration the fluorescence decreased with increasing L-Arg.

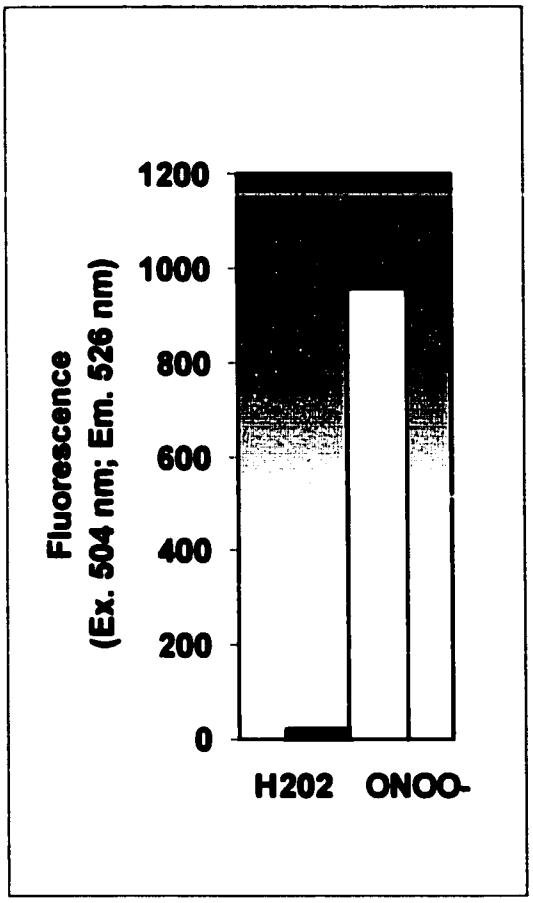

Figure 2.3- Specificity of DCFDA. Effect of H_2O_2 and peroxynitrite on the production of DCFDA fluorescence. H_2O_2 (100 μM) (dark filled bar) or $ONOO^-$ (100 μM) (light filled bar) were incubated with 5 μM DCFDA for 15 min in PBS pH 7.4 at 37°C. Fluorescence of the mixture was then determined (λ_{ex} 475nm, λ_{em} 520 nm).

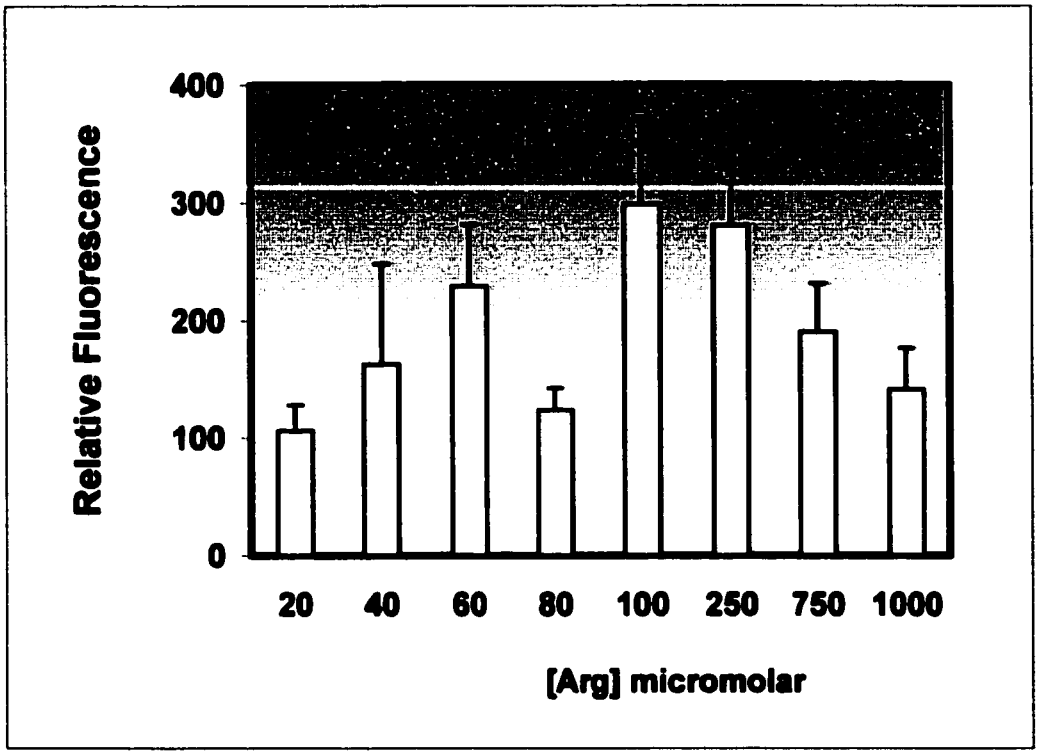

Figure 2.4- Effect of extracellular L-Arg on intraplatelet dichlorofluorescein fluorescence. Washed Platelets (from type I diabetic subjects) were incubated with DCFDA (5 μM) plus increasing L-arginine concentrations (0-1000 μM). Intraplatelet fluorescence was monitored with a spectrofluorometer (λ_{ex} 475nm, λ_{em} 520 nm). The data obtained from are the average of three independent experiments.

Upon using a NOS inhibitor L-NMMA, the fluorescence level in diabetic platelets is diminished (Fig.2.5). Furthermore, confocal microscopy images presented in Fig.2.6 for platelets from diabetic subjects exhibited dramatically higher fluorescence in comparison to controls. This is further confirmed when pixel intensities were plotted with respect to platelet source (Fig.2.7). The average pixel intensities for normal and type I platelets were 0.75 ± 0.49 and 3.79 ± 0.77, respectively.

Quantification of intraplatelet dichlorofluorescein formation revealed that under the conditions employed the standard curve obtained for dichlorofluorescein fluorescence (λ_{ex} 475nm, λ_{em} 520 nm) as a function of authentic concentration of $ONOO^-$, was best fitted by the equation $y = 1078\ x + 48$. Both type I (4.07 ± 2.88 nmol/mg) and type II (1.82 ± 2.12 nmol/mg) diabetic platelets exhibited higher L-Arg/NO-dependent $ONOO^-$ production in comparison to controls (0.58 ± 0.36 nmol/mg) (Fig.2.8).

Representative immunoblots of normal, type 1 and type 2 diabetic platelet proteins with human anti iNOS are presented in Fig.2.9. The blot densities of the bands (Fig.2.10) corresponding to iNOS are plotted as a function of subject category. None of the control subjects (n= 12) had a positive band for iNOS. On the other hand iNOS was evident in both type I (n=7) and type II (n=12) platelets. The average blot densities for type I and Type II were (2.63 ± 0.84) and (7.3 ± 5.11) respectively.

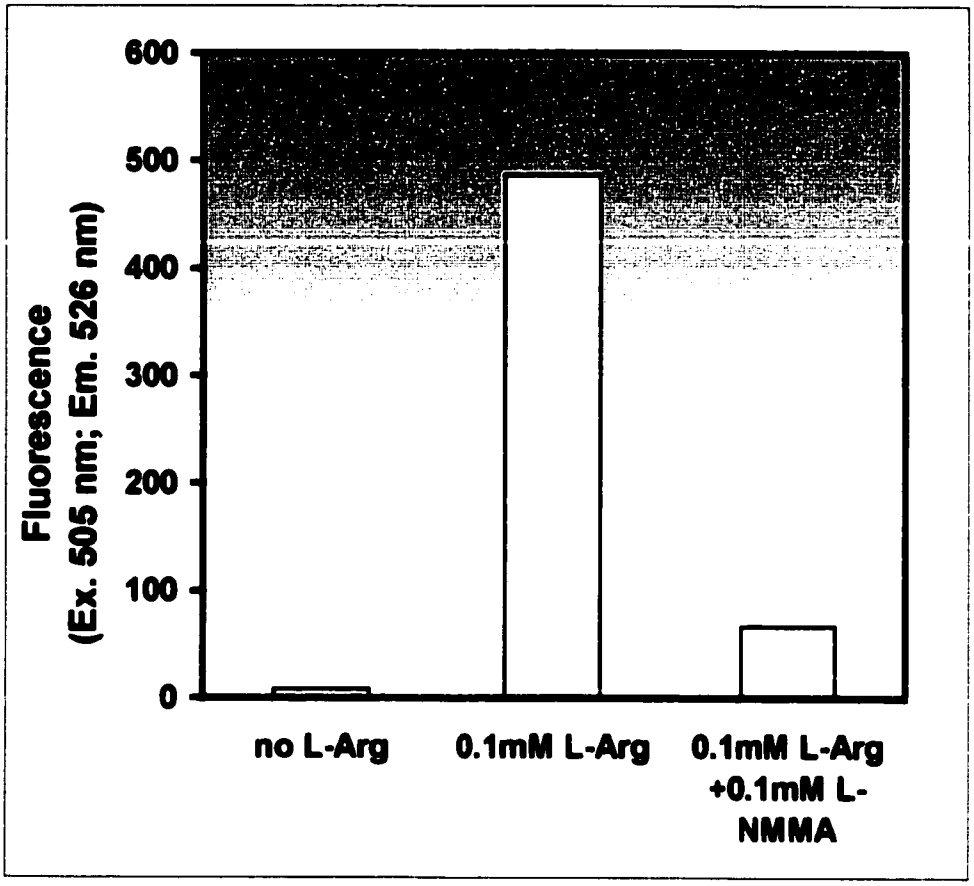

Figure 2.5- Effect of L-NMMA, a non-specific NOS inhibitor on intraplatelet DCF fluorescence. Washed platelets (from type I diabetic subjects) were incubated with L-arginine (100 μM) ± L-NMMA (100 μM) in the presence of DCFDA (5 μM) for 15 min at 37°C. Intraplatelet DCF fluorescence was monitored spectrofluorometically (λ_{ex} 475nm, λ_{em} 520 nm).

Figure 2.6- Confocal images of DCFDA preloaded normal and type I diabetic platelets. Washed normal (A) and type I diabetic (B) platelets were preloaded with 5 μM DCFDA for a 15 min pre-incubation and washed 2x. They were exposed to L-Arg (100 μM) for 15 min, washed, then transferred to a microscope slide. The cover slip was attached onto the slide with clear nail polish. The platelets were viewed with a U-V laser on a Zeiss LSM 410 confocal microscope, under a 60 x objective.

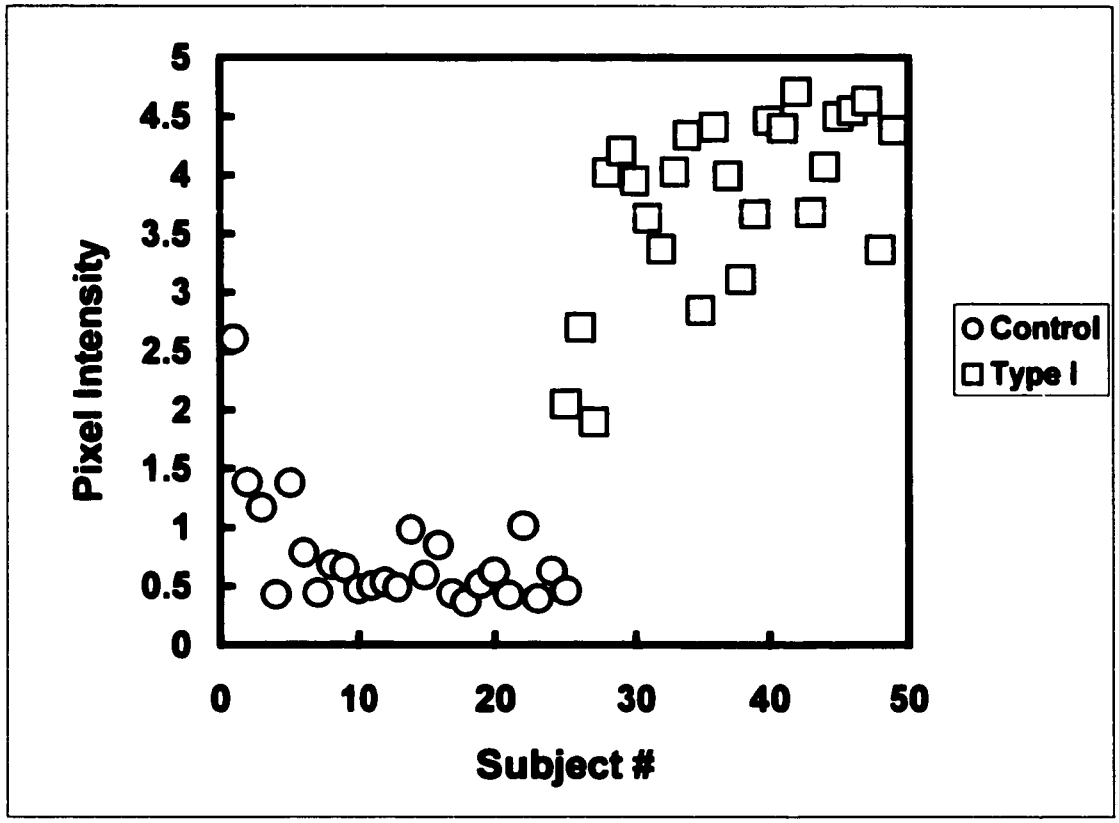

Figure 2.7- Quantification of the fluorescence of confocal images of DCFDA/L-Arg treated control and type I diabetic platelets. Confocal images in *.gif format, were scanned on a Bio-Rad 620 scanning densitometer. The total pixel intensity values from circular areas slightly smaller than the areas covered by the platelets are presented as a function of subject number: 1 to 25 controls; 26 to 50 Type I.

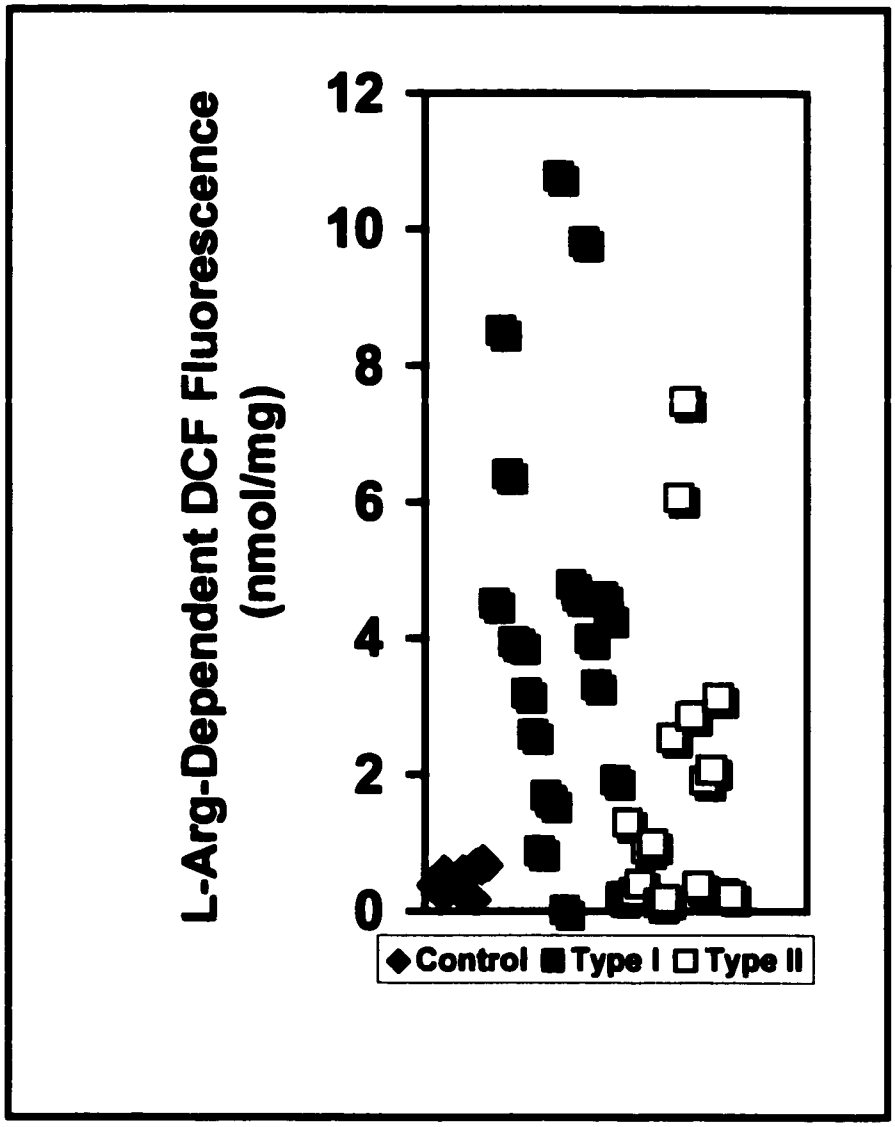

Figure 2.8- Effect of L-Arginine on intraplatelet DCF fluorescence. L-Arg (100 μM) was incubated with DCF loaded PRP of control, type I and type II diabetics for 15 min at 37°C. Washed platelets were lysed with H_2O. The fluorescence (λ_{ex} 475 nm, λ_{em} 520 nm) was converted to peroxynitrite concentration/mg of protein by comparing to a standard curve of DCF fluorescence as a function of authentic peroxynitrite. This standard curve was best described by the linear equation, fluorescence = 1078 * nmol $ONOO^-$ + 48.

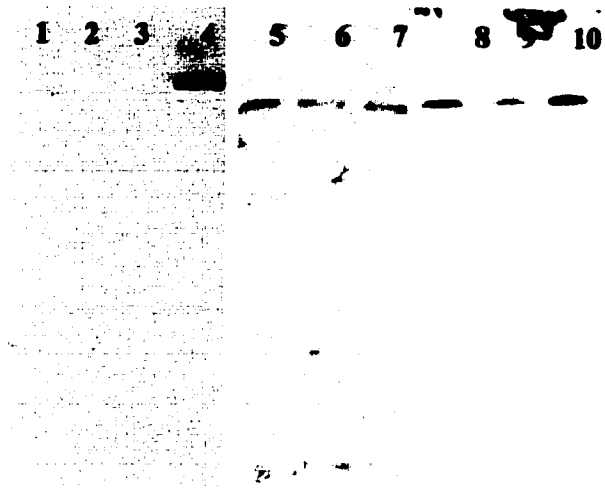

Figure 2.9- Evidence of iNOS in diabetic platelets. Western immunoblot analysis of normal type I and type II diabetic intraplatelet proteins with anti-iNOS monoclonal antibodies. Intraplatelet proteins from the three subject categories were separated by 8% SDS-PAGE, transferred to nitrocellulose membrane, probed with primary and secondary antibodies and exposed to ECL reagents and the blot density was recorded on hyperfilm. Three of each category shown: Lanes 1, 2, 3 normal; Lane 4 positive control *mac* NOS; Lanes 5, 6, 7, Type I; Lanes 8, 9, 10 Type II.

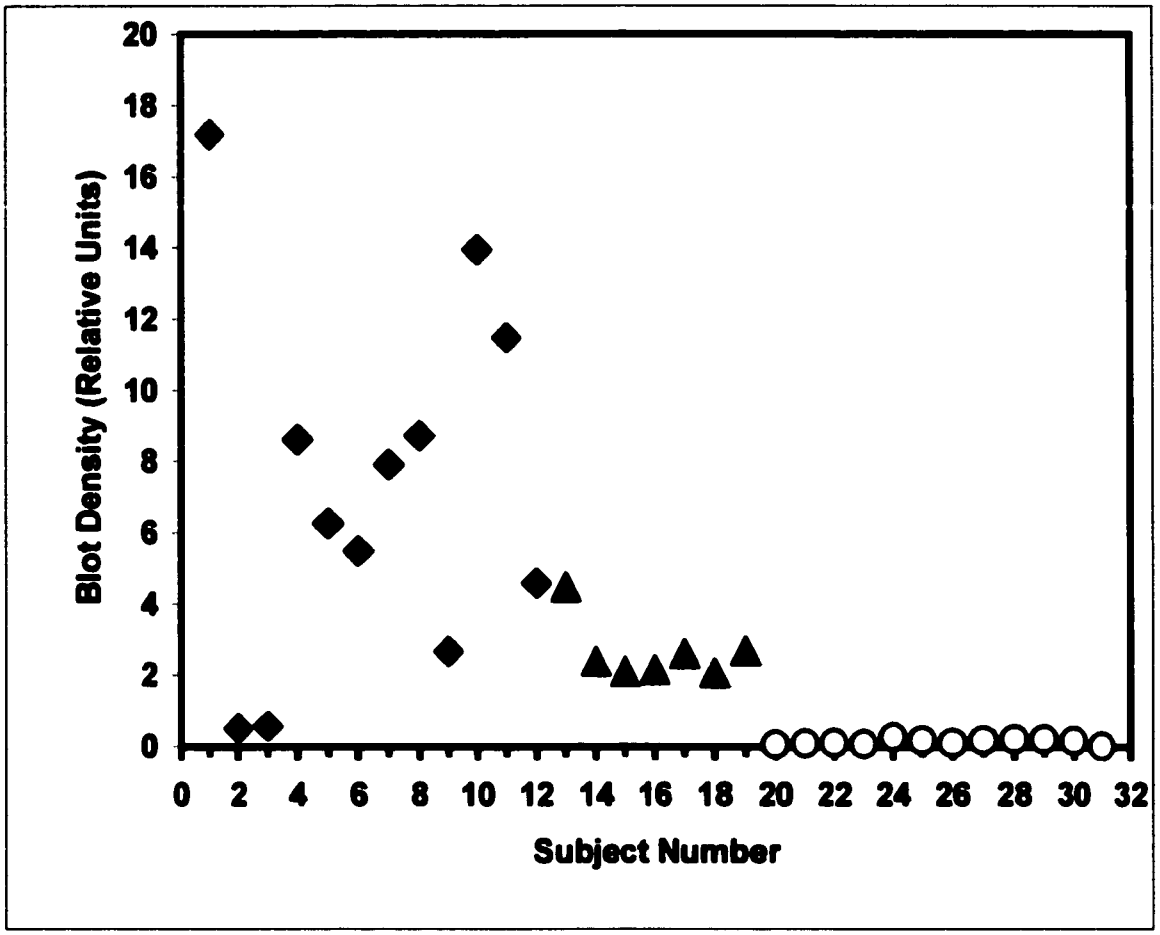

Figure 2.10- Western immunoblot iNOS-specific densities as a function of subject number. Hyperfilm exposed to western immunoblot probed with anti iNOS, was scanned on a Bio-Rad 620 densitometer. The blot densities are plotted with respect to blot number: Subjects 1 to 12 Type II; subjects 13 to 19 Type I; subjects 20 to 31 normals.

4.2 The effects of Atorvastatin on NOS in platelets

In this study, men and women with dyslipidemia were placed on a three weeks washout period where they were on no medication but on a low lipid diet. After this point the subjects were given a daily dose of 10 mg of Atorvastatin or Placebo for four weeks and *vice versa* for another four weeks. Blood samples were withdrawn every four weeks and analyzed for triglycerides, total as well as LDL and HDL cholesterol, intraplatelet eNOS, iNOS and nitrotyrosylated proteins.

Platelet proteins were electrophoresed, immnunoblots analysis for eNOS, iNOS, and nitrotyrosine were performed. The blot densities for eNOS levels were significantly higher in drug treated patients (Fig 2.11, P = 0.005, paired t-test). In contrast, iNOS levels in the presence of the drug showed a decreased in protein level with a higher statistical significance (Fig. 2.12, P= 0.33, paired t-test). Interestingly, nitrotyrosine levels, an indication of peroxynitrite damage to proteins, were reduced (Fig. 2.13, P= 0.17, paired t-test).

Furthermore the effect of Atorvastatin on lipids was investigated. As expected Atorvastatin lowered total cholesterol (Fig 2.14, P <0.001 paired t-test) and LDL (Fig. 2.15, P <0.001, paired t-test) in all subjects. Whereas triglycerides were lowered in 70 % of the subjects in the presence of Atorvastatin (Fig. 2.16, P < 0.1, paired t-test). HDL was not affected by the drug (Fig. 2.17, P=0.11, paired t-test) (table 2.1). These results are in agreement with previously published data on the anti-lipid effects of Atorvastatin (Lea *et al.*, 1997).

Table 2.1: Paired t-test (P) values.

	P values
eNOS	0.004987784
Chol	4.67779 E-08
Trig	0.090582549
LDL	3.32396 E-08
HDL	0.111453178
iNOS	0.331126993
Nitro-Tyr	0.166869

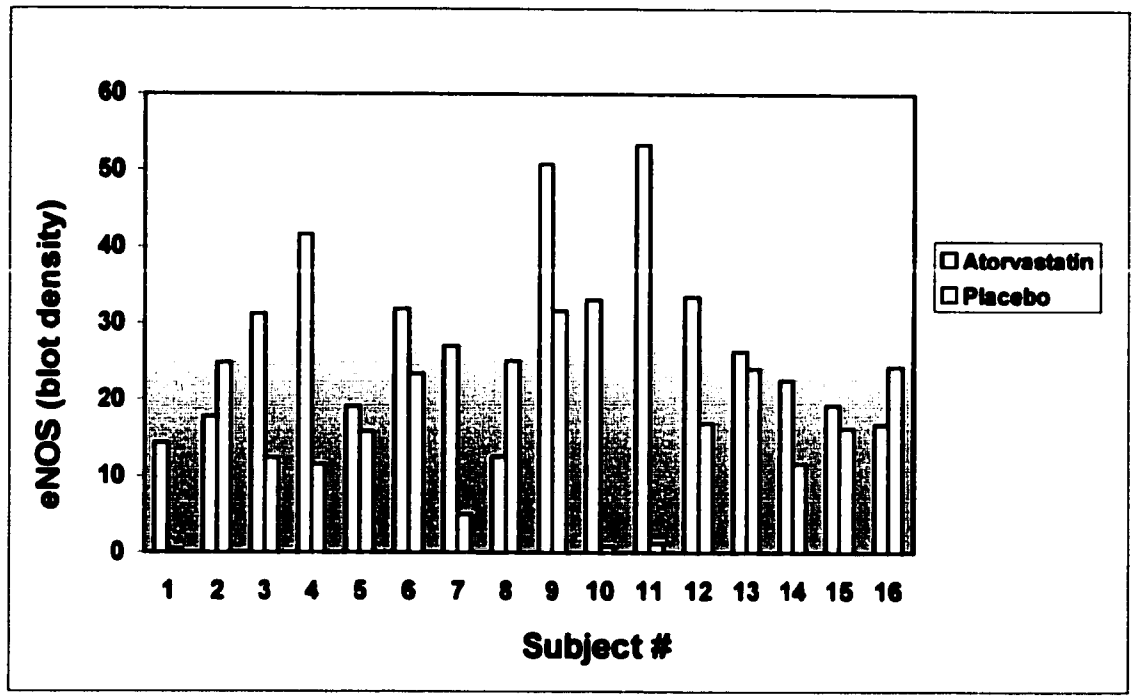

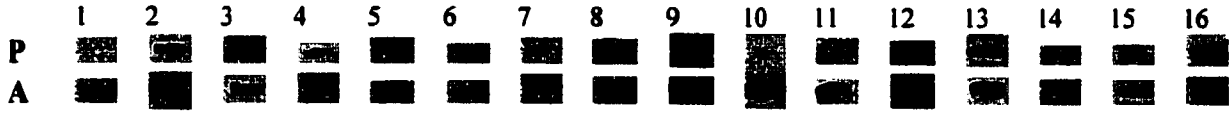

Figure 2.11- Monitoring eNOS level during Atorvastatin therapy. Immunoblot eNOS-specific densities of platelets from hypercholesterolemic subjects receiving Atorvastatin (10 mg/day) (A) or placebo (P) at each stage of the study. Intraplatelet proteins were separated by 8% SDS-PAGE, transferred to nitrocellulose membrane, probed with primary monoclonal antibody for eNOS. eNOS was visualized using HRP-conjugated secondary antibody followed by exposure to ECL reagents. The blots were then scanned on a Bio-Rad 620 densitometer. The blot densities are plotted with respect to subject numbers.

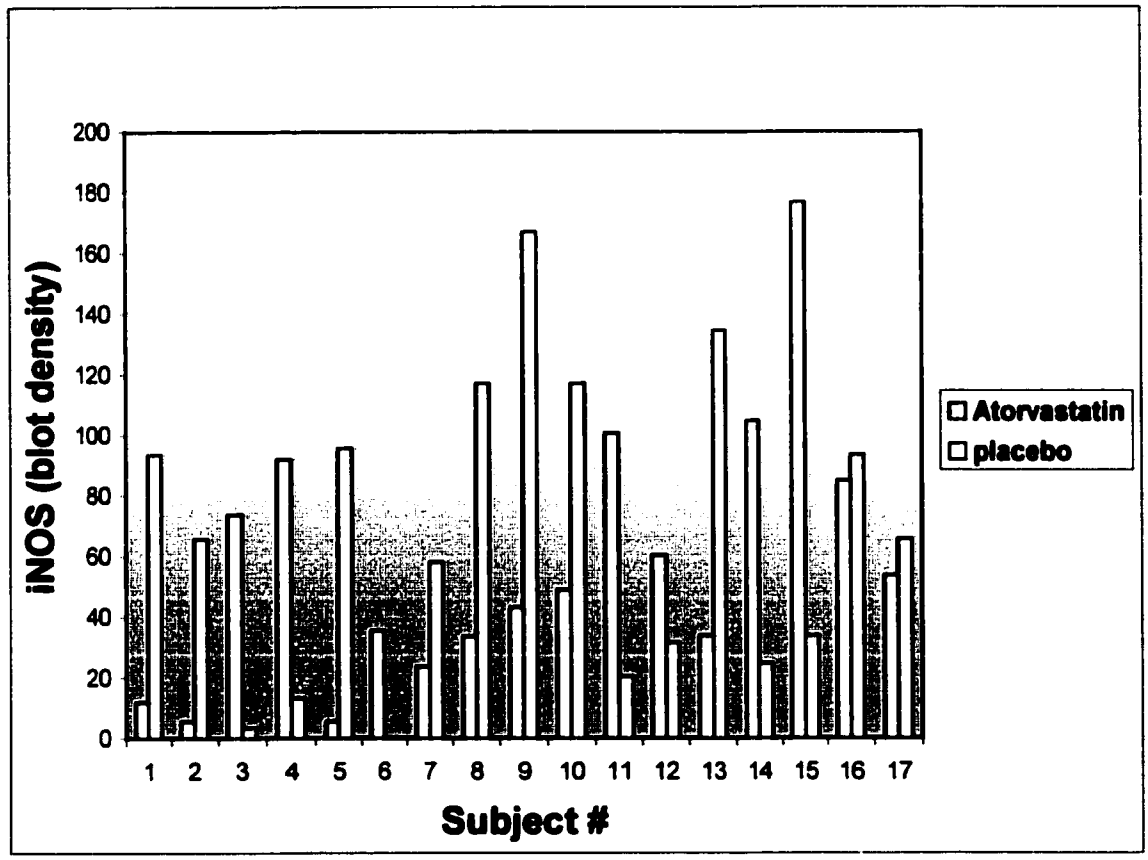

Figure 2.12- Monitoring iNOS level during Atorvastatin therapy. Immunoblot iNOS-specific densities of platelets from hypercholesterolemic subjects receiving Atorvastatin (10 mg/day) (A) or placebo (P) at each stage of the study. Intraplatelet proteins were separated by 8% SDS-PAGE, transferred to nitrocellulose membrane, probed with primary monoclonal antibody for iNOS. iNOS was visualized using a HRP conjugated secondary antibody followed by exposure to ECL reagents and the blots were scanned on a Bio-Rad 620. The blot densities are plotted with respect to subject numbers.

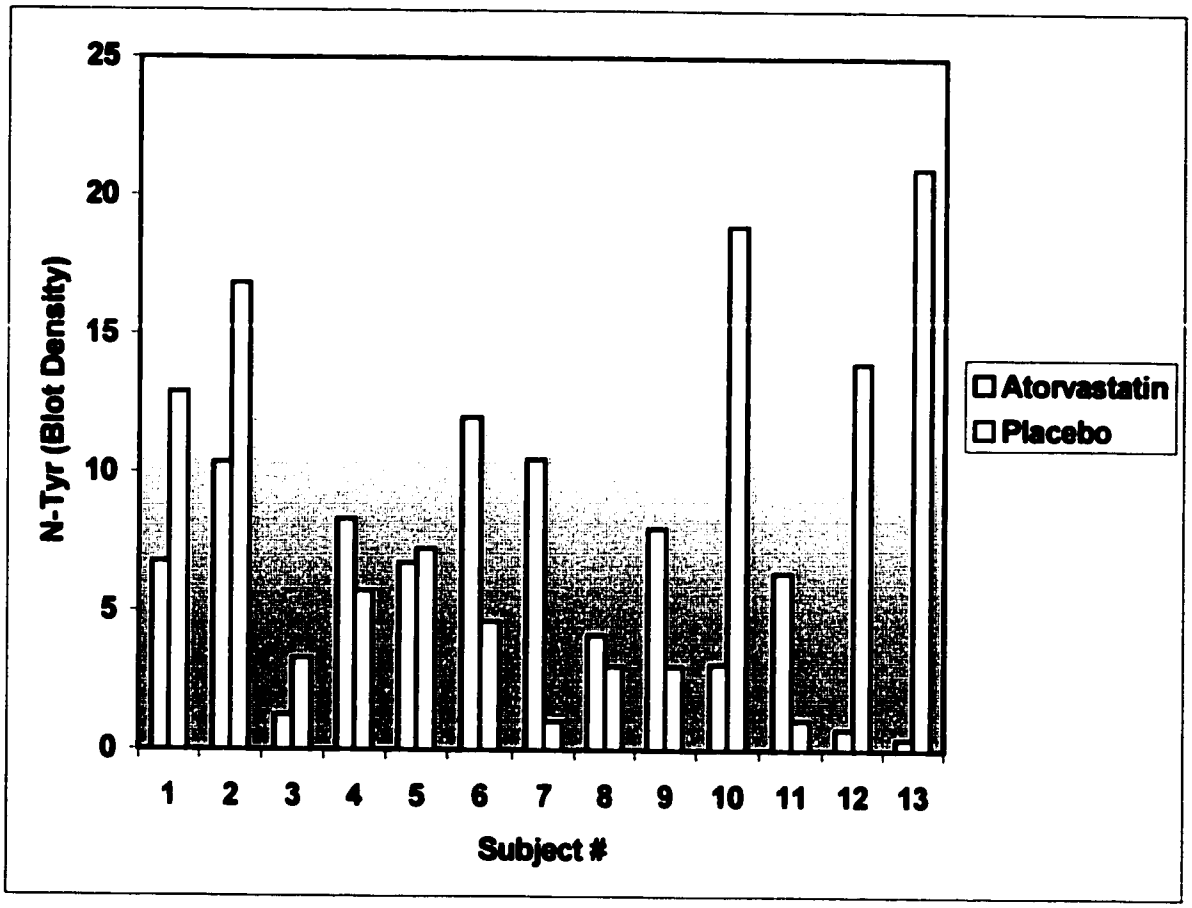

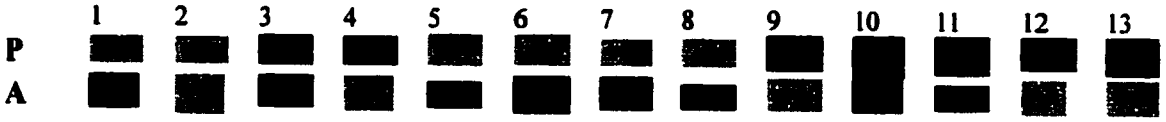

Figure 2.13- Monitoring nitrotyrosine level during Atorvastatin therapy. Immunoblot nitrotyrosine-specific densities of platelets from hypercholesterolemic subjects receiving Atorvastatin (10 mg/day) (A), or placebo (P) at each stage of the study. Intraplatelet proteins were separated by 8% SDS-PAGE, transferred to nitrocellulose membrane, probed with primary monoclonal antibody for nitrotyrosine. Nitrotyrosine band was visualized using HRP-conjugated secondary antibody followed by exposure to ECL reagents and the blots were scanned on a Bio-Rad 620 densitometer. The blot densities are plotted with respect to subject numbers.

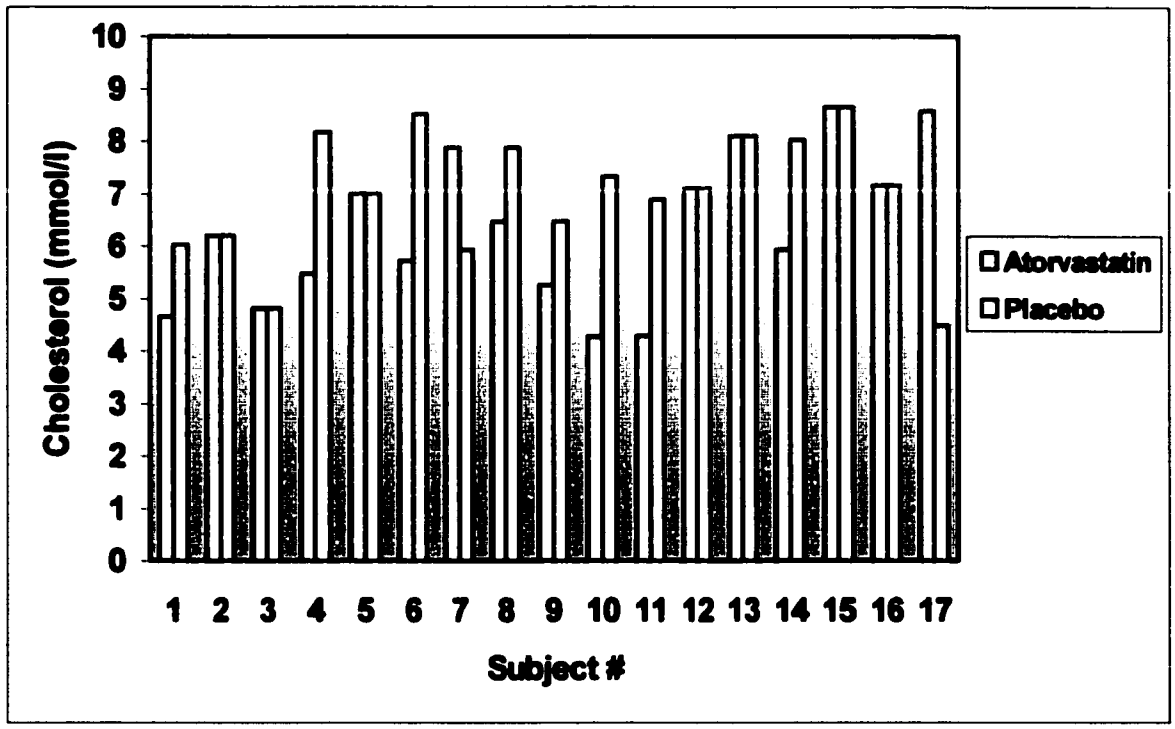

Figure 2.14- Effect of Atorvastatin on cholesterol synthesis. Blood from hypercholesterolemic subjects receiving (+/- Atorvastatin 10 mg/day) was obtained. Samples of pre and post treatment were monitored for cholesterol level.

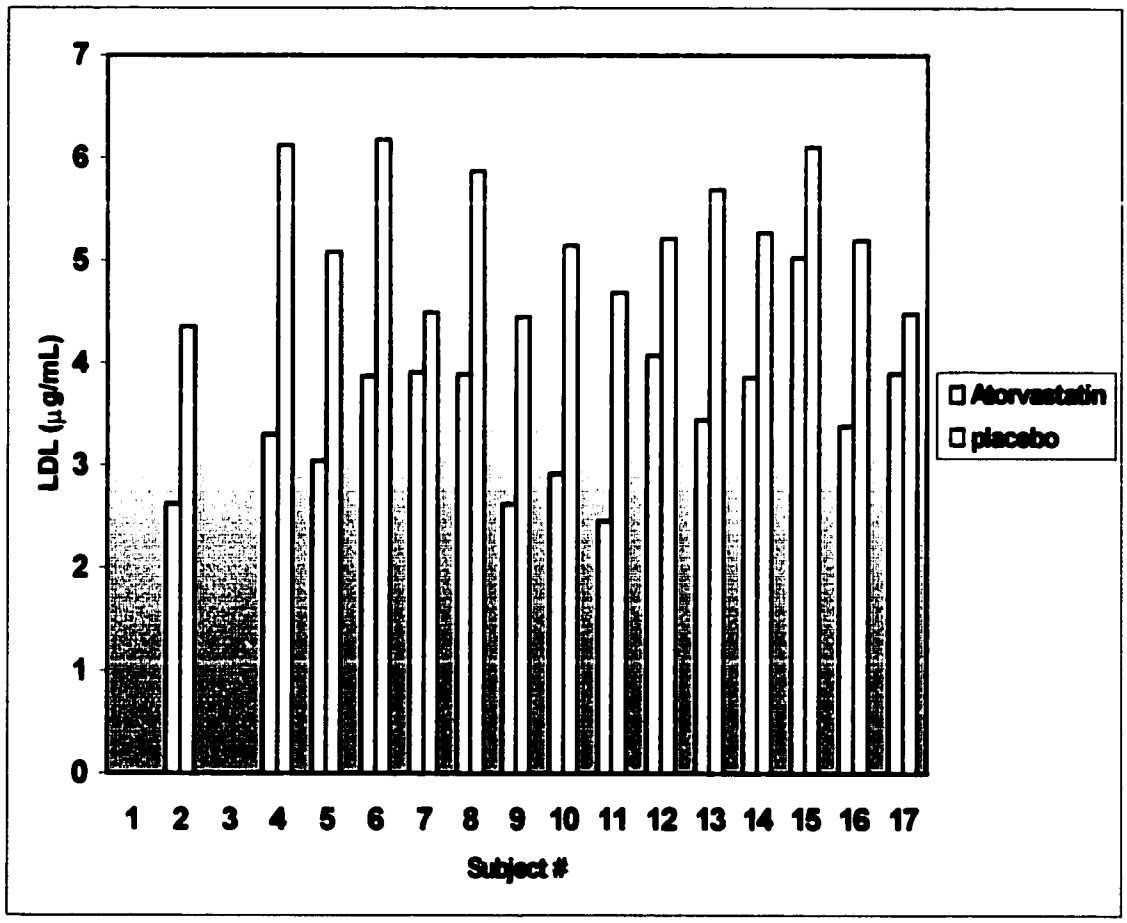

Figure 2.15- Effect of Atorvastatin on Low density lipoprotein (LDL) level. Blood from hypercholesterolemic subjects receiving (+/- Atorvastatin 10 mg/day) was obtained. Samples of pre and post treatment were monitored for LDL level.

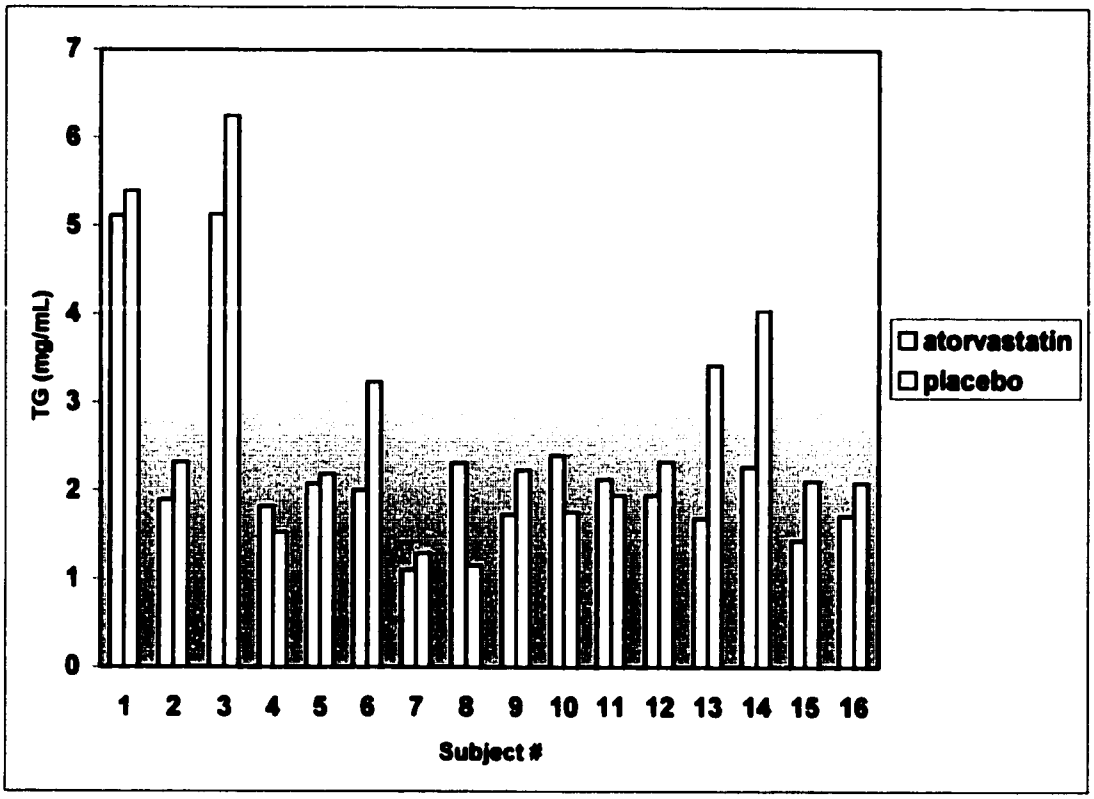

Figure 2.16- Effect of Atorvastatin on Triglycerides (TG) level. Blood from hypercholesterolemic subjects receiving (+/- Atorvastatin 10 mg/day) was obtained. Samples of pre and post treatment were monitored for triglycerides level.

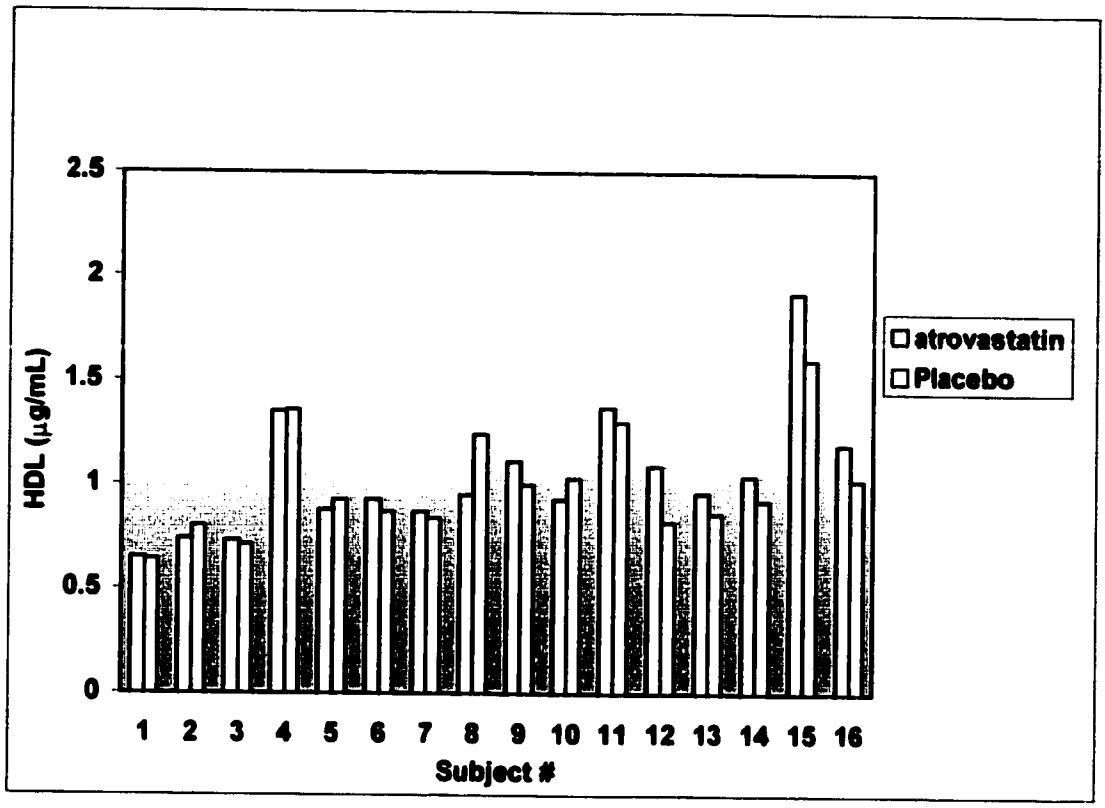

Figure 2.17- Effect of Atorvastatin on high density lipoprotein (HDL) level. Blood from hypercholesterolemic subjects receiving (+/- Atorvastatin 10 mg/day) was obtained. Samples of pre and post treatment were monitored for HDL level.

CHAPTER 5

DISCUSSION

5.1 NOS and diabetes mellitus

Patients with diabetes mellitus show alterations in platelet function, which have been hypothesized to be crucial in the pathogenesis of diabetic angiopathy. The involvement of the L-arginine–nitric oxide pathway in the pathogenesis of diabetes was studied by comparing NOS isozymes level between control and diabetic platelet. In the presence of 100 μM extracellular L-Arg *in vitro* diabetic platelets produced ~5-fold larger levels of DCF fluorescence, evaluated either by confocal microscopy or by fluorimetry.

Moreover, we observed here a significant increase in peroxynitrite production in platelets from both Type I and Type II diabetic subjects. Fluorescent Dichlorofluorescein (DCF) level was increased proportionally to extracellular L-Arg concentration up to 100 μM and then was reduced, as NOS was inhibited by large concentrations of NO. The additional piece of evidence that DCF is a reporter of NOS-derived $ONOO^-$ was the inhibition of intracellular fluorescence by the preincubation of platelets with the non-specific NOS inhibitor L-NMMA.

Of the three NOS isoenzymes, iNOS is known to produce the largest levels of both NO and $O_2^{-\bullet}$, being therefore implicated in peroxynitrite production (Berkels, 1997) which tends to inhibit platelet aggregation and to cause nitrosylation of platelet proteins (Muijsers *et al.*, 1997). In addition iNOS has been detected in megakaryocytes of subjects with coronary heart disease (De Belder *et al.*, 1995). It is therefore conceivable that the large levels of ONOO- production observed here *in vitro* in platelets from diabetic

patients could result from the induction of iNOS by diabetes-related factors. As we expected, iNOS is expressed in all the diabetic samples (both Type I and Type II) examined, while iNOS protein was not expressed in normal platelets. Our data are in agreement with the previous results of Berkels *et al.* (1997) reporting that iNOS protein is not expressed in normal platelets, while the presence of cNOS has been widely described in human platelets (Chen *et al.*, 1996). The observation of the presence of iNOS in diabetic platelets combined with the *in vitro* demonstration of the increased peroxynitrite production suggests that iNOS-dependent peroxynitrite production could play a major role in diabetes pathophysiology. In the event that further studies do show that iNOS-dependent peroxynitrite is responsible for platelet dysfunction *in vivo*, the focus of research should then be on the identification of the diabetes-derived agent(s) that induce iNOS expression in platelets.

5.2 The effects of Atorvastatin on NOS in platelets

In this study Atorvastatin, a new HMG-CoA reductase inhibitor with potent inhibitory effects on the intracellular rate of cholesterol synthesis, was used to investigate the effect of inhibition of cholesterol on NOS isoforms in platelets. Atorvastatin has been shown to decrease cholesterol level to a certain extent *in vitro* and *in vivo* (Bocan *et al.*, 1994). Thus apart from lipid lowering, it also has potentially very beneficial effects in alleviating platelet related cardio-vascular problems. This is due to the observed elevations in the levels of eNOS in the presence of the drug. Increased eNOS leads to overproduction of NO thus inhibiting thrombus formation. Atorvastatin dependent elevation in eNOS has previously been reported in bovine aortic endothelial cells

(Hernandez-Perera *et al.*, 1998). In that study, the authors showed that oxidized-LDL down-regulated eNOS mRNA by up to 57%. On the other hand, Atorvastatin caused a net elevation in eNOS levels by preventing oxidized-LDL-dependent inhibition of eNOS transcription. A similar mechanism might be operative in the platelet. In our study, it is likely to have elevated levels of oxidized-LDL. As a result, eNOS expression would be down-regulated. Atorvastatin might interact at or near the oxidized-LDL receptor thus interfering in the signaling pathway for eNOS down regulation. The overall effect of this would be a net increase in eNOS levels. Another interesting aspect of our study was the observation that in the presence of the drug levels of intraplatelet protein that were nitrotyrosylated decreased. This suggests that Atorvastatin has a role in lowering intraplatelet peroxynitrite levels by an as yet unknown mechanism. This is very desirable as peroxynitrite irreversibly modifies lipids, proteins and nucleic acids. Therefore its presence in the intracellular milieu is likely to lead to cellular damage.

CHAPTER 6

CONCLUSION

This study was focused on intraplatelet NOS isoforms in diabetics and hypercholesterolemic subjects. Significant findings have been outlined below. In the first stage, intraplatelet NOS content as well as peroxynitrite formation were evaluated in type I, type II diabetics, and normal subjects. NO is known to have a major role in the pathological regulation of platelet function. In this study we presented evidence of increased peroxynitrite production in diabetic platelets. The fact that iNOS is detected in diabetic platelets and not in controls, suggests that this increase in peroxynitrite level may be due to overproduction of iNOS. Thus, this iNOS-dependent peroxynitrite production could play a major role in diabetes pathophysiology.

In the second stage of this study the hypolipidemic drug Atorvastatin was assessed for its effect on cholesterol as well as intraplatelet NOS level. Thus aside from its inhibitory effects on intracellular cholesterol synthesis, Atorvastatin was able to influence other cellular functions such as upregulation of eNOS and down regulation of peroxynitrite production in platelets of hypercholesterolemic subjects post therapy.

REFERENCES

Addicks E, Quigley H, Green R, Robin H. Histologic characteristics of filtering blebs in glaucomatous eyes. *Arch. Ophthalmol.* 1983; 101: 795-798.

Ahmad N, Feyes D, Agarwal R, Mukhtar H. Photodynamic therapy results in induction of WAF1/CIP1/P21 leading to cell cycle arrest and apoptosis. *Proc. Natl. Acad. Sci. USA* 1998; 95 (12): 6977-6982.

Ambs S, Hussain P, Harris C. Interactive effects of nitric oxide and p53 tumor suppressor gene in carcinogenesis and tumor progression. *FASEB* 1997; 11: 443-448.

Arnelle D, Stamler J. NO+, NO, and NO- donation by S-nitrosothiols: implications for regulation of physiological functions by S-nitrosylation and acceleration of disulfide formation. *Archives of Biochemistry and Biophysics* 1995; 18(2): 279-285.

Aveline B, Hasan T, Redmond R. Photophysical and photosensitizing properties of benzoporphyrin derivative monoacid ring A (BPD-MA). *Photochem. Photobiol.* 1993; 59 328-335.

Baggiolini M, Wyamann M. Turning on the respiratory burst. *Trends Biochem. Sci.* 1990; 15(2): 69-72.

Barr H, Dix T, Roberts d, Shepard N. Eradication of high grade dysplasia in columnar lined (Barret's) oesophagus by photodynamic therapy with oral 5-aminolevulinic acid and 630 nm light, *Gut* 1994; 35 (suppl.5), 7.

Barth R, Adams D, Soloway A, Alam F, Darby M. Boronated starburst dendrimer-monoclonal antibody immunoconjugates: evaluation as a potential delivery system for neutron capture therapy. *Bioconjug.* 1994; 5: 58-66.

Beckman J, Beckman T, Chen J, Marshall P, Freeman B. Apparent hydroxyl radical production from peroxynitrite implications for endothelial injury by nitric oxide and superoxide. *Proc. Natl. Acad. Sci. USA* 1990; 87: 1620-1624.

Beckman J, Koppenol W. Nitric oxide, superoxide, and peroxynitrite: The good, the bad, and the ugly. *Am. J. Physiol.* 1996; 271, C1424-C1437.

Berg K, Anholt H, Bech O, Moan J. The influence of iron chelators on the accumulation of protoporphyrin IX in 5-aminolevulinic acid-treated cells. *Br. J. Cancer* 1996; 74 (5): 688-697.

Berkels R, Bertsch A, Zuther T, Dhein S, Stockklauser K, Rosen P, Rosen R. Evidence for a NO synthase in porcine platelets which is stimulated during activation/aggregation. *Eur. J. Haematol.* 1997; 58(5): 307-313.

Bielinska A, Kukowska-Latallo J, Johnson J, Tomalia D, Baker Regulation of in vitro gene expression using antisense oligonucleotides or antisense expression plasmids transfected using starburst PAMAM dendrimers. *J. Nucleic Acids Res.* 1996; 24(11): 2176-2182.

Bitterman N, Bitterman H, L-arginine-NO pathway and CNS oxygen toxicity. *J. Appl. Physiol.* 1998; 84 (5): 1633-1638.

Bocan TM, Mueller SB, Brown EQ, Uhlendorf PD, Mazur MJ, Newton RS. Antiatherosclerotic effects of antioxidants are lesion-specific when evaluated in hypercholesterolemic New Zealand white rabbits. *Exp. Mol. Pathol.* 1992 Aug; 57(1): 70-83.

Bonfoco E, Krainc D, Ankarcrona M, Lipton S. Apoptosis and necrosis: Two distinct events induced respectively by mild and intense insults with NMDA or nitric oxide/superoxide in cortical cell cultures. *Proc. Natl. Acad. Sci. USA* 1995; 92, 72: 162-72,166.

Bown SG. Photodynamic therapy to scientists and clinicians-one world or two? *J. Photochem. Photobiol. B.* 1990; 6(1-2): 1-12.

Brunelli L, Crow JP, Beckman JS. The comparative toxicity of nitric oxide and peroxynitrite to Escherichia coli. *Arch. Biochem. Biophys.* 1995; 316(1): 327-334.

Buhler RH, Kagi JH. Spectroscopic properties of zinc-metallothionein. *Experientia Suppl.* 1979; 34: 211-220

Butler A, Rhodes P. Chemistry, analysis, and biological roles of S-nitrosothiols. *Analytical Biochemistry*, 1997; 249: 1-9.

Buttery L, Springall D, Chester A, Evans T, Standfield E, Parums D, Yacoub M, Polak J. Inducible nitric oxide synthase is present within human atherosclerotic lesions and promotes the formation and activity of peroxynitrite. *Lab. Invest.* 1996; 75(1): 77-85.

Caimduff F, Streinger M, Hudson F, Ash D, Brown S. Superficial photodynamic therapy with topical 5-aminoeluvilinic acid for superficial primary and secondary skin cancer. *Br. J. Cancer* 1994; 69,605-608.

Calver A, Collier J, Moncada S, Vallance P. Effect of local infusion on N^G-monomethyl-L-arginine inpatients with hypertension: the nitric oxide dilator mechanism appears abnormal. *J. Hypertens.* 1992; 10: 1025-1031.

Calver A, Collier J, Vallance P. Nitric oxide and the control of human vascular tone in health and disease. *Eur. J. Med.* 1993; 2(1): 48-53

Castro DJ, Saxton RE, Soudant J. The concept of laser phototherapy. *Otolaryngol Clin. North Am.* 1996; 29(6): 1011-1029.

Chen LY, Mehta JL. Further evidence of the presence of constitutive and inducible nitric oxide synthase isoforms in human platelets. *J. Cardiovasc. Pharmacol.* 1996 Jan; 27(1): 154-158.

Cherian M, Chan H. Biological functions of metallothionein- A review, in: Suzuki K, Imura N and Kimura M, (Eds), Metallothionein III, Biological roles and medical implications, *Birkhauser Verlag Basel/Switzerland.* 1993; 87-110.

Cho H, Xie Q, Catatcay J, Mumford R, Swiderrek K, Lee T, Nathan C. Calmodulin is a subunit of nitric oxide synthase from macrophages. *J. Exp. Med.*1992; 176: 599-604.

Cohen John, Apoptosis and its regulation. Adv. Exp. Med. Biol. 1996; 406: 11-20.

Crow J, Spruell C, Chen J, Gunn C, Ischiropoulos H, Tsai M, Smith C, Radi R, Koppenol W, Beckman J. On the pH-dependent yield of hydroxyl radical products from peroxynitrite. *Free Radical Biol. Med.* 1994;16:331-338.

De Belder AJ, Radomski MW, Why HJ, Richardson PJ, Martin JF. Myocardial calcium-independent nitric oxide synthase activity is present in dilated cardiomyopathy, myocarditis, and postpartum cardiomyopathy but not in ischaemic or valvar heart disease. *Br. Heart J.* 1995 Oct; 74(4): 426-430.

Denicola A, Rubbo H, Rodriguez D, Radi R. Peroxynitrite-mediated cytotoxicity to trypanosoma cruzi. *Arch. Biochem. Biophys.* 1993; 304: 279-286.

Desjardins D, Parrish R, Folberg R, Nevarez J, Heuer D, Gressel M. Wound healing after filtering surgery in owl monkeys. *Arch. Ophthalmol.* 1986;104: 1835-1839.

Dewanjee M. Molecular biology of nitric oxide synthases. Reduction of complications of cardiopulmonary bypass from platelets and neutrophils by nitric oxide generation from L-arginine and nitric oxide donors. *ASAIO J.* 1997; 43(3): 151-159.

Dimmeler S, Haendeler J, Nehls M, Zeiher AM. Suppression of apoptosis by nitric oxide via inhibition of interleukin-1beta-converting enzyme (ICE)-like and cysteine protease protein (CPP)-32-like proteases. *J. Exp. Med.* 1997; 185(4): 601-607.

Dougherty T, Activated dyes as antitumor agents. *J. Natl. Cancer Inst.*. 1974; 52(4): 1333-1336.

Drexler H, Zeiher AM. Progression of coronary endothelial dysfunction in man and its potential clinical significance. *Basic Res. Cardiol.* 1991; 86(2): 223-232.

Ellman G. A colorimetric method for determining low concentrations of mercaptans. *Arch. Biochem. Biophys.* 1958; 74: 443-450.

Estevez A, Radi R, Barbeito L, Shin J, Thompson J, Beckman J. Peroxynitrite-induced cytotoxicity in PC12 cells: evidence for an apoptotic mechanism differentially modulated by neurotrophic factors. *J. Neurochem.* 1995; 65: 1543-1550.

Farias-Eisner R, Chaudhuri G, Aeberhard E, Fukuto J. The chemistry and tumoricidal activity of nitric oxide/hydrogen peroxide and the implications to cell resistance/susceptibility *J. Biol. Chem.* 1996; 271: 6144-6151.

Ford P, wink D, Stanbury D. Autoxidation kinetics of aqueous nitric oxide. *FEBS Lett.* 1993; 326: 1-3.

Forrest J, Forrest H. Case report: Malignant melanoma arising during therapy for vitiligo *J. Surg. Oncol.* 1980: 13: 337-340.

Fritsch C, Goerz G, Ruzicka T. Photodynamic therapy in dermatology. *Arch. Dermatol.* 1998; 134: 207-214.

Furuse K, Fukuoka M, Kato H et al. Aprospective phase II study on photodynamic therapy with photofrin II for centrally located early-stage lung cancer. *J. Clin. Oncol.* 1993; 11, 1852-1857.

Gaullier J, Berg K, Peng Q, Anholt H, Selbo P, Ma L, et al. The use of esters of 5-aminolevulinilic acid to improve photodynamic therapy on cells in culture. *Cancer Res.* 1997; 57:1481-6.

Gaullier J, Geze M, Santus R, Melo T, Maziere J, Bazin M, Morliere P, Dubertret L. Subcellular localization of and photosensitization by protoporphyrin IX in human keratinocytes and fibrobalsts cultivated with 5-aminolevulinic acid. *Photochem. Photobiol.* 1995;62,114-122.

Gaw A, Packard CJ, Murray EF, Lindsay GM, Griffin BA, Caslake MJ, Vallance BD, Lorimer AR, Shepherd J. Effects of simvastatin on apoB metabolism and LDL subfraction distribution. *Arterioscler. Thromb.* 1993 Feb; 13(2): 170-189.

Genaro A, Hortelano S, Alvarez A, Martinez A, Bosca L. Splenic B. lymphocyte programmed cell death is prevented by nitric oxide release through mechanisms involving sustained Bcl-2 levels. *J. Clin. Invest.* 1995; 95: 1884-1890.

Gentry P. The mammalian blood platelet: its role in hemostasis, inflammation and tissue repair. *J. Comp. Path.* 1992; 107: 243-270.

Gillies M, Su T. Cytokines, fibrosis and the failure of glaucoma filtration surgery. *Aust. N. Z. J. Ophthalmo*l. 1991; 19(4): 299-304.

Gordge M, Addis P, Noronha-Dutra A, Hothersall. Cell-mediated biotransformation of S-nitrosoglutathione. *Biochem. Pharmacol.* 1998; 55(5): 657-665.

Greenfield D, Suner I, Miller M, Kangas T, Palmberg P, Flynn H. Endophthalmitis after filtering surgery with mitomycin. *Arch. Ophthalmol.* 1996; 114: 943-949.

Hale A, Smith C, Sutherland L, Stoneman V, Longthorne V, Culhane A, Williams G. Apoptosis: molecular regulation of cell death. *Eur. J. Biochem.* 1996; 236:1-26.

Hamer D. Metallothionein, *Annu. Rev. Biochem.* 1986; 55: 913-915.

Haria M, McTavish D. Paravastatin: a reappraisal of its pharmacological properties and therapeutic use in the management for coronary heart disease. *Drugs* 1997; 53(2): 299-336.

Harrison DG. Endothelial function and oxidant stress. *Clin. Cardiol.* 1997; 20(11 Suppl 2): II-II117.

Hart T.W. Tetrahedron Lett. 1985; 26: 2013-2016.

Hausladen A, Fridovich I. Superoxide and peroxynitrite inactivate aconitases, but nitric oxide does not. *J. Biol. Chem.*. 1994 Nov 25; 269(47): 29405-29408.

Hawkins C, Analysis of the role of bcl-2 in apoptosis. *Immunol. Rev.* 1994; 142: 127-139.

Hernandez-Perera O, perez-Sala D, Navarro-Antolin J, Sanchez-Pascuala R, Hernandez G, Diaz C, Lamas S.Effects of the 3-hydroxy-3-methylglutaryl-CoA reductase inhibitors, Atorvastatin, on the expression of endothelin-1 and endothelial nitric oxide synthase in vascular endothelial cells. *J. Clin. Invest.* 1998; 101(12): 2711-2719.

Hill R, Crean D, Doiron D, McDonald T, Liaw L, Ghosheh F, Hamilton A, Berns M. Photodynamic therapy for antifibrosis in a rabbit model of filtration surgery. *Ophthalmic Surg. Lasers* 1997; 28(7): 574-581.

Huang X, Yuang J, Goddard A, Foulis A, James RF, Lernmark A, Pujol-Borrell R, Rabinovitch A, Somoza N, Stewart TA. Interferon expression in the pancreases of patients with type I diabetes. *Diabetes.* 1995 Jun; 44(6): 658-664.

Huie R, Padjama S. The reaction of no with superoxide. *Free Radic Res. Commun.* 1993; 18(4): 195-199.

Ignarro L, Wood K, Wolin M. Regulation of purified soluble guanylate cyclase by porphyrins and metalloporphyrins: a unifying concept. *Adv. Cyclic Nucleotide Protein Phosphoryl Res.* 1984; 17, 267-274.

Ignarro, L., Fukuto J, Griscavage J, Rogers N, Byrns R. Oxidation of nitric oxide in aqueous solution to nitrite but not nitrate: comparison with enzymatically formed nitric oxide from L-arginine. *Proc. Natl. Acad. Sci. USA* 1993; 90, 8103-8107.

Iinuma S, Farshi S, Ortel B, Hasan T. A mechanistic study of cellular photodestruction with 5-aminolevulinic acid induced porphyrin. *Br. J. Cancer.* 1994; 70: 21-28.

Ischiropoulos H, Al-Mehdi A. Peroxynitrite-mediated oxidative protein modifications. *FEBS Lett.* 1995; 364: 279-282.

Ischiropoulos H, Zhu L, Chen J, Tsai M, Martin J, Smith C, Beckman J. peroxynitrite-mediated tyrosine nitration catalyzed by superoxide dismutase *Arch. Biochem. Biophys.* 1992; 298: 431-437.

Jacobson MD, Burne JF, Raff MC. Mechanisms of programmed cell death and Bcl-2 protection. *Biochem. Soc. Trans.* 1994; 22(3): 600-602.

Jampel H, McGuigan L, Dunkelberger M, l'Hernault N, Quigley H. Cellular proliferation after experimental glaucoma filtration surgery. *Arch. Ophthalmol.* 1988;106: 89-94.

Jori G. Photosensitized processes in vivo: proposed phototherapeutic applications. *Photochem. Photobiol.* 1990; 52(2): 439-443.

Jourd'heuil D, Mai C, Laroux S. The reaction of S-nitrosoglutathione with superoxide. *Biochemical and Biophysical Research Communications* 1998; 244: 525-530.

Kagi J, Kojima J. Chemistry and biochemistry of metallothionein, *Experientis Supplementum* Birkhauser, Basel 1987; 52: 25-62.

Kagi JH, Kojima Y, Kissling MM, Lerch K. Metallothionein: an exceptional metal thiolate protein. *Ciba Found Symp.* 1979; 72: 223-237.

Kane DJ, Ord T, Anton R, Bredesen DE. Expression of bcl-2 inhibits necrotic neural cell death. *J. Neurosci. Res.* 1995; 40(2): 269-275.

Kennedy J, Marcus S, Pottier R. Photodynamic therapy (PDT) and photodiagnosis (PD) using endogenous photosensitization induced by 5-aminolevulinic acid (ALA): mechanisms and clinical results. 1996; 14(5): 289-304.

Kennedy J, Pottier R, Pross D. Photodynamic therapy with endogenous protoporphyrins IX, basic principles and present clinical experience. *J. Photochem. Photobiol. B.* 1990; 6: 143-148.

Kennedy J, Pottier R. Endogenous protoporphyrin IX, a clinically useful photosensitizer for photodynamic therapy. *J. Photochem. Photobiol. B.* 1992; 14: 275-292.

Kershaw WC, Klaassen CD. Degradation and metal composition of hepatic isometallothioneins in rats. *Toxicol. Appl. Pharmacol.* 1992 Jan; 112(1): 24-31.

Kerwin J, Lancaster J, Feldman P, Nitric oxide: a new paradigm for second messengers. *J. Med. Chem.* 1995; 38: 4343-4362.

Ketabchi A, MacRobert A, Speight PM, Bennett JH. Induction of apoptotic cell death by photodynamic therapy in human keratinocytes. *Arch. Oral. Biol.* 1998; 43 (2): 143-149.

Kharitonov V, Sundquist A, Sharma V. Kinetics of nitrosation of thiols by nitric oxide in the presence of oxygen. *The journal of Biological Chemistry* 1995; 270 (47): 28158-28164.

Kitazawa Y, Kawase K, Matsushita H, Minobe M. Trabeculectomy with mitomycin. A comparative study with fluorouracil. *Arch. Ophthalmol.* 1991; 109(12): 1693-1698.

Klatt P, Schmidt K, Uray G, Mayer B. Multiple catalytic functions of brain nitric oxide synthase. Biochemical characterization, cofactor-requirement, and the role of N omega-hydroxy-L-arginine as an intermediate. *J. Biol. Chem.* 1993; 268(20): 14781-14787.

Kluck R, Bossy-Wetzel E, Green D, Newmeyer D.The release of cytochrome c from mitochondria: a primary site for Bcl-2 regulation of apoptosis. *Science* 1997; 275(5303): 1132-1136.

Knowles R, Moncada S: Nitric oxide synthases in mammals. *Biochem. J.* 1994; 298: 249-258.

Kooy N, Royal J, Ishiropoulos H. Oxidation of 2'-7'-dichlorofluorescein by peroxynitrite. *Free Radic. Res.* 1997;27(3):245-254.

Koppenol W, Moreno J, Pryor W, Ischiropoulos H, Beckman J. peroxynitrite, a cloaked oxidant formed by nitric oxide and superoxide. *Chem. Res. Toxicol.* 1992;5:834-842.

Korsmeyer SJ, Shutter JR, Veis DJ, Merry DE, Oltvai ZN. Bcl-2/Bax: a rheostat that regulates an anti-oxidant pathway and cell death. *Semin Cancer Biol* 1993 Dec; 4(6): 327-332.

Krammer B, Uberriegler K. In-vitro investigation of ALA-induced protoporphyrins IX. *J. Photochem. Photobiol. B.* 1996; 36:121-126.

Kukowska-Latallo J, Bielinska A, Johnson J, Spindler R, Tomalia D, Baker Efficient transfer of genetic material into mammalian cells using Starburst polyamidoamine dendrimers. *Proc. Natl. Acad. Sci. U S A.* 1996; 93(10): 4897-4902

Lane D.P. Cancer. p53, guardian of the genome. *Nature* 1992; 358(6381): 15-16.

Lea A, McTavish D. Atorvastatin: A review of its pharmacology and therapeutic potential in the management of hyperlipidaemias. *Drugs* 1997; 53(5); 828-847.

Leist M, Nicotera P. Apoptosis, Excitotoxicity, and Neuropathology. *Experimental Cell Research* 1998; 239: 183-201.

Leske M, Rosenthal J. Epidemiologic aspects of open-angle glaucoma. *Am. J. Epidemiol.* 1979; 109, 250-256.

Levy J, Obochi M. New applications in photodynamic therapy. Introduction. *Photochem. Photobiol.* 1996; 64(5): 737-739.

Liang H, Fesik S. Three-dimensional structures of proteins involved in programmed cell death. *J. Mol. Biol.* 1997; 274: 291-302.

Lin K, Xue J, Nomen M, Spur B, Wong P. Peroxynitrite-induced apoptosis in HL-60 cells. *J. Biol. Chem.* 1995 Jul 14; 270(28): 16487-16490

Lin K, Xue J, Wong P. Peroxynitrite an apoptotic agent in HL-60 cells. *Adv. Exp. Med. Biol.* 1997; 407: 413-419.

Lindenboim L, Haviv R, Stein R. Inhibition of drug-induced apoptosis by survival factors in PC12 cells. *J. Neurochem.* 1995; 64: 1054-1063.

Liu Z, Rudd MA, Freedman JE, Loscalzo J. S-Transnitrosation reactions are involved in the metabolic fate and biological actions of nitric oxide. *J. Pharmacol. Exp. Ther.* 1998; 284(2): 526-534.

Lum B, Torti F. Adjuvant intravesicular pharmacotherapy for superficial bladder cancer. *J. Natl. Cancer Inst.* 1991; 83, 682-694.

MacAllister R, Vallance P. L-arginine: nitric oxide pathway in the human cardiovascular system. *JIFCC* 1996; 8(4): 152-158.

Mannick J, Asano K, Izumi K, Kieff E, Stamler I. Nitric oxide produced by human B lymphocytes inhibits apoptosis and Epstein-Barr virus reactivation. *Cell* 1994; 79: 1137-1146.

Martina V, Bruno G, Trucco F, Zumpano E, Tagliabue M, Di Bisceglie C, Pescarmona G. Platelet cNOS activity is reduced in patients with IDDM and NIDDM. *Thromb. Haemost.* 1998; 79: 520-522.

McCaughan J, Guy J, Hicks W, laufman L, Nims T, Walker J. photodynamic therapy for cutaneous and subcutaneous malignant neoplasms. *Arch. Surg.* 1989; 125, 211-216.

McGuigan L, Mason R. Sanchez R, Quigley H. D-penicillamine and beta-aminopropionitrile effects on experimental filtering surgery. *Invest Ophthalmol. Vis. Sci.* 1987; 28(10): 1625-1629.

Megevand GS, Salmon JF, Scholtz RP, Murray AD. The effect of reducing the exposure time of mitomycin C in glaucoma filtering surgery. *Ophthalmology*. 1995; 102(1): 84-90.

Messmer U, Ankarcrona M, Nicotera P, Brune B. p53 expression in nitric oxide-induced apoptosis. *FEBS Lett.* 1994; 355: 23-26.

Moan J, Bech O, Gaullier JM, Stokke T, Steen HB, Ma LW, Berg K. Protoporphyrin IX accumulation in cells treated with 5-aminolevulinic acid: dependence on cell density, cell size and cell cycle. *Int. J. Cancer*. 1998; 75(1): 134-139.

Moan J, Berg K. Photochemotherapy of cancer: experimental research, *Photochem. Photobiol.*, 1992; 55: 931-948.

Moffat P, Denizeau F. Metallothionein in physiological and physiopathological processes. *Drug Metabolism Reviews*, 1997; 29(1&2), 261-307.

Moshage H. Nitric oxide determinations: much ado about NO.-thing? *Clin. Chem*. 1997; 43(4): 553-556.

Muijsers R, Folkerts G, Henricks P, Sadeghi-hashjin G, Nijkamp F. Peroxynitrite: A two faced metabolite of nitric oxide. *Life Sciences* 1997; 60(21): 1833-1845.

Munger K, Germann U, Beltramini M, Niedermann D, Baitella-Eberle G, Kagi J, Lerch K. (Cu, Zn)-Metallothioneins from fetal bovine liver. *The journal of Biological Chemistry* 1985; 260(18): 10032-10038.

Munzel T, Heitzer T, Harrison D. The physiology and pathophysiology of the nitric oxide/superoxide system. *Herz*. 1997; 22(3): 158-172.

Nathan C. Nitric oxide as a secretory product of mammalian cells. *FASEB J.* 1992; 6(12): 3051-3064.

Noodt B, Berg K, Stokke TM, Peng Q, Nesland J. Apoptosis and necrosis induced with light and 5-aminolevulinic acid-derived protoporphyrin IX. *Br. J. Cancer* 1996; 74 (1): 22-29.

Nyamekye I, Anglin S, McEwan. Photodynamic therapy of normal and balloon-injured rat carotid arteries using 5-amino-levulinic acid. Circulation 1995; 91(2): 417-425.

Ochsner M. Photodynamic therapy: the clinical perspective. Review on applications for control of diverse tumorous and non-tumorous diseases. *Arzneimittelforschung* 1997; 47(11): 1185-1194.

Packer M, Murphy M. Peroxynitrite formed by simultaneous nitric oxide and superoxide generation causes cyclosporin-A-sensitive mitochondrial calcium efflux and depolarization. *Eur. J. Biochem.* 1995; 234(1): 231-239.

Park J, Billman G. Transnitrosation as a predominant mechanism in the hypotensive effect of S-nitrosoglutathione. *Biochem. Mol. Biol. Int.* 1993; 30(5): 885-891.

Peng Q, Warloe T, Berg K, Moan J, Kongshaig M, Giercksky K, Nesland J. 5-aminolevulinic acid-based photodynamic therapy. *American Cancer Society.* 1997; 79(12): 2282-2308.

Possel H, Noack H, Augustin W, Keilhoff G, Wolf G: 2,7-Dihydrodichlorofluorescein diacetate as a fluorescent marker for peroxynitrite formation. *FEBS Letters* 1997; 416:175-178.

Pryor W, Squadrito G. The chemistry of peroxynitrite: A product from the reaction of nitric oxide with superoxide. *Am. J. Physiol.* 1995; 268: L699-L722.

Qin L, Pahud DR, Ding Y, Bielinska AU, Kukowska-Latallo JF, Baker JR Jr, Bromberg JS. Efficient transfer of genes into murine cardiac grafts by Starburst polyamidoamine dendrimers. *Hum. Gene Ther.* 1998; 9(4): 553-560.

Rabini R, Staffolani R, Fumelli P, Mutus B, Curatola G, Mazzanti L. Decreased nitric oxode synthase activity in platelets from IDDM and NIDDM. *Diabetologia* 1998; 41: 101-104.

Radi R, Beckman J, Bush K, Freeman B. Peroxynitrite oxidation of sulfhydryls. The cytotoxic potential of superoxide and nitric oxide. *J. Biol. Chem.* 1991; 266(7): 4244-4250.

Radomski M, Moncada S. Biological role of nitric oxide in platelet function. In: Moncada S, Higgs E, Berrazueta J, eds. Clinical Relevance of Nitric Oxide in the Cardiovascular system. *Madrid : Edicomplet.* 1991; 45-46.

Ramezanian M, Padmaja S, Koppenol W. Nitration and hydroxylation of phenolic compounds by peroxynitrite. *Chem. Res. Toxicol.* 1996; 9 (1): 232-241.

Reed JC, Bcl-2 and the regulation of programmed cell death. *J. Cell Biol.* 1994; 124:1-6.

Roberts J, Adams Y, Tomalia D, Mercer-Smith J, Lavallee D. Using Starburst Dendrimers as linker to radiolabel antibodies. *Bioconjugate Chemistry* 1990; 1(5): 305-308.

Salgo M, Squadrito G, Pryor W. Peroxynitrite causes apoptosis in rat thymocytes. *Biochem. Biophys. Res. Commun.* 1995; 215(3): 1111-1118.

Sandau K, Pfeilschifter J, Brune B. Nitric oxide and superoxide induced p53 and Bax accumulation during mesangial cell apoptosis. *Kidney International* 1997; 52: 378-386.

Savill J, Fadok V, Henson P, Haslett C. Phagocyte recognition of cells undergoing apoptosis. *Immunol. Today* 1993; 14(3): 131-136.

Schmidt HH, Murad F. Purification and characterization of a human NO synthase. *Biochem. Biophys. Res. Commun.* 1991; 181(3): 1372-1377.

Schwartzman R, Cidlowski J. Apoptosis: The biochemistry and molecular biology of programmed cell death. *Endocrine Rev.* 1993; 14: 133-151.

Seo HG, Takata I, Nakamura M, Tatsumi H, Suzuki K, Fujii J, Taniguchi N. Induction of nitric oxide synthase and concomitant suppression of superoxide dismutases in experimental colitis in rats. *Arch. Biochem. Biophys.* 1995; 324(1): 41-47.

Sexton D, Muruganadam A, Mckenney D, Mutus B. Visible light photochemical release of nitric oxide fron S-nitrosoglutathione: potential photochemotherapeutic applications: *Photochem. Photobiol.* 1994; 59(4): 463-467.

Sexton D. Some aspects of glutathione and L-arginine/nitric oxide metabolism in the maintenance of platelet function. Ph. D thesis. 1994.

Sherman M, Griscavage J, Ignarro Nitric oxide-mediated neuronal injury in multiple sclerosis. *Med. Hypotheses.* 1992; 39(2): 143-146.

Singh R, Hogg N, Joseph J, Kalyanaraman. Photosensitized decomposition of S-nitrosothiols and 2-methyl-2-nitrosopropane possible use for site-directed nitric oxide production. *FEBS Lett.* 1995; 360: 47-51.

Singh R, Moll F, Lin S, Ferzli C, Yu K, Koski K, Saul R, Cronin P. Starburst Dendrimers: Enhanced performance and flexibility for immunoassays *Clin. Chem.* 1994; 40(9): 1845-1849.

Smyth R, Nguyen K, Ahn S, Panek W, Lee D. Th effects of photofrin on human Tenon's capsule fibroblasts in vitro. *J. Ocular Pharmacol.* 1993; 9(2): 171-178.

Stamler J, Vaccaro O, Neaton JD, Wentworth D. Diabetes, other risk factors, and 12-yr cardiovascular mortality for men screened in the Multiple Risk Factor Intervention Trial. *Diabetes Care* 1993; 16(2): 434-444.

Stamler JS, Singel DJ, Loscalzo J. Biochemistry of nitric oxide and its redox-activated forms. *Science* 1992 Dec 18; 258(5090): 1898-1902.

Steinbach P, Weingand H, Baumgartner R, Kriegmair M, Hofstadter F, Knuchel R. Cellular fluorescence of the endogenous photosensitizer protoporphyrin IX following exposure to 5-aminolevulinic acid. *Photochem. Photobiol.* 1995; 62(5): 887-895.

Steinman HM. The Bcl-2 oncoprotein functions as a pro-oxidant. *J. Biol. Chem.* 1995; 270: 3487-3490.

Stuer D. Structure-function aspects in the nitric oxide synthases. *Annu. Rev. Pharmacol. Toxicol.* 1997; 37: 339-59.

Suzuki K, Imura N, Kimura M, Metallothionein III: Biological roles and medical implications. *Eds.* Basal Switz: Birkhauser Verlag. 1993.

Szabo C, Ohshima H. DNA damage induced by peroxynitrite: subsequent biological effects. *Nitric oxide: Biology and Chemistry.* 1997; 1(5): 373-385.

Szabo C, Zingaarelli B, O'Connor M, Salzaman A. DNA strand breakage, activation of poly (ADP-ribose) synthetase, and cellular energy depletion are involved in the cytotoxicity of macrophages and smooth muscle cells exposed to peroxynitrite. *Proc. Natl. Acad. Sci. USA* 1996; 93: 1753-1758.

Tomalia D, Naylor A, Goddard W. Starburst cascade polymers: Molecular-level control of size, shape, surface chemistry, topology and flexibility from atoms to macroscopic matter. *Angew. Chem. Int. Ed. Engl.* 1990; 29: 138-175.

Troy C, Derossi D,Prochiantz A, Greene L, Shelanski M. Down-regulation of Cu/Zn superoxide dismutase leads to cell death via the nitric oxide-peroxynitrite pathway. *J. Neurosci.* 1996; 18, 253-261.

Upchurch G J, Welch G, Loscalzo J. S-Nitrosothiols: Chemistry, Biochemistry, and Biological Actions. *Advances in Pharmacology* 1995; 34:343-349.

Vanags D, Porn-Ares M, Coppola S, Burgess D, Orrenius S. Protease involvement in fodrin cleavage and phosphotidylserine exposure in apoptosis. *J. Biol. Chem.* 1996; 271: 31075-31085.

Wever R, van Dam T, van Rijn H, de Groot P, Rabelink T. Tetrahydrobiopterin regulates superoxide and nitric oxide generation by recombinant endothelial nitric oxide synthesis. *Biochem. Biophys. Res. Commun.* 1997; 237: 340-344.

Williams D. The mechanism of nitric oxide formation from S-nitrosothiols (thionitrites). *Chem. Commun.* 1996; 1085-1091.

Wolf P, Rieger E, Kerl H. Topical photodynamic therapy with endogenous porphyrins after application of 5-aminolevulenilic acid, an alternative treatment modality for solar keratoses, superficial squamous cell carcinomas, and basal cell carcinomas *J. Am. Acad. Dermatol.* 1993; 28:17-21.

Wood P, Mutus B, Redmond R. The mechanism of photochemical release of nitric oxide from S-nitrosoglutathione. *Photochem. Photobiol.* 1996; 64(3): 518-524.

Xia Y, Dawson VL, Dawson TM, Snyder SH, Zweier JL. Nitric oxide synthase generates superoxide and nitric oxide in arginine-depleted cells leading to peroxynitrite-mediated cellular injury. *Proc. Natl. Acad. Sci. U S A* 1996; 93(13): 6770-6774.

Zacharia P, Deppermann, S, Schuman J. Ocular hypotony after trabeculectomy with mitomycin C. *Am. J. Ophthalmol.* 1993; 116: 314-326.

Zhong LT, Sarafian T, Kane DJ, Charles AC, Mah SP, Edwards RH, Bredesen DE. bcl-2 inhibits death of central neural cells induced by multiple agents. *Proc. Natl. Acad. Sci. USA* 1993; 90(10): 4533-4537.

Zhou Q, Hellermann G, Solomonson L. Nitric oxide release from resting platelets. *Thromb. Res.* 1995; 77: 87.

Zingarelli B, O'Connor M, Wong H, Salzman A, Szabo C. *J. Immun.* 1996; 156, 350-358.

VITA AUCTORIS

MARIE A. TANNOUS

EDUCATION

1994-1998	**Ph. D** Clinical Chemistry Department of Chemistry and Biochemistry University of Windsor, Windsor, ON
1990-1994	**B.Sc. Biochemistry** (Honours) University of Windsor, Windsor, ON
1987-1990	**Medical Laboratory Technology Diploma** St. Clair College, Windsor, ON

AWARDS

1998	University of Windsor Summer Research Award
1996-1998	NSERC postgraduate Scholarship (PGS B)
1996	The Canadian Society of Clinical Chemists Travel Award
1996	The American Association of Clinical Chemistry Travel Award
1996	University of Windsor Travel Award

PUBLICATIONS

- Tannous M, Vignini A, Cheung R, Mutus B. Atorvastatin induces eNOS in human platelets. (Manuscript in preparation)

- Tannous M, Hutnik C, Tingey D, Mutus B. S-Nitrosoglutathione Photolysis as a Novel Therapy for Antifibrosis in Filtration Surgery. (Submitted).

- Tannous M, Rabini R, Vignini A, Moretti N, Fumelli P, Zielinski B, Mazzanti L, Mutus B. Evidence for iNOS-dependent peroxynitrite production in Diabetic Platelets. (Submitted)

- Dimmock et al. Mutus B, Tannous M. Cytotoxic activities of Mannich bases of Chalcones and related compounds. Journal of Medicinal Chemistry 1998; 41(7): 1014-1026.

- Tannous M, Labbe N, Redmond R, Mutus B. A photo-activated, protein-based, peroxynitrite generating system composed of the nitric oxide derivative of apo-metallothionein (thionein-NO) and glucose oxidase. Journal of Photochem. Photobiol.1997; 41: 249-254.

- Muruganandam A, Tannous M, Mutus B. ELISA for in vivo assessment of nonenzymatically glycated platelet glutathione peroxidase. Clinical Biochemistry 1994; 27(4): 293-298.

ABSTRACTS:

- Tannous M, Labbe N, Mutus B. A photo-activated, protein-based, peroxynitrite generating system composed of the nitric oxide derivative of apo-metallothionein (thionein-NO) and glucose oxidase. AACC/CSCC Annual Meeting (1996), Chicago, IL.

- Tannous M, Mutus B. Assessment of photochemotherapeutic effect of T-NO. Canadian Federation of Biological Societies 39th Annual Meeting, (1996). London, Ontario.

- Tannous M, Mutus B. Assessment of photochemotherapeutic effect of thionein/GOD on tumor cells in culture. The Michigan section of the AACC (1995), Ypsilanti, Michigan.

- Tannous M, Mutus B. Assessment of photochemotherapeutic effect of thionein/GOD on tumor cells in culture (1995), UCI Symposium for Cancer Research, Irvine, California.